Radiation Monitoring and Remediation Following the Fukushima Daiichi Nuclear Power Plant Accident

Cooperation between Fukushima Prefecture and the IAEA

SUMMARY REPORT (2013 to 2017)

[Fukushima Prefecture Initiative Projects]

(temporary translation)

March 2018

Fukushima Prefecture

Introduction

Fukushima Prefecture suffered immense damage from the Great East Japan Earthquake that occurred on 11 March 2011 and the accompanying disaster at Tokyo Electric Power's Fukushima Daiichi Nuclear Power Plant[1]. Radioactive materials released into the environment contaminated the land and forced more than 160,000 prefectural residents to evacuate. About 50,000 residents have still not returned home, even at the creation of this report about 7 years after the disaster.

Concentrating the world's wisdom is important to restore the environment after the unprecedented nuclear disaster, and create an environment where prefectural residents can make a safe living in the future. Therefore, we initiated a collaboration with the International Atomic Energy Agency (hereinafter, IAEA), which has extensive knowledge in the nuclear field. In December 2012, a memorandum of cooperation between Fukushima Prefecture and the IAEA was signed. Based on this memorandum, a practical arrangement in the fields of decontamination and radiation monitoring between Fukushima Prefecture and the IAEA was signed on the same day (projects based on this arrangement are referred to as FCPs).

Following this, additional agreements were signed for five Fukushima Prefecture Initiative Projects (hereinafter, FIPs) with a period of 3 years in April and October 2013 as a new framework in which support from the IAEA was provided for the projects implemented by Fukushima Prefecture. These agreements initiated FIPs. In April and May 2016, agreements were signed to extend the cooperation period until December 2017 and alter the extent of cooperation[2].

[FIPs]

1 Survey of radionuclide movement in river systems
2 Survey of radionuclide movement with wild life
3 Countermeasures for radioactive materials in rivers and lakes
4 Development of environmental mapping technology using GPS walking surveys
5 Study of the proper treatment of waste containing radioactive materials at municipal solid waste Incinerators

Fukushima Prefecture and the IAEA initiated cooperative projects in 2013. This report summarises the achievements about the part of FIPs out of the above projects over the past 5 years and provides a broad overview of the future outlook.

We would like to express our gratitude to IAEA specialists, experts from international and domestic organisations and local governmental staff for their assistance in these cooperative projects.

We expect this report to contribute to the safety and security of prefectural residents as well as people all over the world.

---

1 Tokyo Electric Power's Fukushima Daiichi Nuclear Power Plant transitioned to Tokyo Electric Power Company Holdings' Fukushima Daiichi Nuclear Power Plant on 1 April 2016.

2 In accordance with the change in the scope of cooperation, the names of FIPs have changed.

Contents

1. FIP1 Survey of radionuclide movement in river systems

Abstract

It is important to provide the necessary information for the safe use of river water in the prefectural land contaminated with radioactive materials. We conducted surveys of rivers in Fukushima Prefecture to clarify the dynamics of radioactive materials, and to verify the accuracy of a simulation model.

In particular, we collected necessary data from the Hirose River to predict the dynamics of radionuclides using the TODAM model. The simulation results indicated that the TODAM model could roughly reproduce the concentration changes accompanying the downflow of radiocaesium at each monitoring point along the Hirose River however, improvements in the accuracy of the model results are necessary.

In the Abukuma River system and the major rivers in Hamadori area, we investigated the flow dynamics of suspended radiocaesium adsorbed by microparticles. According to this analysis, the suspended radiocaesium concentrations are still decreasing. In addition, it was also shown that the migration of radiocaesium was affected by dams at the basins and decontamination practices.

1.1. Purpose

River water is widely used for drinking water and farming. In 2011, however, the accident at Tokyo Electric Power's Fukushima Daiichi Nuclear Power Plant resulted in wide contamination of the prefectural area with radioactive materials. Since river basins were also contaminated, it is important to clarify the dynamics of radioactive materials in rivers and to provide the necessary information for the safe use of river water. If radiocaesium absorbed by suspended particulate matter and flows downstream in a suspended form, re-deposition after events, such as floods, may affect the ambient air dose rate. Accordingly, the migration of dissolved radiocaesium through the ecosystem should be considered (Figure 1). Thus, we evaluated the dynamics of radiocaesium depending on its form. The purpose of this survey is to investigate the dynamics of radiocaesium with river flow down in Fukushima prefecture and to verify it by model simulation based on the monitoring data.

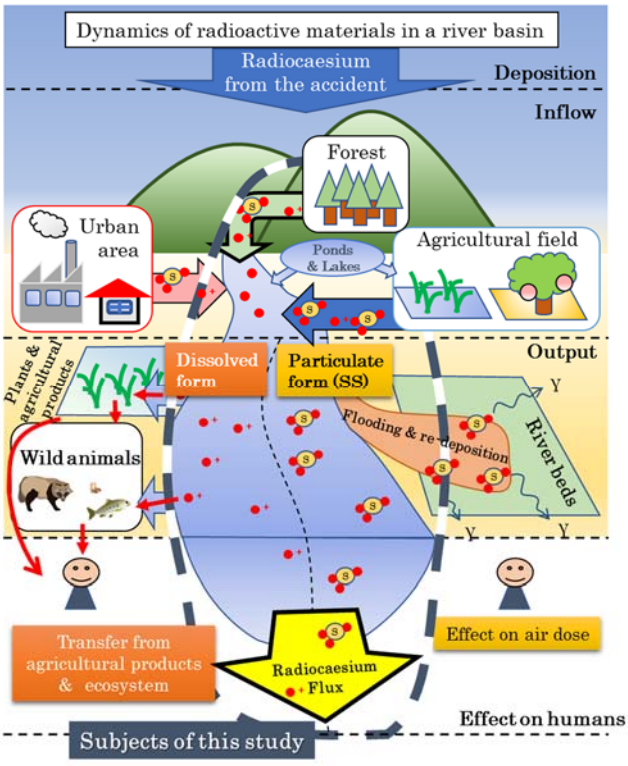

Figure 1: Schematic diagram describing dynamics of radiocaesium in a river basin.

1.2. Content of implementation

(1) Survey of the Hirose River basin

A survey was conducted at the Hirose River and its tributaries during 5 year periods beginning in fiscal year 2013. The Hirose River is a tributary of the Abukuma River. The Hirose River has catchments close to an area of substantial radiocaesium deposition. Figure 2(a) shows a quantitative summary of radiocaesium deposition on the ground surface in this basin. The amount as of 2 July, 2011 is refered ti as the initial deposition in this document. We could find a red area, indicating high radiocaesium levels, near the southeast boundary of the Hirose River basin. Radiocaesium deposition was also high in the basins of the tributaries, the Nuno River and the Oguni River (Table 1).

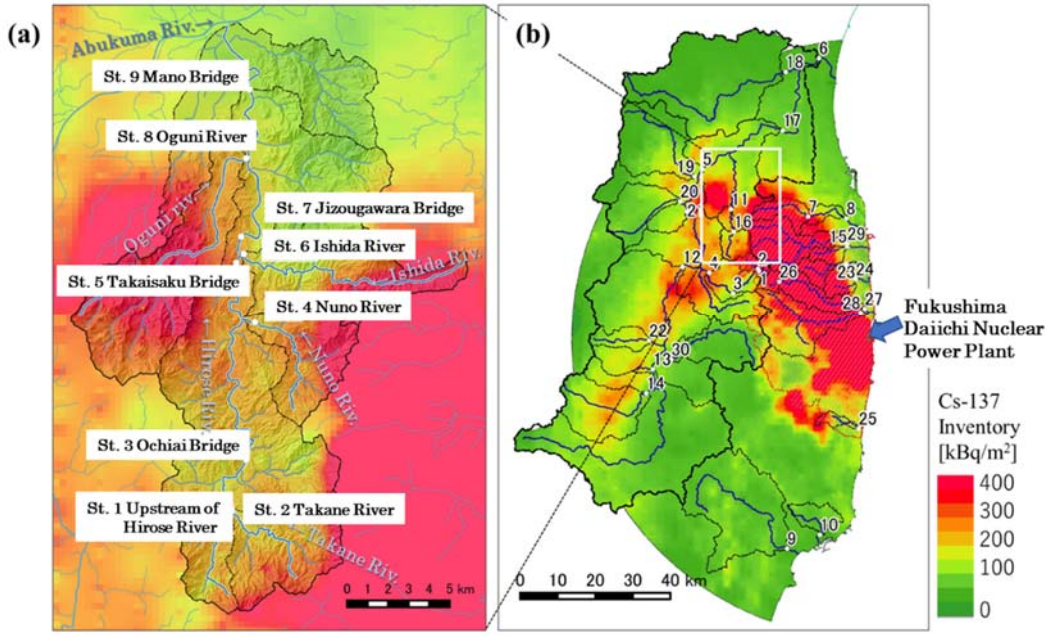

Figure 2: Monitoring points in this survey and the initial amounts of Cs-137 in these areas (as of 2 July, 2011).

(a) Hirose River basin. Numbers in the figure correspond to those in Table 3.

(b) Area included in the wide area river survey.

*Source: Results of the Third Airborne Monitoring by MEXT (2011). http://radioactivity.nsr.go.jp/ja/contents/5000/4858/24/1305819_0708.pdf. In (b), the area outside the third airborne monitoring range was evaluated by both the airborne monitoring results by the prefecture (http://emdb.jaea.go.jp/emdb/en/portals/b224/) and the radiocaesium deposition results from the first unattended helicopter survey within 3 km from the Fukushima Daiichi Nuclear Power Plant (http://emdb.jaea.go.jp/emdb/portals/b225/).

Table 1: Catchment area and initial Cs-137 deposition within the Hirose River basin.

	Catchment area [km^2]	Average Cs-137 deposition [kBq/m^2]
Hirose River	267.9	231
Takane River	19.2	270
Nuno River	18.6	343
Ishida River	30.1	290
Oguni River	40.4	343

Figure 2(a) showed the nine monitoring points and table 2 listed the major monitoring items. River water samples of about 100 L were obtained at the points to measure of radiocaesium concentration. Suspended and dissolved caesium were collected separately from the river water. Their concentrations were measured using a germanium semiconductor detector. To determine the radiocaesium concentration, we used gamma-ray spectrometry with a germanium semiconductor detector, one of a series of measurements established by the Ministry of Education, Culture, Sports, Science and Technology.

Based on the monitoring data, we applied the Time-dependent One-dimensional Degradation And Migration (TODAM) model for the verification of radiocaesium dynamics in the Hirose River. The TODAM model can simulate temporal changes in radionuclides in waters and sediments. For example, the TODAM model enables us to estimate the amounts of radionuclides transported to the Pacific Ocean via rivers, to predict the places in rivers which sediments deposited frequently, and evaluate the effects of decontamination within basins on the amounts of sediment discharge. In this survey, we used the TODAM model to estimate the amounts of radiocaesium transported during flood events, to predict the radiocaesium adsorbed by sediments is deposited, and to estimate the amount of radiocaesium from the Hirose River to the Abukuma River.

Table 2: Major monitoring items.

River Shape		Cross-sectional diagram, latitude, longitude, and vegetation
Air dose rate		Air dose rates at heights of 1 m and 1 cm
Consecutive monitoring		Water level and turbidity.
Ordinary water level	Monitoring	Discharge and velocity.
	Water sampling	Turbidity, suspended solids, pH, and radiocaesium concentrations (Cs-134 · Cs-137)
	Soil sampling	Particle size distribution, mineral composition, and radiocaesium concentrations
Flooding event	Monitoring	Discharge and velocity.
	Water sampling	Radiocaesium, Ca^{2+}, and NH_4^+ concentrations

(2) Wide-area river survey

From the fiscal year 2015, we performed a multipoint survey of the Abukuma River basin and eight

water systems in the Hamadori area. Figure 2(b) shows the positions and characteristics of the monitoring points. In survey (1) of the Hirose River, a single basin was investigated in detail. On the other hand, in this wide-area survey, many rivers were investigated continuously by the same method to clarify long-term changes and relationships with the basin characteristics. This survey was a continuation of a survey performed by Tsukuba University. Until the end of the fiscal year 2014, the university performed a survey on consignment from the Ministry of Education, Culture, Sports, Science and Technology and Nuclear Regulatory Agency. This report also includes those past monitoring data.

At each monitoring point, we set a suspended sediment sampler to collect suspended sediments (SS), a water gauge to measure the water level, and a turbidimeter to measure the turbidity of river water. At some points, however, we used the water-level telemetry data by Fukushima Prefecture or the Ministry of Land, Infrastructure, Transport and Tourism instead of installing a water gauge. Suspended sediments captured in the samplers were collected every month or every several months. The samples were dried at 110 °C for 24 h, and the concentrations of the suspended caesium-134 and caesium-137 were measured using a germanium semiconductor detector. The turbidity and water level were measured every 10 min. We calculated SS concentrations [g/L] and flow rates [m^3/s] by the generated calculation using the appropriate formulas. For the suspended caesium-137 migration [Bq], we multiplied the SS concentrations by the flow rate and by the caesium-137 concentration in the same period.

1.3. Results

(1) Survey of the Hirose River basin

Figure 3 showed river bed cross sections and status photos at the monitoring points of the Ochiai Bridge and the Mano Bridge on the Hirose River. Both points are about 24 km away from each other. Although the water depth was comparable, the river width at the Mano Bridge including the floodplains was about twice as long as that at the Ochiai Bridge. This result indicates that a lot of sediments transported by the river have deposited on the floodplains.

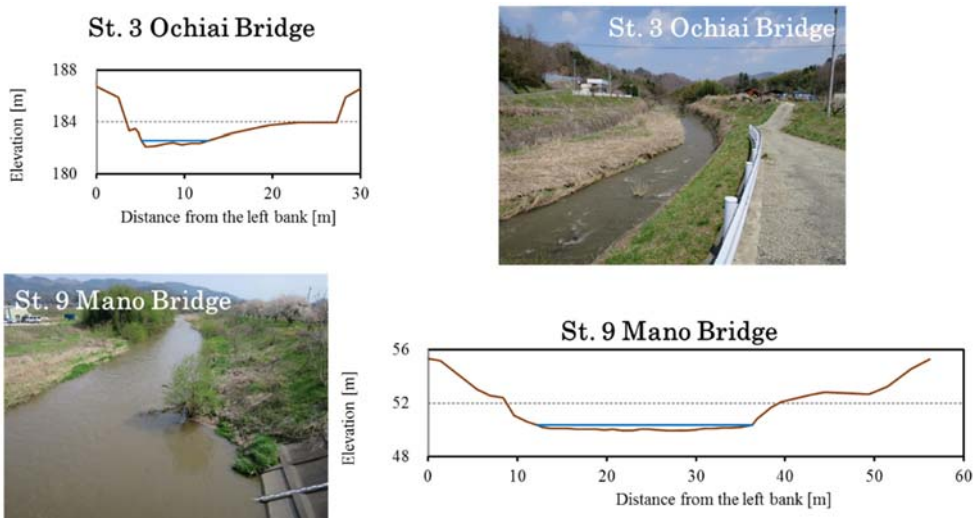

Figure 3: The cross sections and site photographs at the monitoring points in the Hirose River basin (ex. St. 3 Ochiai Bridge and St. 9 Mano Bridge).

During the monitoring period, it was sometimes observed disruptions of the riverbeds and banks during some flood events and depositions of new sediments on the riverbed. However, the cross sections of riverbed at all monitoring points did not show any great change.

Table 3 shows the observed suspended and dissolved caesium-137 concentrations in the river water at each monitoring point of the Hirose river basin in April 2016. The K_d values are also presented and were defined as follows: (solid-liquid distribution coefficient (K_d) = suspended radiocaesium concentration/dissolved radiocaesium concentration). The concentrations of both suspended and dissolved radiocaesium were high in the Oguni River, where radiocaesium deposition was greater than that at other monitoring points. The K_d value, that is the ratio of the radiocaesium concentrations between the solid and liquid phases, varied between 10^5 to 10^6 at every point. These values were greater than those reported in Europe after the Chernobyl accident (8×10^3 to 4.2×10^5 ; Smith et al., 2005).

Table 3: Suspended and dissolved Cs-137 concentrations and K_d values at each monitoring point within the Hirose River basin.

		Suspended Cs-137 [Bq/kg]	Dissolved Cs-137 [mBq/L]	K_d value [L/kg]
St. 1	Upstream of Hirose River	4982	1.8	2.76×10^6
St. 2	Takane River	2889	3.0	9.62×10^5
St. 3	Ochiai Bridge	5012	3.7	1.34×10^6
St. 4	Nunokawa River	4385	1.3	3.44×10^6
St. 5	Takaisaku Bridge	3865	3.2	1.21×10^6
St. 6	Ishida River	3432	2.7	1.25×10^6
St. 7	Jizougawara Bridge	5626	2.8	2.01×10^6
St. 8	Oguni River	11790	15.7	7.50×10^5
St. 9	Mano Bridge	3210	2.7	1.21×10^6

Figure 4 shows the changes in suspended caesium-137 and suspended solid (SS) concentrations at each monitoring point along the Hirose River at the ordinary water level. The suspended caesium-137 concentration was high in the some of the tributaries, as mentioned above. This parameter is greatly affected by the initial deposition in thee basins. The results varied among monitoring points, probably owing to river wall construction. This is supported by the higher SS concentrations in the river water despite the ordinary water level.

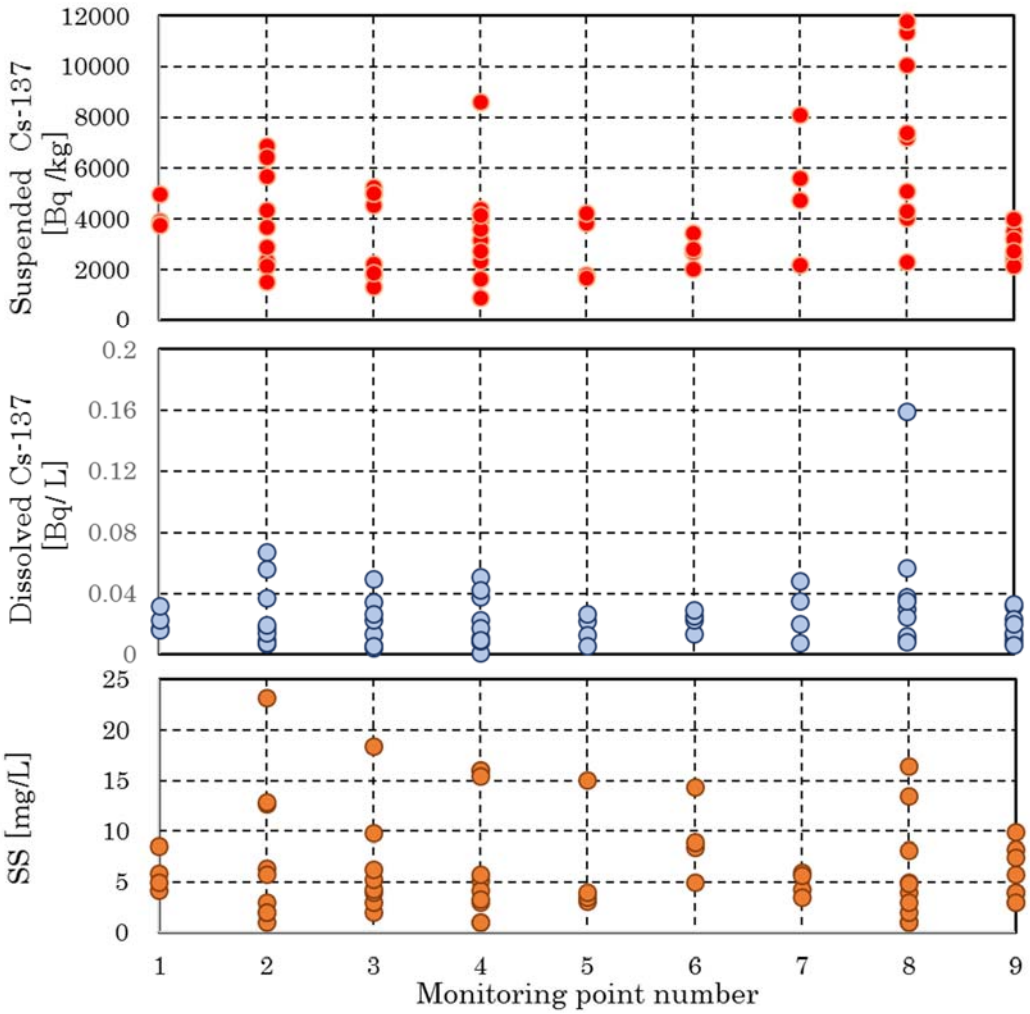

Figure 4: Suspended and dissolved Cs-137, and SS concentrations at each monitoring point.

The TODAM model was provided by Prof. Yasuo Onishi, an IAEA specialist, in fiscal year 2015. Figure 5 shows a schematic of the monitoring network used to apply the TODAM model to the Hirose River. The distance was assumed to be 31,732 m from the mouth of the Hirose River, where it merges with the Abukuma River, to the point where the Takane River and the Hirose River merge. We included the inflows from the Takane River, Nuno River, Ishida River, and Oguni River, which are main tributaries of the Hirose River in the simulation. For the Hirose River, the simulation was performed every 200 mm in the flow channel direction, and 150 calculation points were set in the Hirose River basin.

We simulated the radiocaesium dynamics in the Hirose River based on the monitoring data. For this simulation, we received technical supports from Prof. Onishi. Figure 6 shows a simulation result, that is, radiocaesium concentrations by the TODAM model. The ordinary water level and flow rate conditions were set for the simulation, and measured radiocaesium concentration at the upstream end (St.1) of the main stream of the Hirose River and the main tributary were set as boundary conditions.

Near the downstream end (St. 9), the measured and estimated values differed slightly. However, concentration changes at each monitoring point along the Hirose River could be roughly reproduced.

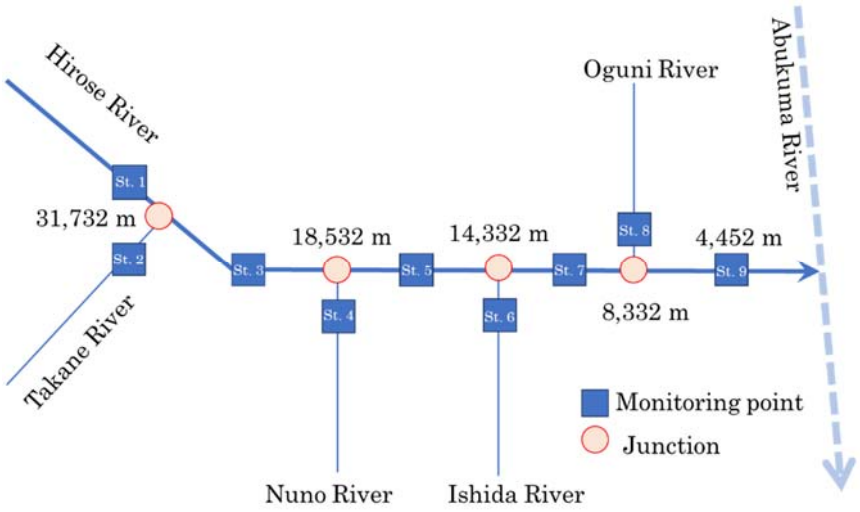

Figure 5: A schematic representation of the monitoring network in the Hirose River basin.

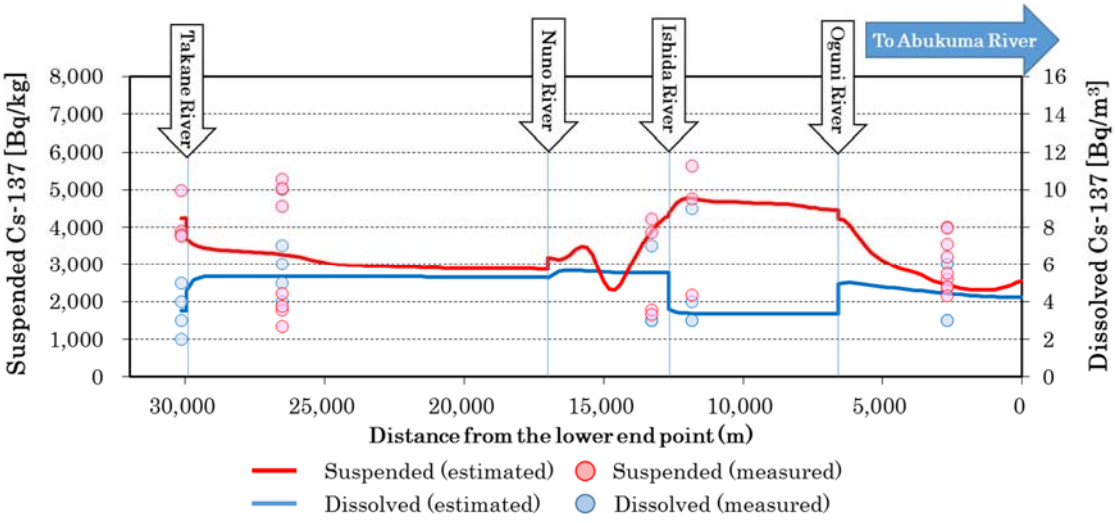

Figure 6: A result of simulation by TODAM model.

(2) Wide-area river survey

Figure 7 showed caesium-137 concentrations in the Abukuma River system and rivers in the Hamadori area until May 2017. Variation in the concentrations can be explained by differences in the initial caesium-137 deposition among the basins. However, significant decreasing trends in the caesium-137 concentrations were commonly observed at all monitoring points for about one year after the accident. The rate of decrease slowed slightly thereafter, but this general trend has continued to the present time. The Nuclear Regulatory Agency indicated that differences in the rate of decrease in the

caesium-137 concentration result from variation in land use types among the basins[2].

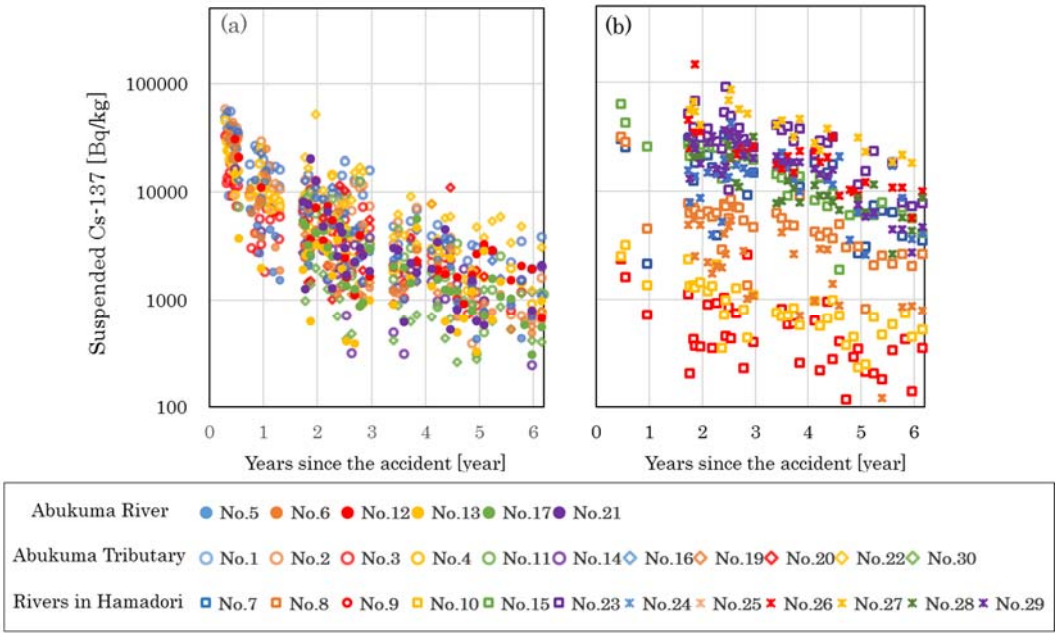

Figure 7: Changes in suspended Cs-137 concentrations in river waters.
(a) Abukuma River system and (b) rivers in the Hamadori area.

Figure 8 shows the monthly changes in suspended caesium-137 at six monitoring points from 2011 to August 2015 (flux at each monitoring point). These amounts did not show a clear trend owing to the extensive temporal variation in river flow and SS concentrations. The ratio of the integrated suspended caesium-137 migration amount to the amount of caesium-137 deposited in the basin at each point (basin area × the initial caesium-137 deposition) was 2.7% to 3.4% at two points along the Abukuma River, and 0.7% to 1.4% at four points along its tributaries.

Figure 9 showed the suspended caesium-137 migration standardized by both the initial amount of caesium-137 deposition and river flow (upper graph) and the proportion of the watersheds of a dam to the total area (excluding No.12, 17, 18 due to several problems during the monitoring period. lower graph) from October 2012 to October 2014. Small caesium-137 migrations were detected at the points where the watershed area of the dam was occupied most area of the basin (red hatched part in the graph).

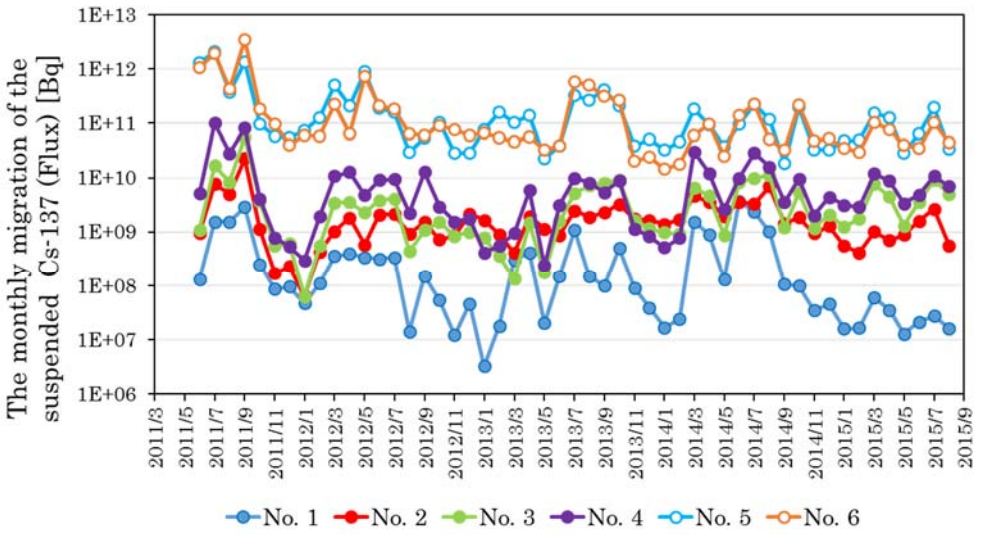

Figure 8: Monthly migration of the suspended Cs-137 at monitoring points (No.1-6) from May 2011 to September 2015.

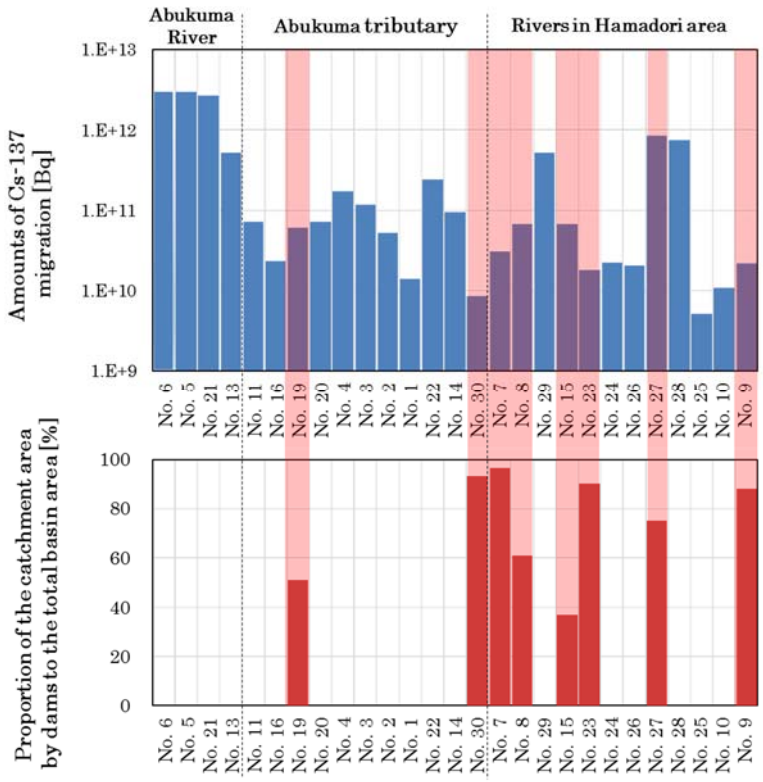

Figure 9: Migration of the suspended Cs-137 from Oct. 2012 to Oct. 2014. Red shadow bars indicate the monitoring point with higher proportion of the watershed area for dams to the total basin area.

Finally, we evaluated the effects of surface decontamination practices by the national and municipal governments on caesium-137 concentrations in the river waters. Because the observed decreases in caesium-137 concentrations, as shown in Figure 7, were similar to the trends observed in European rivers after the Chernobyl accident, this decline is expected to result from the natural attenuation process[1]. It is difficult to determine the effect of surface decontamination practices on the caesium-137 concentrations in rivers owing to the extremely small area subjected to decontamination relative to the total basin area. Thus, at two monitoring points in the Kuchibuto River basin (No.1 and 2. Fig. 2), we investigated the relationship between the progress in surface decontamination and the concentrations of the suspended caesium-137 in river waters (Fig. 10). The effects are expected to be pronounced at those points because the basin was entirely within the special decontamination area. The intensive surface decontamination practices were conducted in the area from Apr. 2014 to Dec. 2015. During this period, the suspended caesium-137 concentrations at both points were decreased substantially. The rapid decrease can be attributed to surface decontamination because the observed changes exceed those that can be explained by natural attenuation (Fig. 10).

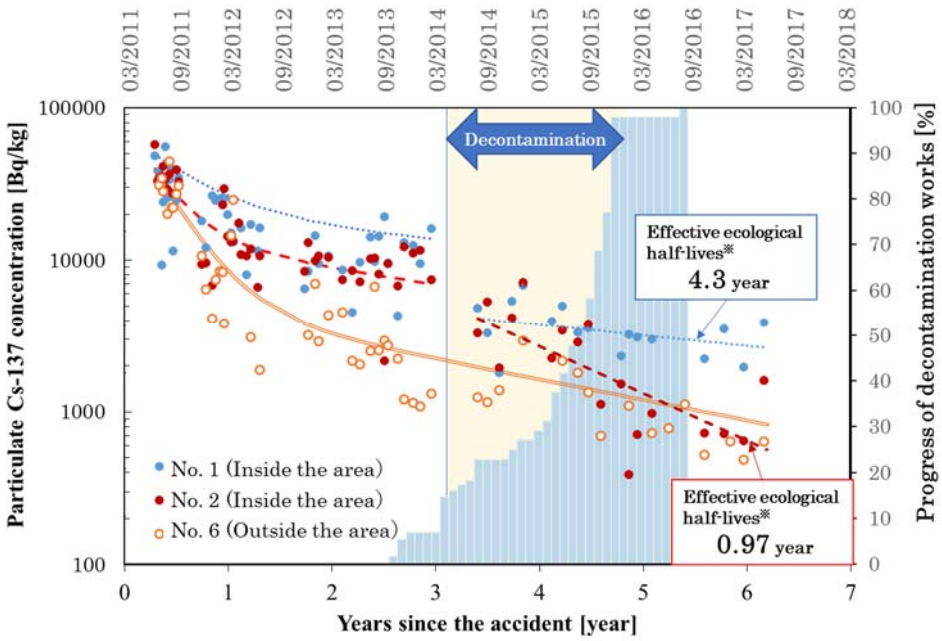

Figure 10: Suspended Cs-137 concentrations at the monitoring points in the special decontamination area (No.1 and 2) and outside the area (No. 6). The effective ecological half-lives are also shown[3].
Blue bars indicate the progression of the surface decontamination for farmlands after Apr. 2014.

1.4. Conclusions

We conducted continuous monitoring and applied the TODAM model to the Hirose River basin to investigate the dynamics of radiocaesium. The simulation was able to roughly reproduce the actual changes in radiocaesium at each monitoring point with the river flow. Further studies are needed to improve the prediction accuracy by continuous monitoring and the re-evaluation of the effects of high initial

radiocaesium amounts in the Oguni River basin.

The suspended radiocaesium concentrations showed decreasing trends over time in the Abukuma River systems and major rivers in the Hamadori area in the wide-area multipoint survey. In addition, it was shown the reduction of radiocaesium migration at points with watersheds including dams therein. Furthermore, effects of surface decontamination were detected at some monitoring points. Continuous monitoring and subsequent assessments are important owing to potential changes in radiocaesium concentrations in river waters in response to various processes, such as the recovery of vegetation and resumption of agricultural practices. Accordingly, we will continue to provide information for the safe and secure use of water by the residents in Fukushima Prefecture.

References

1) Smith, J.T., Voitsekhovitch, O. V., Konoplev, A. V., Kudelsky, A. V., 2005. Radioactivity in aquatic systems, in: Smith, J.T., Beresford, N.A. (Eds.), Chelnobyl - Catastrophe and Consequences. Praxis Pablishing, pp. 139–190.

2) The Nuclear Regulatory Agency (2015), Fiscal 2014 Project Report about Integration of Radioactive Material Distribution Data and Development of Migration Model Accompanying Disaster at Tokyo Electric Power's Fukushima Daiichi Nuclear Power Plant - Part 2 "Radiocaesium migration status survey on river water systems" at http://radioactivity.nsr.go.jp/ja/list/560/list-1.html

3) Pröhl, G., Ehlken, S., Fiedler, I. G. Kirchner, G. Klemt, E. Zibold G. (2006). Ecological half-lives of ^{90}Sr and ^{137}Cs in terrestrial and aquatic ecosystems, Journal of Environmental Radioactivity, 91(1–2), 41-72.

2. FIP2: Survey of radionuclide movement with wild life

Abstract

To understand radionuclide behavior in the ecosystem, Fukushima Prefecture is conducting survey and research on radionuclide migration in wild animals that are part of the ecosystem. Radiocaesium concentrations in wild animals will be measured to investigate changes with the passage of time and differences between species.

We also investigated the behaviors of wild animals because radionuclide behavior in wild animals is considered to be closely related to the behaviors of the animals.

2.1. Purpose

The accident at Tokyo Electric Power's Fukushima Daiichi Nuclear Power Plant caused wide-area environmental contamination with radioactive materials. Radionuclides were detected in many wild animals inhabiting the natural environment because they took radioactive materials from the natural environment through food.

Since 2011 immediately after the accident, Fukushima Prefecture has been monitoring radionuclide concentrations in the muscles of wild animals that are possibly hunted for consumption to contribute the safe and secure of prefectural residents. As a result, caesium-134 and caesium-137 were mainly detected in the muscles of wild animals as artificial gamma-ray emitting nuclides. However, there were not enough information as regards radiocaesium migration from the ecosystem to wild animals. This is why we started investigation and research into the dynamics of radiocaesium in the ecosystem to understand the implications for the lifting of restrictions, and make prefectural residents feel safe. The behaviors and food habits of wild animals are considered to have a close relationship with radiocaesium migration to those animals. However, much is still unknown about the ecology of wild animals, such as behaviors and dietary habits. In particular, almost no research has been carried out about the behaviors of wild animals in areas evacuated by residents because of the evacuation order. Therefore, we carried out a home range survey as part of a series of surveys to clarify the ecology of wild animals.

2.2. Content of implementation

We selected wild boars which inhabit wide areas of the prefecture as the main subjects of this research, because even studies assessing the impact of the Chernobyl disaster did not show any clear tendency of decrease in the time-series changes of radiocaesium taken into living things.

(1) Radionuclide dynamics in wild animals

A. Measurement of gamma-ray emitting radionuclide concentrations in wild animals

We measured gamma-ray emitting nuclides (wet weight) contained in the muscles of game species (wild boars, Asian black bear, copper pheasant, green pheasant, spot-billed duck, and mallard) captured by nuisance kill or by hunting. Figure 1 shows the measuring procedure. By using the measurement result, we investigated the dispersion of caesium-137 contained in the muscles of wild

boars and other animals between individuals, and the tendency of fluctuation with the passage of time after the accident. We also measured gamma-ray emitting radionuclide concentrations in stomach contents and of various organs in the same way to check radionuclide distributions in wild boars.

We checked the caesium-137 soil ground deposition at the capture points of target wild animals from their capture information, and analyzed relationships between caesium-137 soil ground deposition and caesium-137 concentration in muscle. As to the soil ground deposition, we used the results of UAV surveys carried out by the Japan Atomic Energy Agency.

Example of sample (Muscle) Cell U-8 Measurement of radionuclide concentration (Germanium semiconductor detector)

Figure 1: Measurement of radionuclides in wild animals.

B. Radionuclide migration from the environment into wild animals

To investigate the effect of foods on caesium-137 concentrations in the muscles of wild animals, we measured caesium-137 concentrations in the stomach contents of wild boars captured in Nihonmatsu City from fiscal 2013 to 2015. Then, we investigated relationships between caesium-137 concentrations in stomach contents and in the muscles of the same individuals.

C. Physicochemical fractions of radiocaesium in stomach contents

There are three physicochemical fractions of radiocaesium in soil (Figure 2). In the case of plants, they mainly absorb radiocaesium of exchangeable fractions. However, for plants, radiocaesium of strongly bound fraction like as strongly bound clay ores is difficult to absorb. In the case of wild boar, it is thought that they are considered to take in soil when eating foods or gaining minerals intentionally. Because of soil intake and the influence of physicochemical fractions of radiocaesium in soil, there is also possibility that caesium-137 concentration in the muscles of boars is higher than those in other wildlife. However, it is much remains unknown about amounts of absorption and migration of caesium-137 from soil and foods eaten by boar into their bodies.

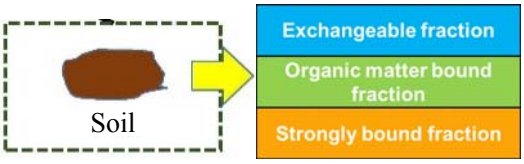

Figure 2: Physicochemical fractions of radiocaesium in soil.

Exchangeable fraction: Comparatively, easily to elute.
Organic matter bound fraction: Coupled with organic matter.
Strongly bound fraction: Exist in soil particle.

In this study, we focus on about concentrations and ratios of physicochemical fractions of caesium-137 in stomach contents, and research about relationships between physicochemical fractions of

caesium-137 in stomach contents and migration into their body.

The physicochemical fractions of radiocaesium is related to the absorption of the radiocaesium from soil to plants. Collaborate with the Institute of Environmental Radioactivity at Fukushima University, we are verifying the possibility that the physicochemical fractions of radiocaesium in stomach contents affects radiocaesium migration into wild boars.

(2) Investigating the home ranges of wild animals

We attached GPS data loggers (hereinafter, GPS collars) (Figure 3) to wild boars and investigated their behaviors. We set the GPS fix schedule of GPS collars as 1 GPS fix / 15 minutes, and recorded wild boar behaviors for more than one month. We investigated wild boar behaviors inside and outside the evacuation order zone (Figure 4).

Figure 3: GPS collar.

Figure 4: Attaching a GPS collar to an anethesized wild boar captured with the cooperation of a harmful bird and animal capture team.

2.3. Results

(1) Dynamics of radionuclides in wild animals

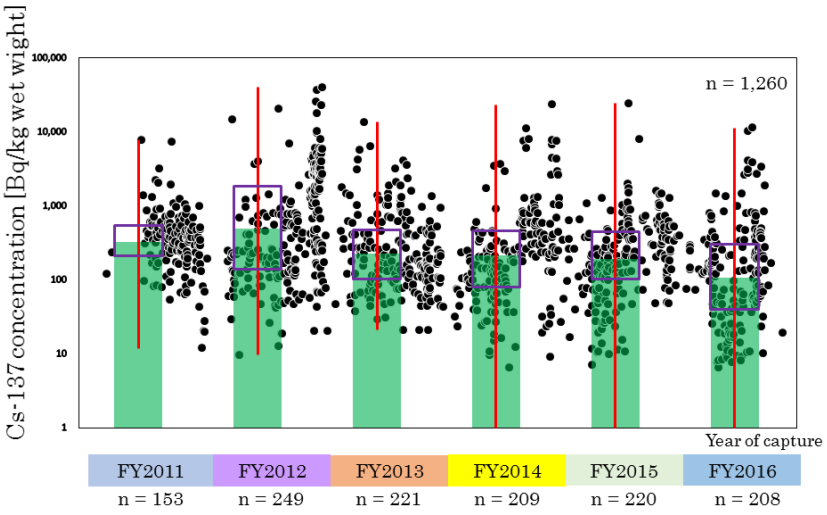

Figure 5: Results of monitoring caesium-137 concentration in wild boar muscles.
The X-axis indicates wild boar capture timing, and the Y-axis indicates logarithmically transformed caesium-137 concentration. The black dots indicate the measured values for individuals. The bar graph shows the geometric mean value of caesium-137 concentration in each year. Each box indicates the reliability section from 75% at the top and 25% at the bottom. The bars indicate the maximum and minimum values (Annual change: May 2011 to March 2017).

A. Results of measuring gamma-ray emitting radionuclide concentrations in wild animals

Figure 5 shows the caesium-137 concentration in the muscles of wild boars captured throughout Fukushima Prefecture from May 2011 until March 2017.

From figure 5, Any clear tendency was not shown because the dispersion between individuals was great.

For comparison with wild boars captured in Fukushima Prefecture, we investigated the annual changes of radiocaesium concentrations in wild boars captured in Europe after the Chernobyl disaster. Figure 6 shows the case of Regensburg in South Germany (Semizhon et al. 2009). Also in the case of Regensburg, caesium-137 concentration varied greatly between individuals and did not show any clear tendency of decrease. Since wild boars in Fukushima Prefecture also showed a similar tendency, we should monitor the contamination trends in wild boars captured in Fukushima Prefecture.

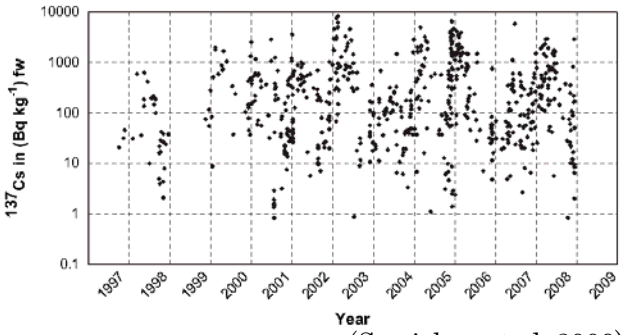

(Semizhon et al. 2009)

Figure 6: Temporal trends of caesium-137 in the muscle of boars (Regensburg, Southern Germany).

Figure 7 shows caesium-137 concentrations in the muscles of Asian black bears that inhabit the forest ecosystem like wild boars. In Asian black bears, caesium-137 concentrations decreased with the passage of years. This indicates that the annual change of caesium-137 concentration in muscles differs depending on the animal species.

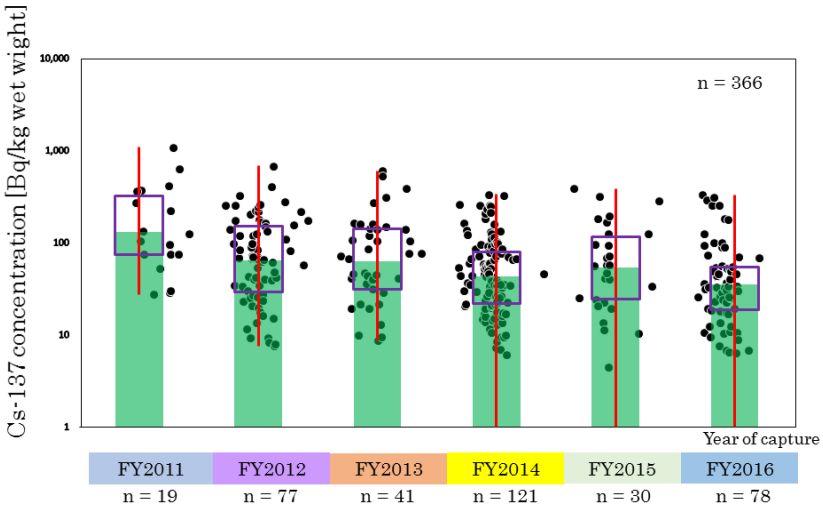

Figure 7: Results of monitoring caesium-137 concentration in Asian black bear muscles.
The X-axis indicates Asian black bear capture timing, and the Y-axis indicates logarithmically transformed caesium-137 concentration. The black dots indicate the measured values for individuals. The bar graph shows the geometric mean value of caesium-137 concentration in each year. Each box indicates the reliability section from 75% at the top and 25% at the bottom. The bars indicate the maximum and minimum values (Annual change: May 2011 to March 2017).

Figure 8 shows relationships between caesium-137 soil ground deposition at the wild boar and Asian black bear capture points, and caesium-137 concentrations in muscles. Both wild boars and Asian black bears showed positive relationships between caesium-137 soil ground deposition at the capture points and caesium-137 concentrations in muscles. Wild boars and Asian black bears captured at points of greater caesium-137 in-soil deposition amounts showed higher caesium-137 concentrations in muscles. From the regression line in the figure, wild boars showed higher concentrations in muscles than Asian black bears captured at points of the same soil ground deposition.

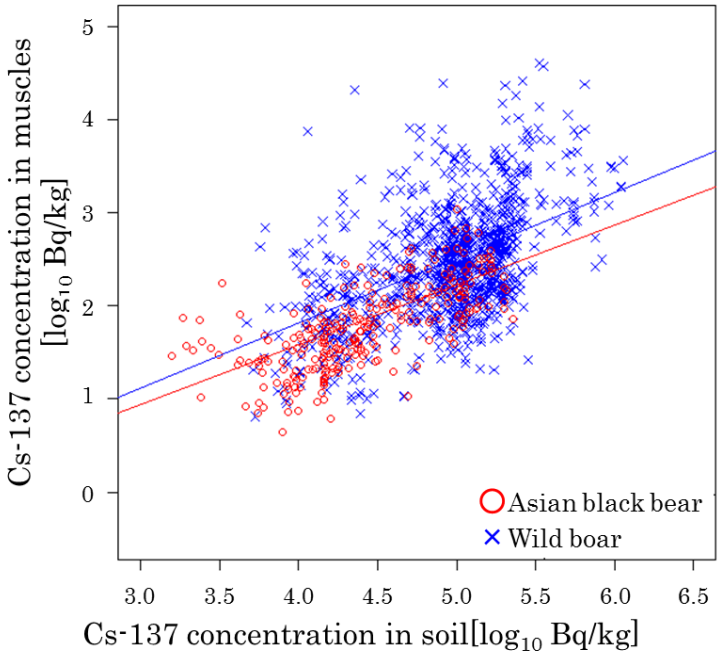

Figure 8: Relationships between caesium-137 concentrations in Asian black bear and wild boar muscles, and the amount of caesium-137 deposition to soil at the capture points.

Figure 9 shows wild boar and Asian black bear monitoring results by coloring depending on the area of capture. Individuals with high caesium-137 concentrations in muscles were frequently captured in the Hamadori region where the caesium-137 soil ground deposition is comparatively great. Individuals with low caesium-137 concentrations in muscles were frequently captured in the Aizu region where the caesium-137 soil ground deposition is comparatively small.

It has also been confirmed with birds that caesium-137 concentration in muscles differs between species.

Figure 10 shows caesium-137 concentrations in the muscles of copper pheasant, green pheasant, spot-billed duck, and mallard captured in the period from October 2011 until February 2017. Consider of the including of N.D. values, the caesium-137 concentration in muscles were higher in copper pheasant that is not a migratory bird and inhabits a forest ecosystem than in the other species.

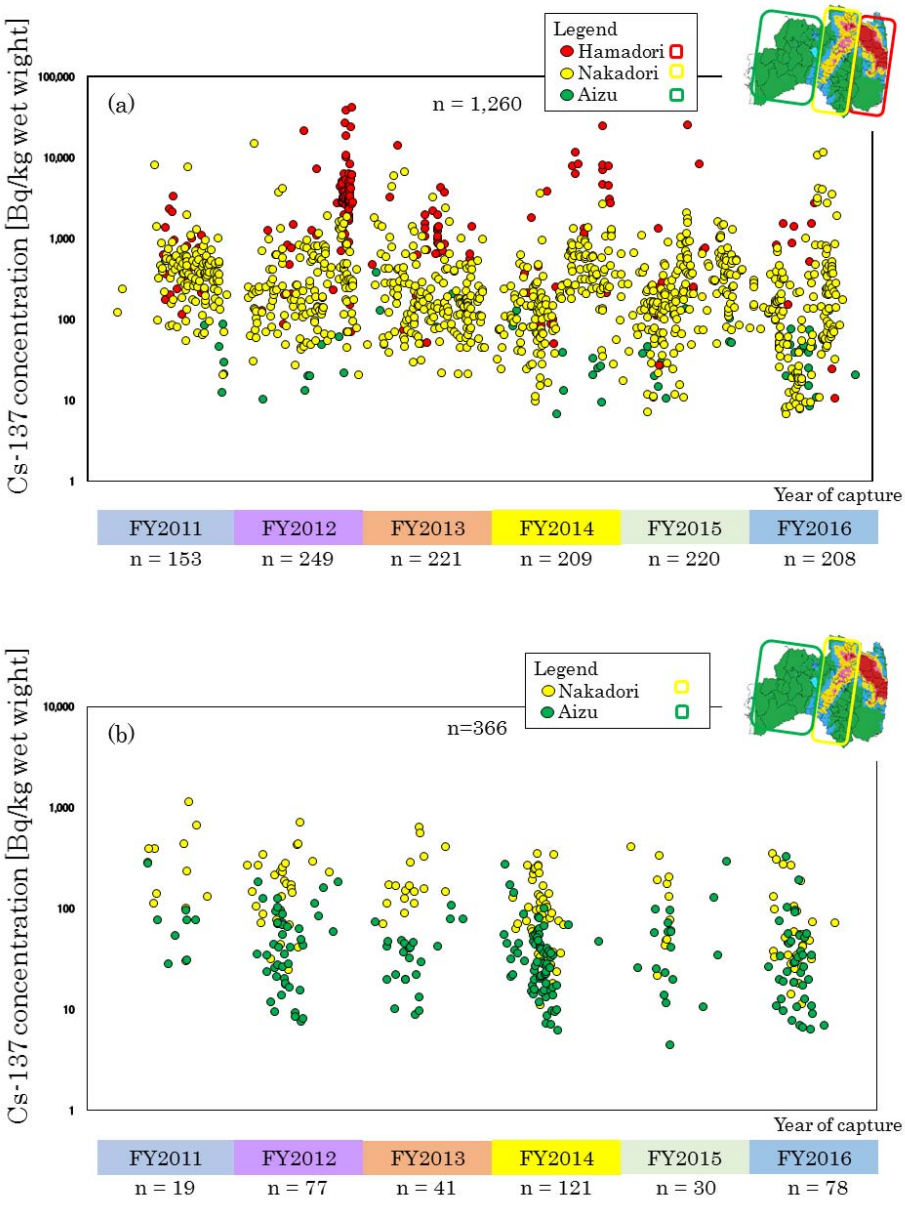

Figure 9: Monitoring results of caesium-137 concentration in the muscles of wild boars and Asian black bear (by the captured area).

The X-axis indicate the capture timing of wild boar and black bear and the Y-axis indicates logarithmically transformed caesium-137 concentration. The dots indicate the measured value for individuals that captured Hamadori (red dot), Nakadori (yellow dot), and Aizu (green dot).

(Annual change: May 2011 to March 2017)

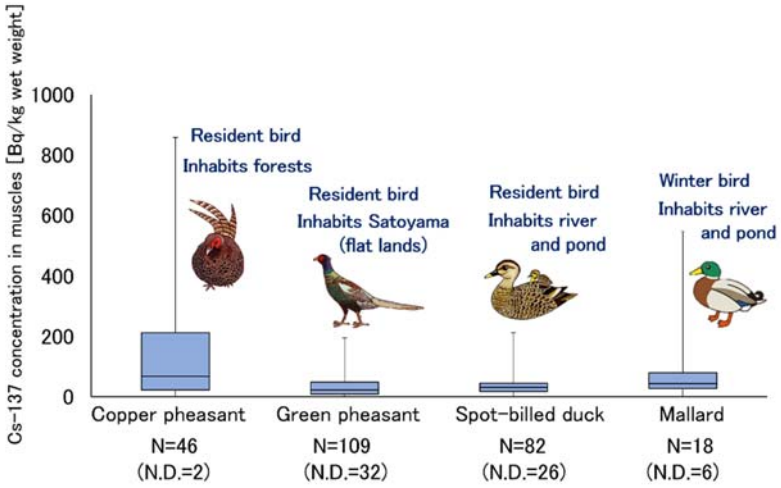

Figure 10: Results of monitoring caesium-137 concentration in muscle of copper pheasants, green pheasants, spot-billed duck, and mallard (Data period: October 2011 to February 2017). N.D., not detected

Figure 11 shows the temporal change of caesium-137 concentration in muscle about copper pheasant and green pheasant. Caesium-137 concentration in muscle decreased gradually in the green pheasant, but no clear trend was observed in the copper pheasant because of great dispersion between individuals like wild boars. The reason for the difference between species is probably because of difference of food habitat and/or the condition of the accumulation of radionuclides in their environmental habitat; copper pheasant mainly inhabits forests, while pheasant mainly inhabits the Satoyama ecosystem.

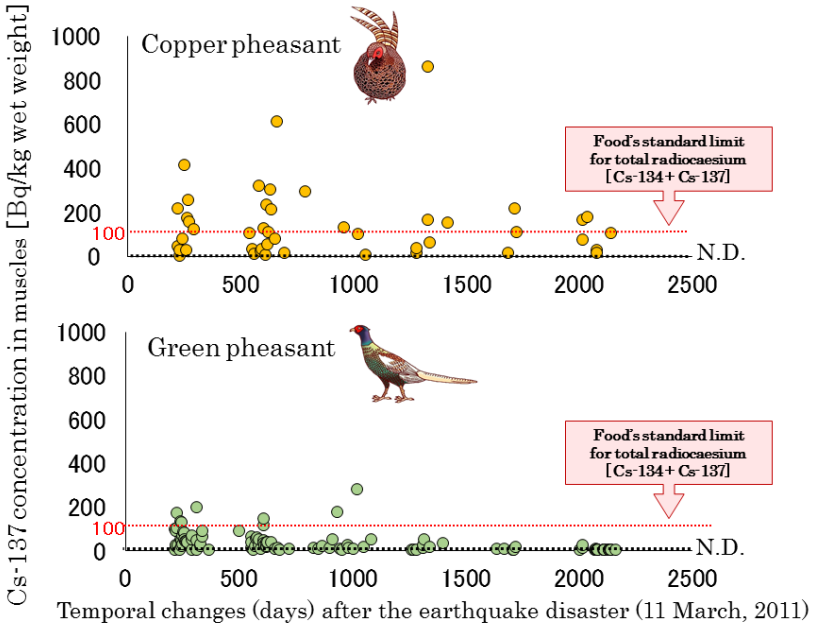

Figure 11: Changes caesium-137 concentrations in muscle of copper pheasant and green pheasant.

B. Radionuclide migration from the environment into wild animals

Figure 12 shows relationships between caesium-137 concentrations in the muscles and stomach contents of the same wild boars. The caesium-137 concentrations in the muscles and stomach contents showed positive relationships. These relationships indicate the strong effect of intake of caesium-137 such as food item and soil on caesium-137 concentrations in wild boars.

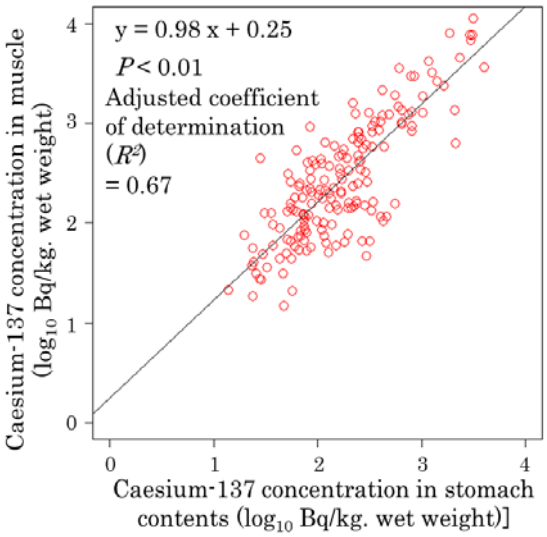

Figure 12: Relationship between caesium-137 concentration in muscle and in stomach contents of wild boar.

According to research on the impact of the Chernobyl disaster, caesium-137 concentrations in the muscles of wild animals vary with the seasons because of such biological factors as food habits and habitat use. Thus, we analyzed relationships between caesium-137 concentrations in the muscles of wild boars and Asian black bears, and the months in which the animals were captured. Figure 13 shows the results.

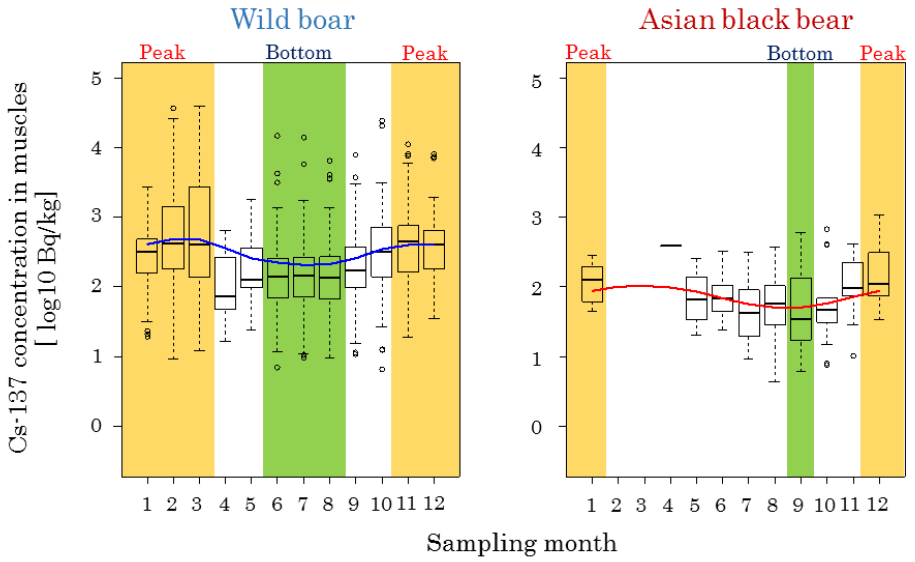

Figure 13: Seasonal variation of caesium-137 concentration in wild boar and Asian black bear muscles.

Both species of wild boar and Asian black bear showed seasonal variation of caesium-137 concentration in muscles. However, the variation pattern differs between the species. Caesium-137 concentrations in the muscles of wild boars were low in May to August, and high in November to March. Caesium-137 concentrations in the muscles of Asian black bears decreased from May to September, then increased until January.

C. Physicochemical fractions of radiocaesium contained in stomach contents

Figure 14 shows correlations between caesium-137 concentrations in muscles of wild boars captured in the prefecture in 2015, and caesium-137 concentrations of each fraction in stomach contents. Caesium-137 concentrations in muscles showed significant correlations with concentrations in exchangeable fractions, and concentrations summed of exchangeable fractions and organic matter-bound fractions in the stomach contents. However, caesium-137 concentrations in muscles did not show significant correlations with concentrations of strongly bound fractions. Therefore, there is a possibility that exchangeable fractions and organic matter-bound fractions contained in ingesting food item and soil are strongly related to caesium-137 migration into the bodies of wild boars.

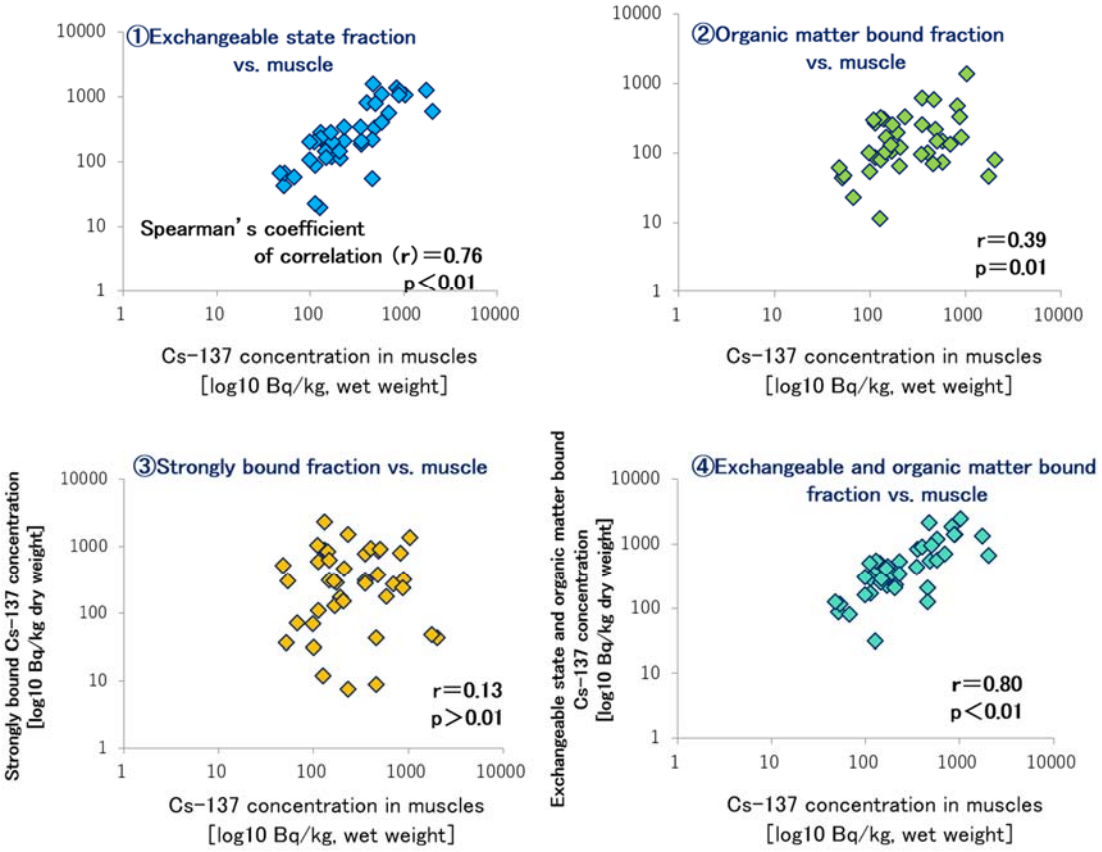

Figure 14: Correlations of caesium-137 concentration from fractions between wild boar muscles and stomach contents.

(2) Investigating the home ranges of wild animals

We tracked behaviors by using a GPS collar, and could define a home range as shown in Figure 15. The home range was separated into core area of high point concentration (area containing almost 95% of points by concentration analysis), and a roaming area containing all points (outermost area). This individual had two core area. The total area was about 37 ha and the home range area was 244 ha.

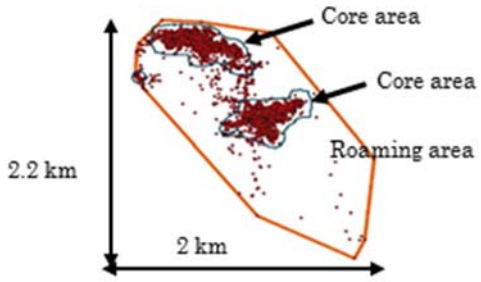

Figure 15: Example of sample structure of home range area.

We carried out wild boar home range surveys in Fukushima City and Tazawa, Iwashiro-chiku, Nihonmatsu City outside the evacuation order zone. Figure 16 shows the survey results on the samescale (one-kilometer mesh in the figure). Fukushima City has urban and suburban environments, while Tazawa, Iwashiro-chiku, Nihonmatsu City is located between plains and mountains. The wild boars surveyed on this occasion had core area of about 20 to 50 ha and home ranges of about 100 to 250 ha.

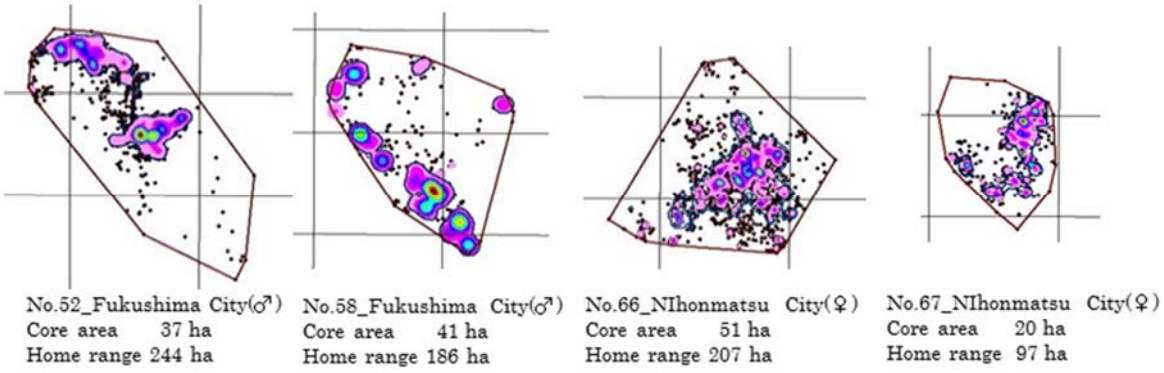

Figure 16: Size of wild boar home range outside the evacuation order zone.

We investigated wild boar home ranges in Tomioka-town, inside the evacuation order zone, to see how the ranges would change if human activities became weak. Figure 17 shows the core area and home range areas of individuals tracked inside and outside the evacuation order zone. No. 50, 85, and 208 are in the evacuation order zone. No. 52 and 58 are in an environment around cities without the evacuation order zone. No. 66 and 67 are in mountainous areas outside the evacuation order zone. They seem to be receiving damage control pressure. In the current survey, the number of samples is small and the sex, weight and duration of GPS collar attachment differ between individuals (Table 1). Therefore, human pressure increases seem to be reducing the home ranges.

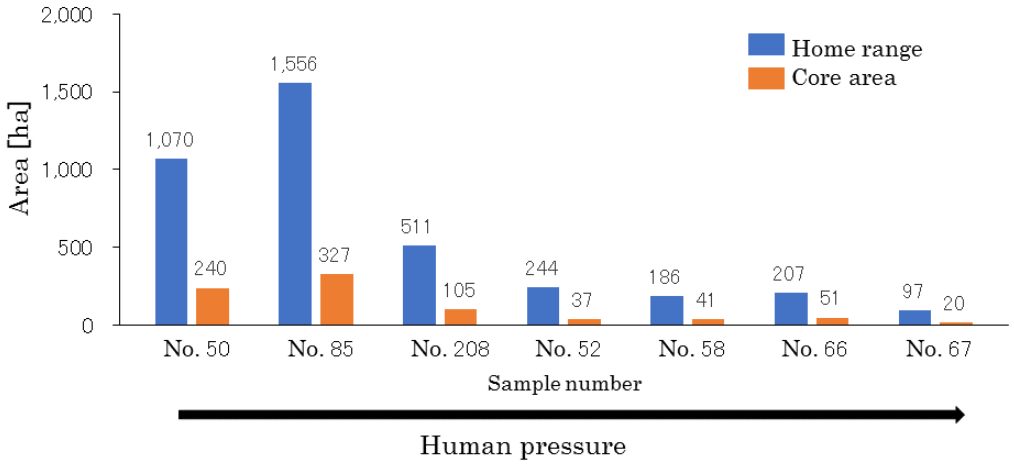

Figure 17: Comparison of home range and core area.

Table 1: Sexes, weights, and numbers of days with GPS collar

ID	No. 50	No. 85	No. 208	No. 52	No. 58	No. 66	No. 67
Sex	♂	♀	♀	♂	♂	♀	♀
Weight (kg)	37	48	51	44	70	35	37
Numbers of days with GPS collar	81	99	117	99	50	110	34

Wild boar home ranges may change depending on the timing of survey. Therefore, we compared the home range sizes of eight individuals whose data could be acquired for one month or longer in November to December (winter), and January to February (the breeding season). Although the number of samples was small, the home ranges tended to be larger inside the evacuation order zone than outside (Figure 18).

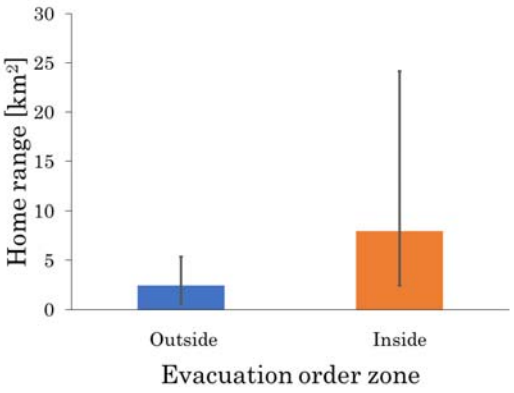

Figure 18: Average of home range size of wild boars inside and outside the evacuation zone. The error bars indicate the minimum and maximum values.

We investigated habitat type in the home ranges of individuals. In home ranges of individuals at inside the evacuation order zone, farmland occupied a high percentage. It suggested that the home ranges of individuals in inside the evacuation order zone tended to extend to farmland (Figure 19).

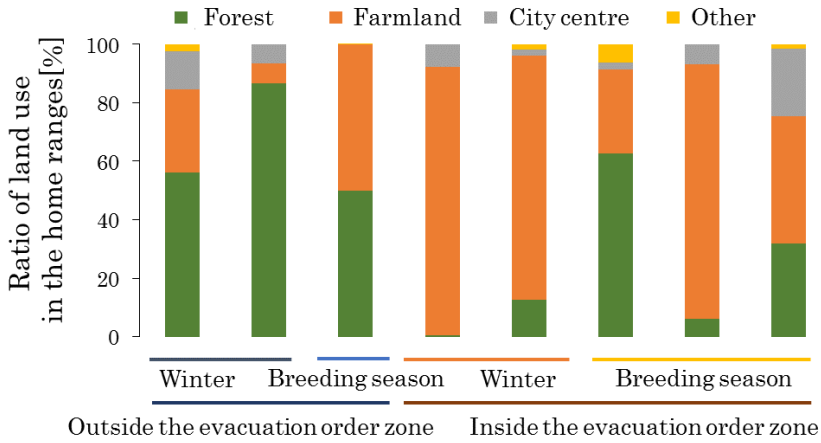

Figure 19: Ratio of land use in the home ranges of wild boars inside and outside the evacuation order zone (each bar indicates the value for an individual).

2.4. Conclusions

① When caesium-137 concentrations in the muscles of wild boars and Asian black bears were compared, wild boars showed higher concentrations. When copper pheasant and green pheasant were compared, copper pheasant showed high concentrations. The tendency differed between species.

② Caesium-137 concentrations in the muscles of wild boars were found to have been strongly affected by food habits. Both wild boars and Asian black bear showed high concentrations in winter although their variation patterns were different.

③ Compared with wild boars outside the evacuation order zone, individuals inhabiting inside the evacuation order zone tend to have larger home ranges and shifted to farmland.

From ① and ② above, food habits greatly affect caesium-137 migration from the environment to wild animals. In Europe, high radiocaesium concentrations in the muscles of wild boars is considered attributable to the foraging of Deer Truffle that is a kind of mushroom. However, the compositional analysis of wild boar stomach contents in Fukushima Prefecture has not yet shown any mushroom pieces. When a kind of wild mushroom called Koutake was fed to captured wild boars, some of the boars ate the mushroom, but not decisively. Since it is necessary to know the detailed food habits of wild boars in Fukushima Prefecture and cesium concentrations in foods, we started studying foraging behaviors by using GPS collars with cameras, and food habits by DNA analysis of wild boar stomach contents. We are also proceeding with the detailed analysis of the physicochemical fractions of caesium-137 in foods because they may affect caesium-137 absorption from foods into the body. We will conduct these investigations on animals of other species, particularly Asian black bears inhabiting the same forest ecosystem as wild boars, and compare the acquired data with those of wild boars. These investigations will clarify the mechanism of radiocaesium migration from the environment into wild animals. They will also clarify why caesium-137 concentrations are higher in the muscles of wild boars than in those of other wild animals, and why radiocaesium concentrations in muscles differ between species.

Wild boar home ranges showed the tendency of ③ above but the number of surveyed individuals was small. In addition to the above food habits survey, we are continuing the home range survey to know the

behavioral characteristics of wild boars in more detail. The findings and survey techniques regarding the behavior of wild boars obtained this time will be applied to ways of dealing with wild animals in evacuation order-lifted areas where residents have begun to return.

We will keep monitoring the transitions of radiocaesium concentrations in the bodies of wild boars and other animals to study the prediction of fluctuation tendency. As to some species showing in-muscle caesium-137 concentration decrease, we will study survey methods to discuss the lifting of shipping and intake restrictions.

3. FIP3: Countermeasures for radioactive materials in rivers and lakes

Abstract

We synthesised findings concerning the behaviour of and countermeasures against radiocaesium in rivers and lakes. We devised a decontamination measure for radiocaesium in riversides and verified its effectiveness and sustainability. In addition, we investigated the contamination state of public sites in Fukushima prefectural riversides and discussed suitable measures to address contamination.

3.1. Purpose

The Fukushima Daiichi Nuclear Power Plant (FDNPP) accident of Tokyo Electric Power Company emitted radioactive materials (particularly radiocaesium) into the environment. This disturbed the use and management of rivers and lakes and caused public anxiety. Governments and research institutions have monitored water, sediments, and fishery products, investigated the behaviour of radioactive materials, and devised countermeasures. In this project, we selected suitable countermeasures against radiocaesium in Fukushima Prefecture by organizing results obtained worldwide. We also performed a decontamination test at a riverside; this method has been not established previously, and accordingly we verified its effectiveness and sustainability. We investigated the contamination state of riverside parks in Fukushima Prefecture and discussed appropriate countermeasures.

3.2. Content of Implementation

(1) Selection of suitable measures against radiocaesium in Fukushima Prefecture

We organized suitable countermeasures against contamination in rivers and lakes after the Fukushima nuclear accident.

(2) Riverside decontamination and the sustainability of its effect

A. Purpose

Countermeasures against external exposure at riversides, particularly decontamination strategies, have not been established. Rivers are a major transport route for radiocaesium, and sediments with radiocaesium are frequently and heavily deposited onto riversides. Soil decontamination methods in farmland, forest, and residential areas are based on the assumption that radiocaesium is distributed within a depth of several centimeters, and thus these methods may be unsuitable for riversides. We tested a sediment removal method that considers the spatial distribution of radiocaesium in riversides and investigated the sustainability of the effect for 2 years after decontamination. The following results have been published, in part, by Nishikiori and Suzuki.[1)]

B. Methods

The test site was located 55 km northwest of FDNPP and at the lower part of the Kami-Oguni River (Figure 1a, 1b), a tributary of the Abukuma River (Figure 1a, 1b). The total deposition density of caesium-134 and caesium-137 was 300–600 kBq/m^2. Most of the watershed is covered with forests,

and agricultural land and residential land are found along the river (Figure 1b). The test site consisted of a river bank, which is approximately 170 in length and 2–6 m in width, and the total width of the river and banks was 15 m on average (Figures 1c, 1d). The left bank, right bank, and flood channel were used as a school route, an orchard, and a place for outdoor education, respectively. The school route on the left bank was decontaminated before this experiment.

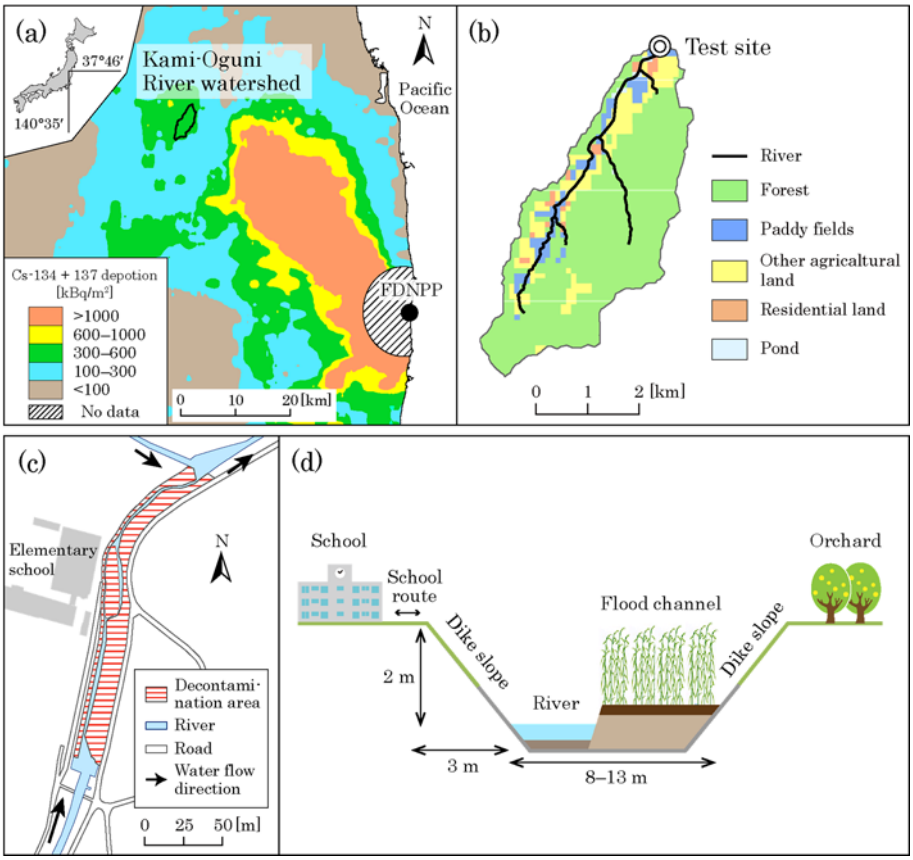

Figure 1: Outline of test site.
Radiocaesium deposition densities (decay correction date: July 2, 2011) were obtained from the third airborne monitoring survey data.[2)]

Figure 2 shows the test procedures. The air dose rates at a height of 1 m were measured using a NaI scintillation survey meter before decontamination and for 2 years after decontamination. Sediments in the flood channel and in the river bed were collected just before and for 2 years after decontamination. The radiocaesium concentration and weight of the mud fraction (silt and clay) were measured for sediment samples after gravel was removed.

Additional annual external exposure doses before and after decontamination were estimated by multiplying the time spent on the dikes and the flood channel and the average air dose rates at a height of 100 cm on the left dike and the flood channel. A value of 0.04 mSv/h measured before the accident[3)] was subtracted from the average air dose rates to account for natural background levels. The durations were 35 h per year for commuting (10 min per day, 210 days per year) and 24 h for outdoor education (2 h per day, 12 days per year).

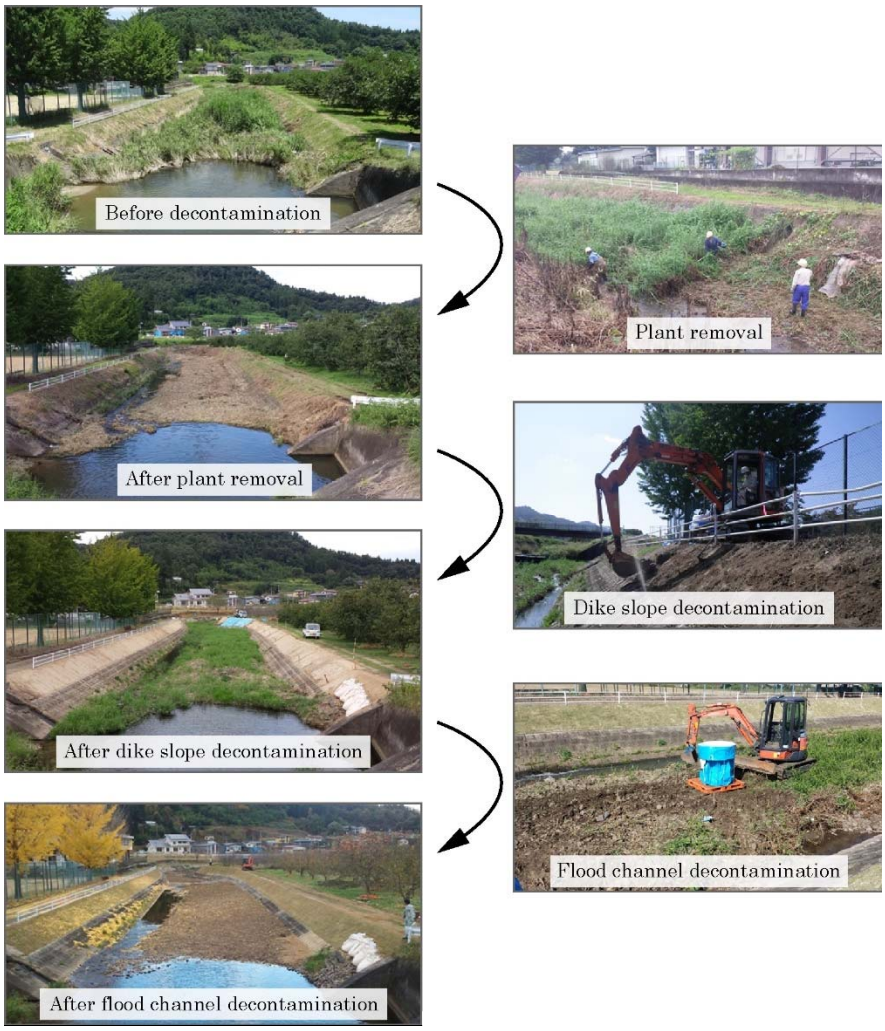

Figure 2: Photographs of the decontamination test procedures.

(3) Investigation of contamination in riverside parks and the selection of countermeasures

A. Purpose

As mentioned above, radiocaesium frequently accumulates on riversides via sediment deposition. The upstream areas of the coastal region in Fukushima Prefecture were heavily contaminated, and the downstream riversides are likely contaminated to a greater extent than the surrounding area. Therefore, we investigated the contamination condition of riverside parks in the coastal region and discuss countermeasures.

B. Methods

We investigated two downstream points along the Niida River in the coastal region (Figure 3). Park A is located along the main stream of the Niida River, and park B is located along the Mizunashi River, a tributary of the Niida River. A dam is located 5 km upstream of park B. The total deposition density of caesium-134 and caesium-137 was greater than 1000 kBq/m^2 in the upstream area but less than 100 kBq/m^2 in the most downstream area. The deposition densities were 490 and 210 kBq/m^2 in parks A and B, respectively.[4)] The area of parks A and B are 2.7 and 1.6 ha, respectively.

In August 2015, the air dose rate was measured 1 m above the ground using a portable gamma-ray-measuring device (Gamma Plotter H, Japan Radiation Engineering Co., Ltd.). A map of the air dose rate was generated using Restoration Support System for Environment software [RESET] (developed by the Japan Atomic Energy Agency).

Just after obtaining the measurements (6–11 September, 2015), an extreme flood inundated nearly half the area of the parks. According to data obtained at an AMeDAS meteorological station located 6 km southeast of park A, the total precipitation during the period was 385.5 mm.[5] The air dose rate was measured again on September 28, 2015. The external exposure doses for activities in the parks, such as recreation, walking, and maintaining flowerbeds, were also measured using a dose meter (DOSE e nano, Fuji Electric Co., Ltd.). The durations of the activities were assumed to be 36 h per year (park A, 12 h per year for recreation, 12 h per year for walking, and 12 h per year for maintaining flowerbeds; park B, 24 h per year for recreation and 12 h per year for walking). Soil was sampled to investigate the radiocaesium distribution in the parks.

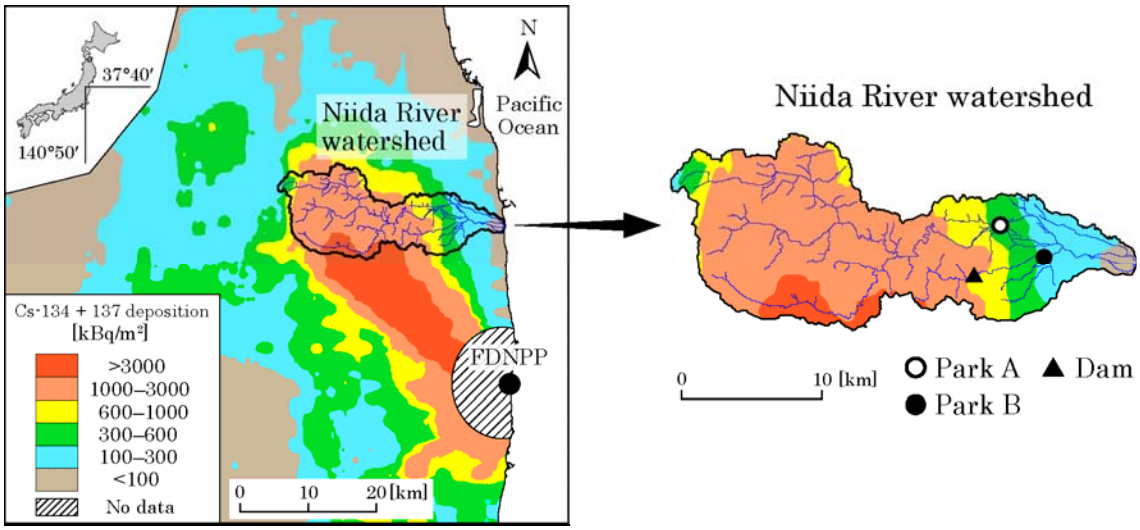

Figure 3: Location of study sites. Radiocaesium deposition densities.
(decay correction date: July 2, 2011) were obtained from the third airborne monitoring survey data.[2]

(4) Interview survey on issues related to the water environment and investigation of temporal trends

A. Purpose

Five years have passed since the FDNPP accident. To evaluate medium- and long-term countermeasures, it is necessary to understand the major issues related to the water environment in Fukushima Prefecture and their temporal trends. The aims of this study are were to clarify these issues by conducting interviews with parties interested in the water environment and to elucidate the temporal changes in the view of Fukushima prefectural residents regarding the safety of the water environment based on an annual public opinion survey.

B. Methods

We conducted interviews about issues related to radioactive materials in the water environment with Fukushima governmental staff involved in water use measures and synthesized these issues. A public opinion survey on prefectural policies is conducted every year by the Fukushima Prefecture government to investigate the awareness and needs of residents as a basis for policy on countermeasures.[6] We obtained the raw data from the survey for 2010 to 2015. In the public opinion survey, the following questions were used for the analysis: "Do you feel that your living environment is safe from environmental pollution including water and air pollution? (safety view on the water and air environments)" and "Is your living space secure from radiation? (low anxiety about radiation risks)". We analyzed temporal changes in the view of the safety of the water and air environments with respect to sex, age, and living region. We also investigated the relationship between the view of safety regarding the water and air environments and the low anxiety about radiation risks.

3.3. Results

(1) Selection of suitable measures against radiocaesium in Fukushima Prefecture

Issues and measures concerning the use of rivers and lakes were well organized in the guidelines established by concerned ministries[7),8)] and in a report concerning the Chernobyl accident.[9)] Table 1 briefly lists the main points.

Table 1: Issues and measures for specific purposes in rivers and lakes.

Issue	Related media	Measures
Internal exposure by drinking	Rivers and lakes	Changing water sources
Transfer from irrigation water to agricultural products and external exposure during farming	Rivers and lakes	Reducing sediment inflow using silt fences Sediment deposition in dams
	Irrigation ponds	Reducing sediment outflow using silt fences Decontamination of bottom sediment
	Agricultural products	Potassium fertilization to suppress uptake
Internal exposure by consuming fishery products	Rivers and lakes	Shipping restrictions Potassium input (effective only in closed lakes)
External exposure by using watersides (Parks, roads, residences, etc.)	Rivers and lakes	Use restriction and soil decontamination Removing riverbed sediments to reduce sediment deposition onto riversides Embankment for inundation control
	Irrigation ponds (at drainage)	Use restriction, decontamination, and covering of exposed bottom sediments
Common to all issues		Source decontamination and sediment discharge prevention Risk communication to reduce anxiety about use

(2) Riverside decontamination and the sustainability of its effect

Figure 4 shows the vertical distribution of radiocaesium concentrations in flood channel sediments before decontamination. The caesium-134 concentration was several kBq/kg because 3.5 years had passed since the FDNPP accident. However, at points 1 and 2, the caesium-137 concentration exceeded 10 kBq/kg, even at layers deeper than 10 cm. The layers had a high percentage of mud fraction (39% to 56%). Since radiocaesium has strong adsorption properties in clay and silt[10], radiocaesium in layers rich in mud are unlikely to migrate into underlying layers. Therefore, the high level of radiocaesium in the lower layer was likely caused by sediment deposition. In contrast, the radiocaesium concentrations were relatively low at points 3 to 5. We considered the heterogeneity in the vertical and horizontal radiocaesium distributions and adjusted the removal depth of the flood channel sediment to 15 to 35 cm. Since a similar depth distribution of radiocaesium has been reported for floodplains[11),12)], it is important to investigate the depth distribution prior to riverside decontamination.

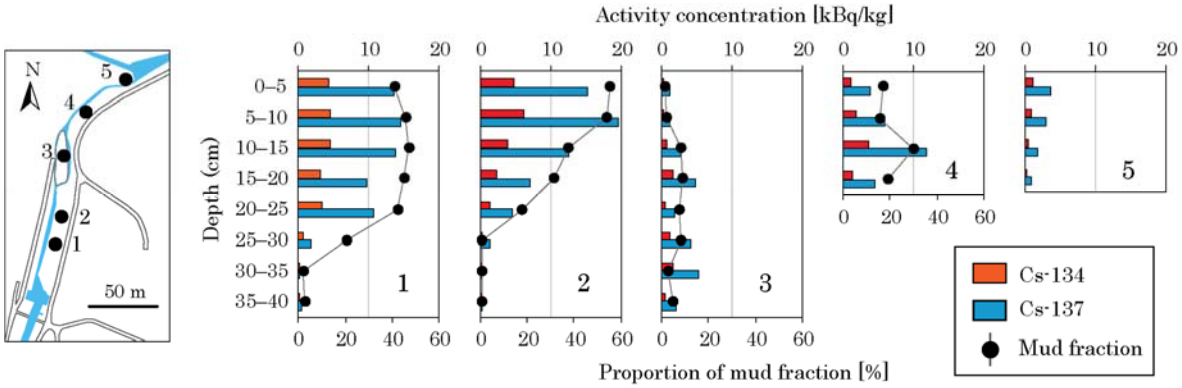

Figure 4: Vertical distribution of the radiocaesium concentration and the mud fraction in flood channel sediment.

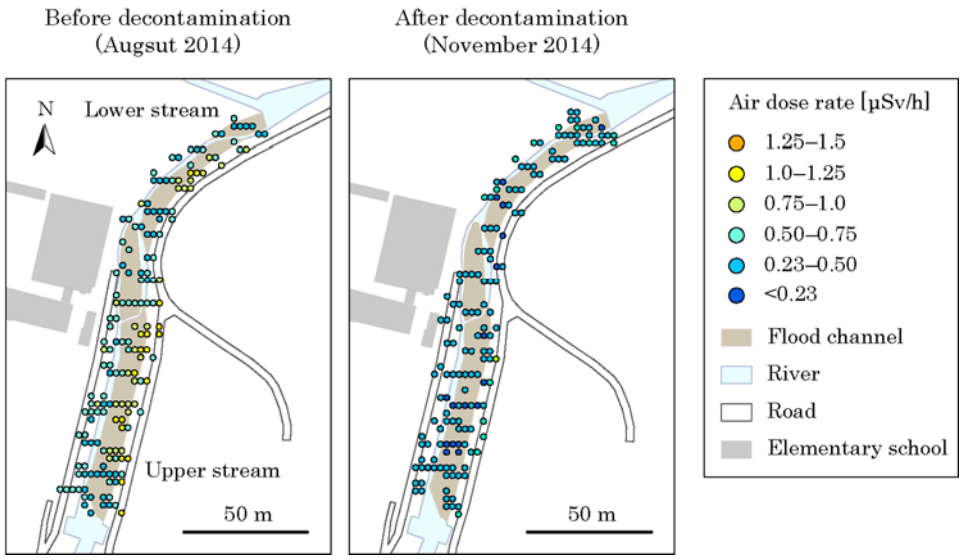

Figure 5: Maps of the air dose rate 1 m above the ground before and after decontamination.

Figure 5 shows the air dose rate distribution before and after decontamination. The mean dose rate 1 m aboveground was 0.66 μSv/h (standard deviation, 0.22 μSv/h) before decontamination. The value decreased by a factor of approximately two at the completion of decontamination to 0.34 μSv/h (standard deviation, 0.11 μSv/h), indicating that the method was effective.

Figure 6 shows the mean air dose rate for 2 years after decontamination. The values for the control area 20 m upstream from the decontaminated area are also given. Four rainfall events of ≥50 mm were observed at AMeDAS Yanagawa station, 9 km north of the test site[5)], during the 2-years period after decontamination, and accordingly the flood channel was likely inundated several times. However, the air dose rate gradually decreased, as in the control area. The caesium-137 concentrations in the top layer (a depth of 5 cm) of flood channel sediments were <3 kBq/kg at five points, shown in Figure 4. Thus, the decontamination effect was maintained. The plant community in the flood channel was removed after decontamination, and sediment deposition was likely difficult. It is necessary to investigate whether the decontamination effect is maintained, even when the the plant community regrows.

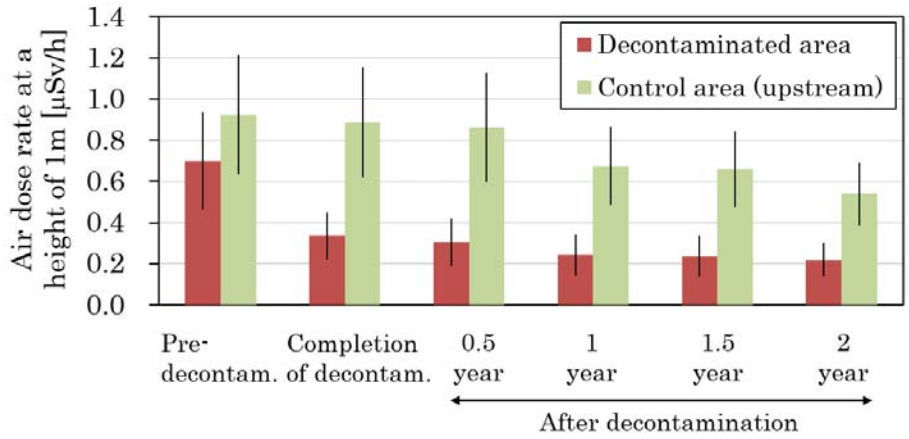

Figure 6. Temporal change in the air dose rate at 1 meter above the ground.
Results are presented as means and standard deviations.

The additional annual external exposure doses during commuting and outdoor education at the test site were estimated to be 0.029 and 0.016 mSv before and after decontamination, respectively. In Kami-Oguni and Shimo-Oguni Districts, similar to the area of our test watershed, annual external exposures doses were determined for daily life based on glass dosimeter measurements. The average additional external exposure during the period from July 2013 to June 2014 was 1.23 mSv.[13)] The dose during the activities at the test site (commuting and outdoor education) accounted for only 2.3% and 1.3% of the total value before and after decontamination, respectively. As described in 3.3.(4), some Fukushima Prefecture residents still feel anxiety about the water environment. Decontamination is one of the tangible measures described in Table 1. The effectiveness of intangible measures, such as risk communication, should also be examined.

(3) Investigation of contamination in riverside parks and the selection of countermeasures

Figure 7 shows maps of the air dose rate at 1 m above the ground in park A in August and September 2015 (before and after an extreme flood). Before the flood, a high air dose rate (≥1.0 μSv/h) was detected in the riverside and the northeastern area. After the flood, however, the air dose rate dropped to <1.0 μSv/h in these areas. In park B, there were no significant differences before and after the flood (Figure 8).

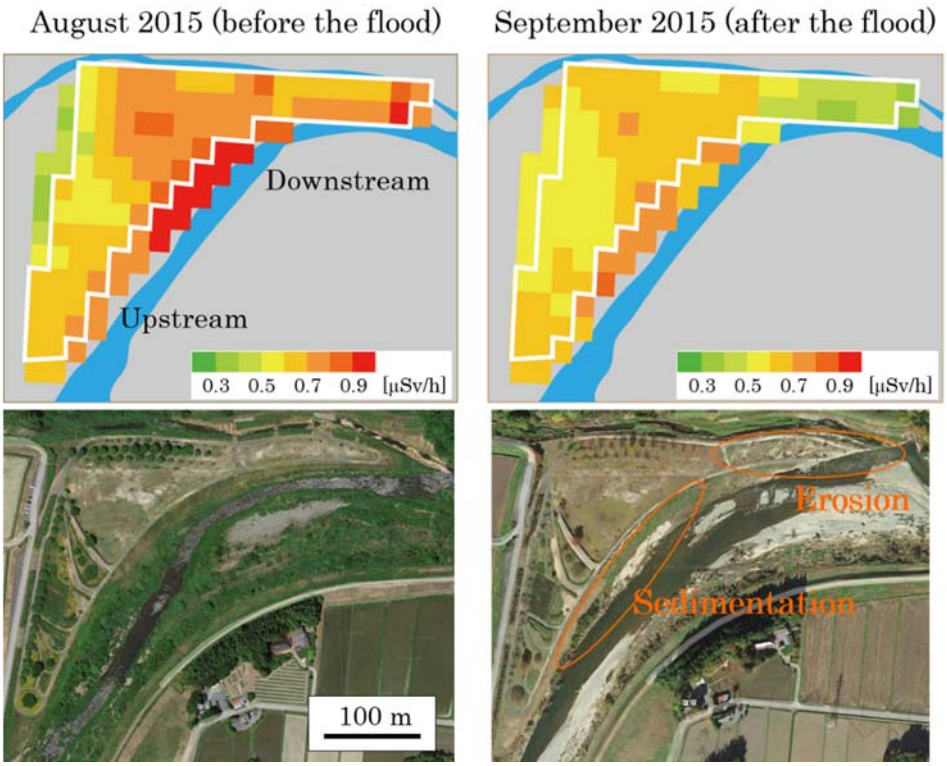

Figure 7: Map of the air dose rate at 1 m above the ground in park A. The park is area surrounded by a white line.

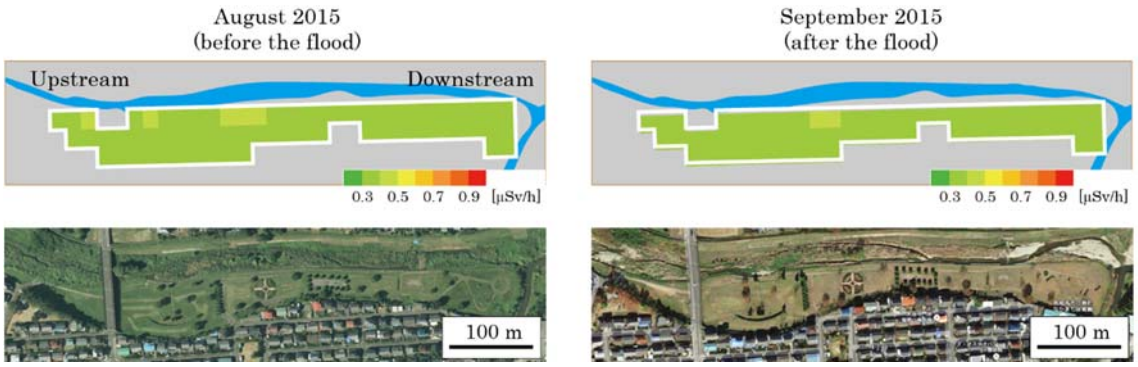

Figure 8: Map of the air dose rate at 1 m above the ground in park B. The park is area surrounded by a white line.

Figure 9 shows the radiocaesium inventory and concentration in the soil of park A. The total inventory to the sampled depth was 200 to 400 kBq/m^2 at the lawn and the flowerbed and was approximately 2400

kBq/m^2 at the riverside (i.e., approximately 10-fold greater than observed at the lawn and the flowerbed). The high air dose rate at the riverside before the flood likely reflected this radiocaesium distribution. For the caesium-137 vertical distribution, the concentration was high only at a depth of several centimeters at the lawn, and it was low and uniform to a depth of 15 cm at the flowerbed due to tilling. At the riverside, the concentration was low to a depth of 25 to 30 cm, and the peak was observed at depth of about 40 to 50 cm. When observing the soil profile at point 3, the color and particle size of the sediment clearly changed at a depth of around 30 cm. Thus, the upper 30 cm of the sediment was likely deposited during the flood in September 2015. The drop in the air dose rate after the flood probably reflected this deposition of sediment with the low concentration and erosion at the northeastern part of the park (Figure 7). In the Niida River watershed, it was reported that this extreme flood caused severe erosion in the upstream area and the deposition of sediment with a low concentration in the downstream area, leading to natural decontamination.[14] Our study results in park A are consistent with this.

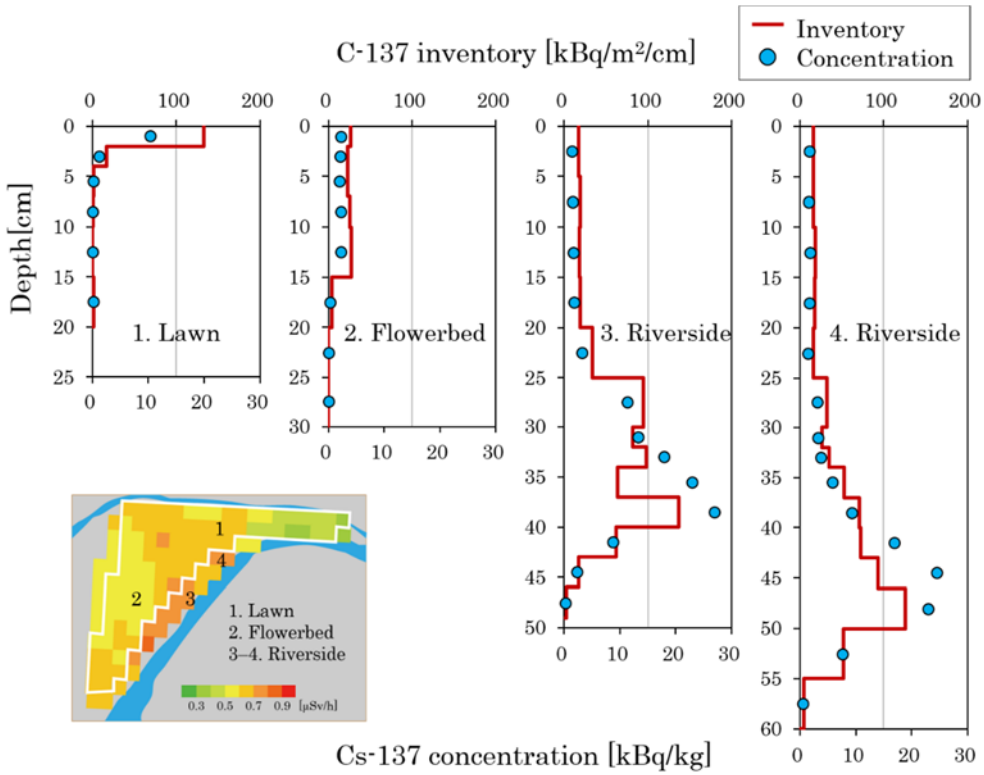

Figure 9: Vertical distribution of radiocaesium in the soil in park A. Samples were collected after the extreme flood in September 2015.

In park B, the total inventory of caesium-137 was in the same range (130 to 220 kBq/m^2) in areas affected and unaffected by the extreme flood. Most caesium-137 was retained in the surface layers (Figure 10). This state shows little sediment deposition, and therefore shows no significant changes in the air dose rate after the flood. The difference in sediment deposition and caesium-137 accumulation in these parks may be explained as follows. First, the riverside of park B was lawn, whereas that of park A was covered with a plant community with a height of around 1 m. The plant community may favor sediment deposition. Second, a dam in the upstream area of park B likely catches sediments and reduces

the sediment supply to the park. Third, sediment with a high radiocaesium concentration is unlikely to be transferred to park B because a heavily contaminated area (≥1000 kBq/m^2) is located in the upstream area of the dam (Figure 3).

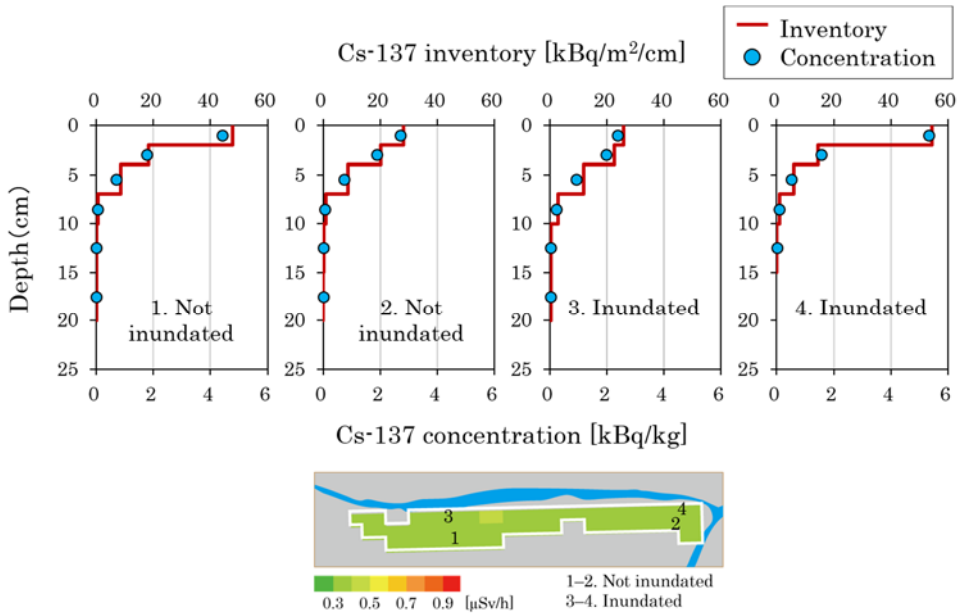

Figure 10: Vertical distribution of radiocaesium in the soil in park B. Samples were collected after the extreme flood in September 2015.

Additional annual external exposure doses during activities in parks A and B were estimated to be 0.018 mSv and 0.009 mSv, respectively. In the administrative district where the parks are located, external exposure was determined for daily life based on glass dosimeter measurements. The additional annual external exposure dose was 0.44 mSv (for a 3-month measurement period from July to September 2015, the value quadrupled).[15] The dose during the activities in the parks accounted for 2% to 4% of the total value. Therefore, effect of decontamination on exposure reduction in the parks is limited. Considering the results obtained for the Kami-Oguni River, time spent at the riverside is usually limited, and natural decontamination occasionally occurs. Tangible countermeasures, such as decontamination, are not necessarily suitable for the riverside. However, radiocaesium occasionally accumulates during small- and medium-scale floods in riversides, where sediments are easily deposited and the upstream area is heavily contaminated. The air dose rate may increase in these riversides. Therefore, to effectively mitigate anxiety, continued monitoring and predictions of the contamination state may be useful in the future.

(4) Interview survey on issues related to the water environment and investigation of temporal trends

The Fukushima Prefecture government indicated the following issues related to radioactive materials in the water environment 5 years after the FDNPP accident:

- interference with activities perforemed before the accident;
- impact of radioactive materials on the future; and

- continuation of countermeasures.

We found that the recovery of the view of residents regarding the safety of the water and air environments differed among regions, based on the public opinion survey results. The recovery was slower in the Nakadori (central) and Hamadori (coastal) regions than in the Aizu (eastern) region (Figure 11). The safety view was significantly associated with the perception of radiation risk.

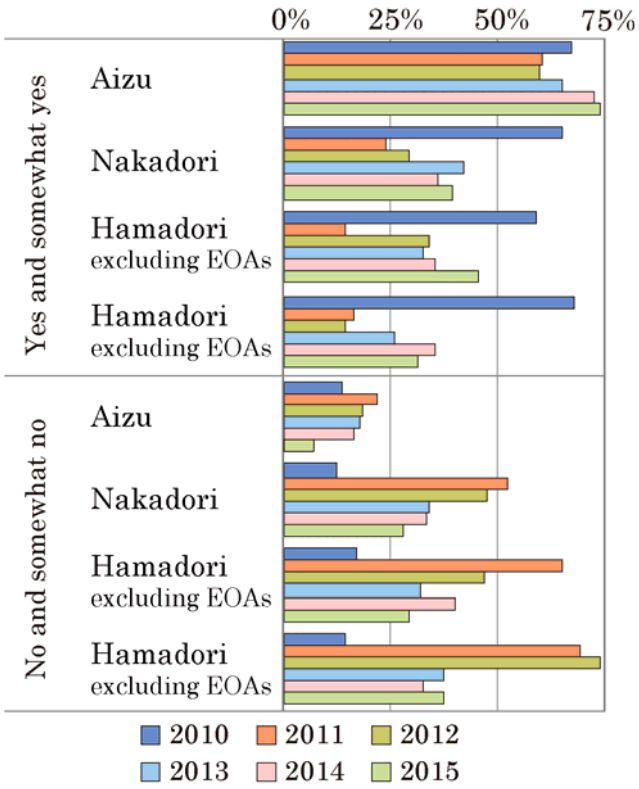

Figure 11: Temporal changes in the response to the question "Do you feel that your living environment is safe from environmental pollution including water and air pollution?". EOAs represents evacuation order areas.

3.4. Conclusions

In this project, we selected suitable countermeasures against radiocaesium in freshwater systems in Fukushima Prefecture by reviewing findings obtained worldwide. We also performed a decontamination test at a riverside, accounting for the spatial distribution of radiocaesium, and verified its effectiveness. Although radiocaesium sometimes accumulates in downstream riversides, extreme floods act as natural decontamination process. In addition, external exposure at riversides is limited. However, residents in heavily contaminated regions (e.g., the Hamadori region, including evacuation areas) have persistent anxiety regarding the water environment. For addressing anxiety, it is necessary to clarify the factors that determine anxiety and discuss appropriate solutions.

Information about the main results of this project has been provided to relevant divisions of the Fukushima Prefectural Government, and the riverside decontamination technique may be a general river improvement strategy, as evidenced by the study results.

References

1) Nishikiori, T., Suzuki, S. (2017) Radiocesium decontamination of a riverside in Fukushima, Japan. Journal of Environmental Radioactivity, 177, 58-64.

2) Ministry of Education, Culture, Sports, Science and Technology (2011) Results of deposition of radioactive cesium of the third airborne monitoring survey. http://emdb.jaea.go.jp/emdb/portals/b224/

3) Minato, S. (2006) Distribution of terrestrial γ ray dose rates in Japan. Journal of Geography, 115 (1), 87-95.

4) Nuclear Regulation Authority (2017) Extension site of distribution map of radiation dose. http://ramap.jmc.or.jp/map/

5) Japan Meteorological Agency (2017) Data and Material. http://www.jma.go.jp/jma/menu/menureport.html.

6) Fukushima Prefectural Government (2017) Fukushima Prefectural Public Opinion Survey. https://www.pref.fukushima.lg.jp/sec/01010e/koucho1-439.html.

7) Ministry of the Environment, Government of Japan (2014) Decontamination Guidelines, second ed. https://josen.env.go.jp/material/

8) Ministry of Agriculture, Forestry and Fisheries (2015) Manual of countermeasure techniques against radioactive materials in irrigation ponds.

9) IAEA (2006) Environmental consequences of the Chernobyl accident and their remediation: Twenty years of experience report of the Chernobyl forum expert group ‘environment’. Vienna.

10) Nakao, A., Funakawa, S., Tsukada, H., Kosaki, T. (2012) The fate of caesium-137 in a soil environment controlled by immobilization on clay minerals. SANSAI Environ. An Environmental Journal for the Global Community, 6, 17-29.

11) Tanaka, K., Kondo, H., Sakaguchi, A., Takahashi, Y. (2015) Cumulative history recorded in the depth distribution of radiocesium in sediments deposited on a sandbar. Journal of Environmental Radioactivity, 150, 213-219.

12) Konoplev A., Golosov V., Wakiyama Y., Takase T., Yoschenko V., Yoshihara T., Parenyuk O., Cresswell A., Ivanov M., Carradine M., Nanba K., Onda Y. (in press) Natural attenuation of Fukushima-derived radiocesium in soils due to its vertical and lateral migration. Journal of Environmental Radioactivity. doi:10.1016/j.jenvrad.2017.06.019.

13) Date City (2015) Reconstruction and recovery news at Date City, 22, 1-4. http://www.city.date.fukushima.jp/soshiki/12/763.html

14) Konoplev, A., Golosov, V., Laptev, G., Nanba, K., Onda, Y., Takase, T., Wakiyama Y., Yoshimura, K. (2016) Behavior of accidentally released radiocesium in soil–water environment: Looking at Fukushima from a Chernobyl perspective. Journal of environmental radioactivity, 151, 568-578.

15) Minami-Soma City (2016) Result of second measurement of individual cumulative dose in 2015 (July to September 2015). http://www.city.minamisoma.lg.jp/index.cfm/10,28438,61,367,html.

4. FIP4: Developing of environmental mapping technology using GPS walking surveys

Abstract

Fukushima Prefecture developed environmental mapping technology with GPS walking surveys as a tool for surveying the regional distribution of air dose rates.

This report covers the results of parameter verification necessary for the development of this technology and the history of development.

4.1. Purpose

To understand the air dose rate (hereinafter simply referred to as the dose rate) in Fukushima Prefecture after the accident at the Fukushima Daiichi Nuclear Power Plant, we have conducted fixed-point measurements with monitoring posts and dose rate measurements in car-borne surveys using the GPS-linked dose rate measurement device KURAMA (Kyoto University RAdiation MApping System), and have provided information to prefecture residents on the prefecture homepage (Figure 1 and 2).

Figure 1: Example of current monitoring.
(a): Example of a fixed-point measurement(using a real-time dose-rate measurement system)
(b): Example of a car-borne survey (KURAMA-II installed on the back of a local bus)

Figure 2: Fukushima Prefecture radiation measurement map.
(http://fukushima-radioactivity.jp/pc/)
(a): Example of a fixed-point measurement
(b): Example of a traveling survey

As of March 2016, measurements are being made at 3500 fixed points with monitoring posts in Fukushima Prefecture. Car-borne surveys using local buses are also being conducted with the purpose of interpolating the fixed-point measurements.

It is, however, difficult to conduct fixed-point measurements or car-borne surveys in some places, including parks, forests, and alleys near residential areas, and dose rates sometimes differ between fixed measuring points at the same facility or site (Figure 3). For these reasons, in addition to fixed-point measurements and car-borne surveys, we require measurement technology with which to grasp a more detailed distribution of dose rates, and we need to present the measurement results in a format that is easy to understand.

Therefore, to employ interpolation to obtain dose rates for parks, forests, and alleys near residential areas where fixed-point measurements and car-borne surveys are difficult, we developed environmental mapping technology using GPS walking surveys together with unmanned aerial vehicles (UAVs) developed by the IAEA.

The prefecture and IAEA have shared the development of environmental mapping technology with GPS walking surveys (FIP4) and environmental mapping technology with unmanned aerial vehicles (FCP3), and by combining these technologies and visualizing measurement results, we were able to create dose distribution maps that are more detailed and effective.

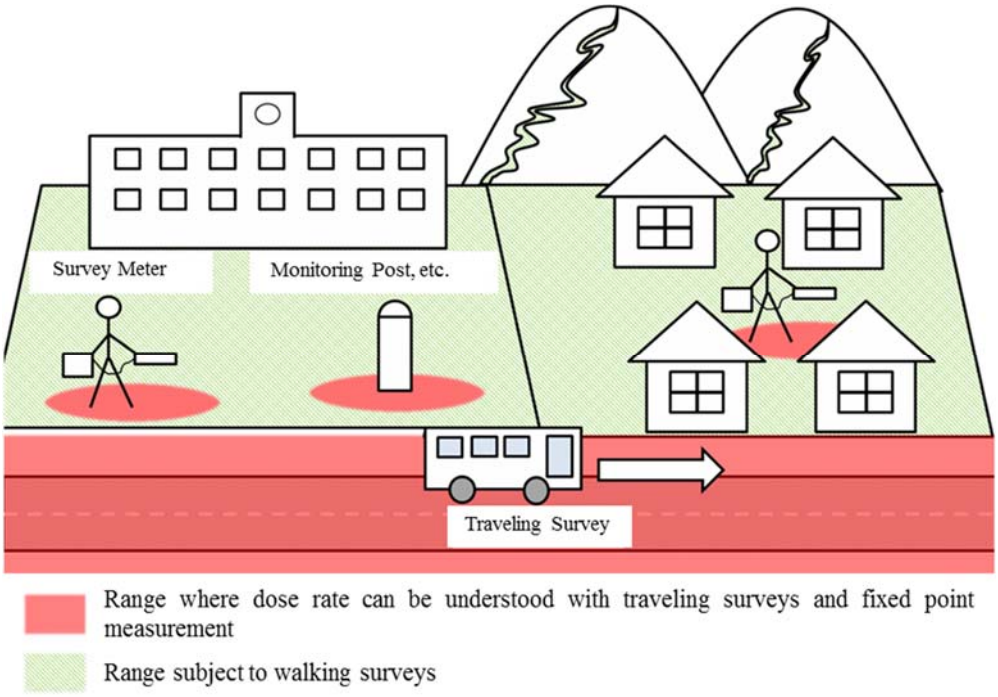

Figure 3: Measurement ranges of conventional measurement methods.

4.2. Content of implementation

(1) Development of equipment

We used the KURAMA-II, which was developed by Kyoto University, for walking surveys, and assembled five pieces of equipment in a way suited to walking surveys (Figure 4). The orange backpack contains a CsI (T1) scintillation detector, which is a low-dose-rate detector, and a high-

precision GPS unit. The back packer measures the dose rate by walking on a transverse course while merging dose rate data from the low-dose CsI detector and position information from the high-precision GPS device.

Figure 4: Walking survey equipment.
(a): Appearance of the devices
(b): Low-dose-rate CsI detector (Hamamatsu Photonics K.K. C12137-01) and high-precision GPS unit (SOKKIA GIR1600)

The measurement screen is shown in Figure 5. The measurement interval may be selected as 3 seconds, 5 seconds, and so on. At the start of the measurement, information such as the current position and dose rate are recorded to a notebook computer, and the position information, dose rate, trends, and mapping results are displayed on the computer screen.

Measurers can look at the screen to check the measurement position and dose rate while conducting detailed measurements.

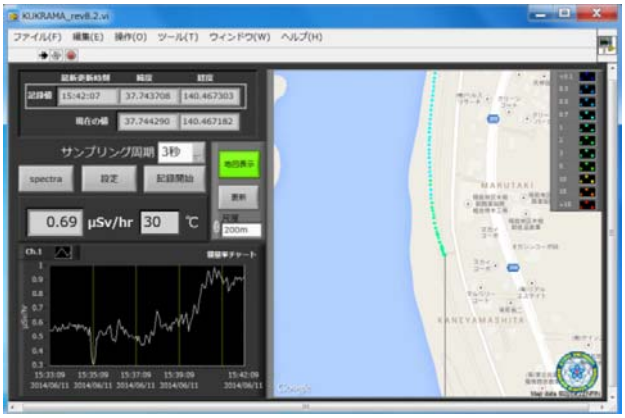

Figure 5: Display screen on a personal computer.

(2) Development of mapping technology using Geographic Information System (GIS)

We conducted a specification study and developed a GIS tool for capturing, combining, and mapping the dose rate and position information gained from walking surveys and UAVs. An overview of the tool is shown in Figure 6.

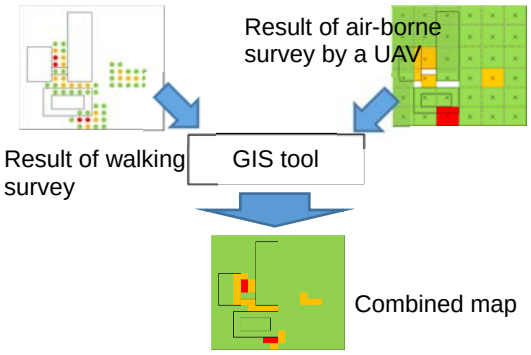

Figure 6: Overview of the GIS tool.

	年月日	時間	緯度	経度	標高	速度	方位	線量率	補正線量率	検出器温度
2	2013/12/12	13:58:19	37.476833	140.857184	27.2	0.7	202.37	1.9		10.37
3	2013/12/12	13:58:22	37.476829	140.85771	27.1	0.4	213.87	1.85		10.37
4	2013/12/12	13:58:25	37.476831	140.857181	26.9	0.5	341.95	1.82		10.37
5	2013/12/12	13:58:28	37.476828	140.857186	27.2	4.4	148.06	1.93		10.37
6	2013/12/12	13:58:31	37.476825	140.857184	27.3	6	182.24	2.09		10.37
7	2013/12/12	13:58:34	37.476824	140.85781	28.1	3.2	52.5	2.1		10.37
8	2013/12/12	13:58:37	37.476825	140.857241	28.2	6.9	111.9	2.48		10.37
9	2013/12/12	13:58:40	37.476828	140.857289	28.3	8.2	125.81	2.55		10.38
10	2013/12/12	13:58:43	37.476785	140.857283	28.2	8.4	168.08	2.67		10.38
11	2013/12/12	13:58:46	37.476758	140.857284	28.3	8.7	155.82	2.75		10.38
12	2013/12/12	13:58:49	37.476735	140.857319	28.2	8.4	112.81	2.9		10.38
13	2013/12/12	13:58:52	37.476717	140.857348	28.2	7.5	132.18	2.7		10.38
14	2013/12/12	13:58:55	37.4767	140.857374	28.1	8.4	133.22	2.68		10.38
15	2013/12/12	13:58:58	37.476684	140.857384	28.2	7	130.08	2.92		10.38
16	2013/12/12	13:59:01	37.476682	140.857384	28.2	0.2	222.58	2.13		10.38

Figure 7: Data including the dose rate.

It is possible to produce a contour map using the GIS tool. Data in comma-separated-value format recorded in walking surveys are converted to Microsoft Excel file format (Figure 7), and point data with dose rate information are created from the latitudinal and longitudinal information contained in the data (Figure 8). With the GIS tool, it is possible to estimate the dose rate at unmeasured positions and to produce contour maps from the point data created using any interpolation algorithm, such as Inverse Distance Weighting (IDW) algorithm (Figure 9).

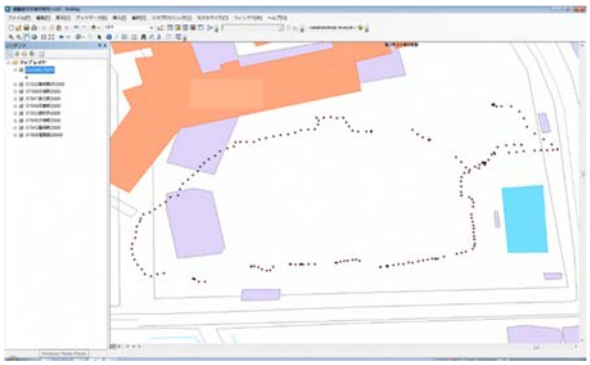

Figure 8: Map data and dose rate plotting.

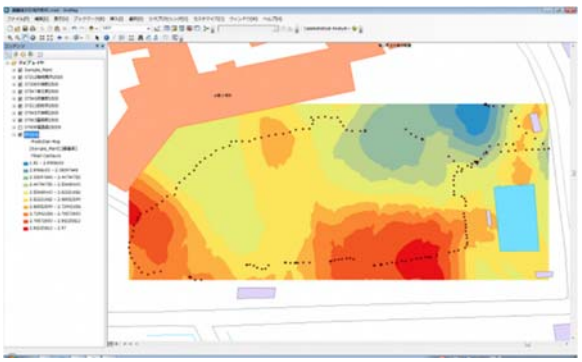

Figure 9: Interpolated dose map.

(3) Walking survey implementation

We collected parameters necessary for walking surveys, and carried out the survey in several areas.

(4) Manual preparation

We created a manual surveying the walking survey method. Photos and sentences are combined in this manual for easy understanding.

4.3. Results

(1) Gathering parameters necessary for walking surveys

We conducted a field test of walking surveys, and gathered data for evaluation and analysis (Figure 10). Data were gathered to check the direction characteristics and appropriate measurement density, as well as to determine correction factors.

Figure 10: View of a walking survey.

A. Checking direction characteristics

Shielding from the measurers themselves affects the contribution from the radiation source depending on the walking direction in walking surveys (Figure 11). Walking surveys were therefore conducted by changing the walking speed and by walking back and forth so as to straddle the radiation source and check the effect of direction characteristics.

As a result, while shifts occurred in places where peaks appeared, they fell within a range of about 2 meters, and measurements showed that the maximum value of the dose rate was nearly the same during forward and reverse passes (Figure 12). We also confirmed that reducing the walking speed caused the peaks of the dose rate distribution to grow sharply (Figures 13 and 14).

Judging from the above result, the impact of directional characteristics on a measured value of a walk survey was considered small at a constant walking speed.

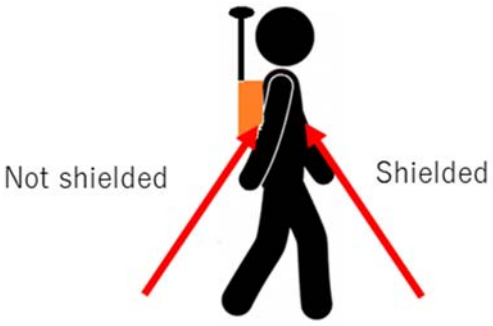

Figure 11: Measurement of direction characteristics.

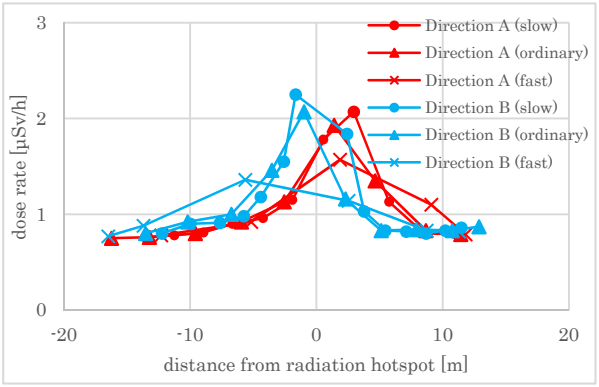

Figure 12: Measurements after changing speed and direction.

Figure 13: Change in walking speed.

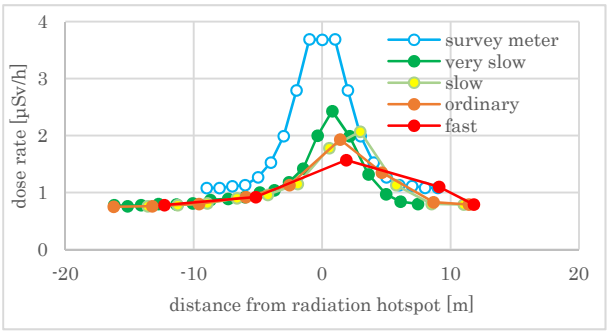

Figure 14: Change in measurements due to walking speed.

B. Determination of correction factors in a comparison test with survey meters

We assumed measurements made with a NaI (Tl) scintillation survey meter (TCS-172B) at a height of 1m to be the most reliable, and the survey meter was calibrated with traceability. We compared measurements made using a survey meter with those obtained in a walking survey (Figure 15). A comparison was made at several points with differing dose rates. At each point, we faced north, south, east, and west and made measurements five times in each direction to mitigate direction characteristics. We then took the average value for all directions as the measurement for that point. We next plotted the measurements of walking surveys against the survey meter to determine the correction factor.

Figure 15: Images of measuring.
(a): Measurement with a survey meter
(b): Measurement with a walking survey
Both measurements were made facing four directions.

The results of the comparison are shown in Figure 16(a). There was good linearity between the measurements of walking surveys and the survey meter below a survey meter measurement of 1 μSv/h, whereas the linearity deteriorated above approximately 1 μSv/h. This phenomenon is due to count loss caused by excessive radiation incidence on the low-dose CsI detector.

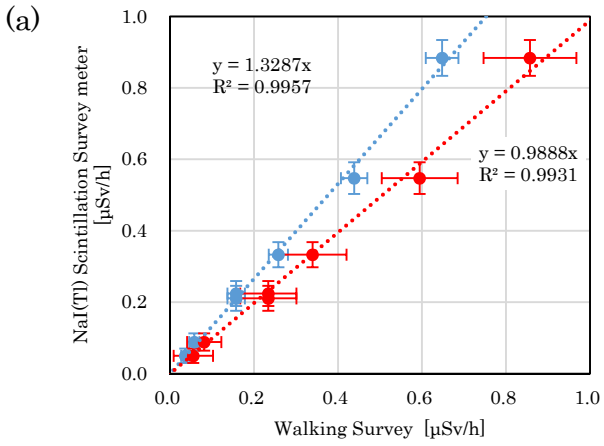

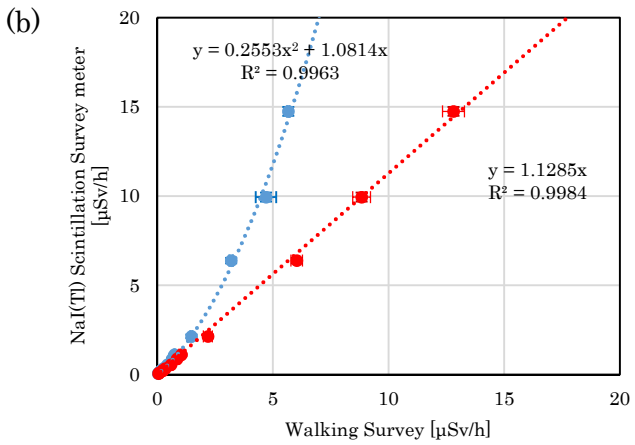

Figure 16: Comparison of measurements of the survey meter and walking survey.
(a): Chart plotting data below 1 μSv/h
(b): Chart plotting all data
- Comparison of the measurements of the low-dose-rate CsI detector (Cs-137, 662keV measuring range: 0.001 to 10 μSv/h) and NaI survey meter.
- Comparison of the measurements of the high-dose-rate CsI detector (Cs-137, 662keV measuring range: 0.01 to 100 μSv/h) and NaI survey meter.

Note that the approximate curve is not affected by the self-dose from the measurement detector, with the intercept being zero.

In light of the above results, we changed the detector to a high-dose-rate CsI detector (Figure 17) and compared the results obtained using the survey meter with measurement results of walking surveys again. The results are shown in Figure 16(b). We confirmed that as a result of changing the detector, the linearity of walking survey measurements against survey meter measurements is obtained even in the high dose range.

We also confirmed that the high-dose CsI detector can make better measurements than the low-dose rate CsI detector in the high dose range in field tests. This is also confirmed in Figure 18, which shows the walking survey results having changed detectors at the same geographic point. The maximum indicated value is higher for the high-dose-rate CsI detector than for the low-dose-rate CsI detector, and the high-dose-rate area represented by red markers appears, indicating that measurements are made without counting loss of radiation.

Figure17: High-dose CsI detector (Hamamatsu Photonics C12137).

According to the above comparisons, we set the correction factor of walking surveys to 1.3 when using the low-dose-rate CsI detector at points with a dose rate less than 1 μSv/h and 1.1 when using the high-dose-rate CsI detector.

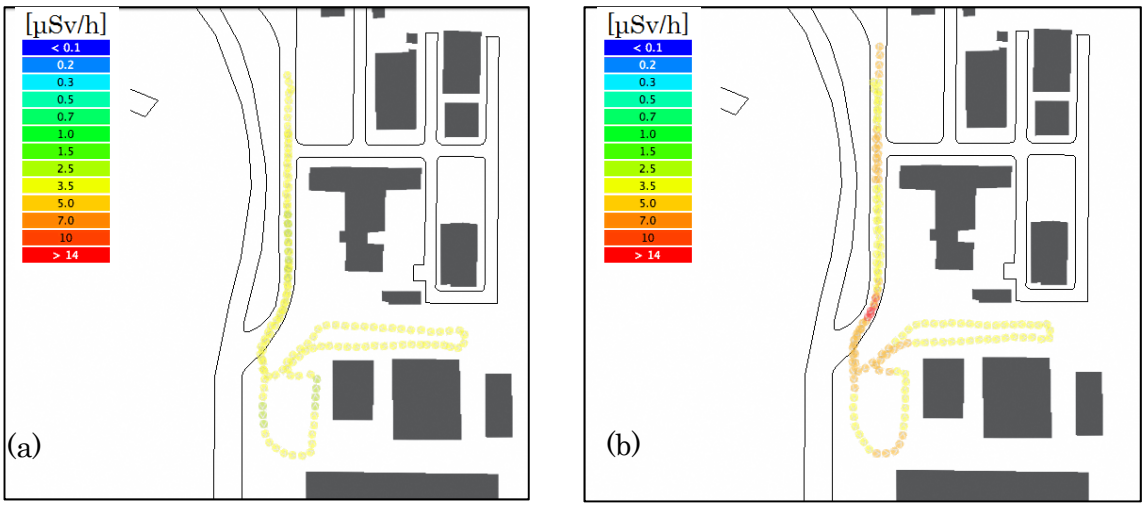

Figure 18: Walking surveys having changed the detector.
(a): Walking survey with the low-dose-rate CsI detector.
The indicated value range is 2.77 to 5.99 μSv/h.
(b): Walking survey with the high-dose-rate CsI detector.
The indicated value range is 5.00 to 29.5 μSv/h.

C. Confirming variations in measurements

We conducted-fixed point measurements to confirm variations in measurements for a measurement time of 3 seconds in the low dose rate range. Fixed-point measurements were made with both the low-dose-rate CsI detector and the high-dose-rate CsI detector.

Results showed that the variation in measurement results was larger for the high-dose-rate CsI detector at points with a low dose rate (Figure 19). The variation coefficient obtained from dividing the standard deviation of measurements by the average value was 19.7% for the low-dose-rate CsI detector but 42.7% for the high-dose-rate detector. Error in measurements made with the low-dose-rate detector was small because of the high counting rate achieved with the large crystal while error in measurements made with the high-dose-rate detector was large because of the small counting rate achieved with the small crystal.

On this basis, we decided to use the low-dose-rate CsI detector, which has a small

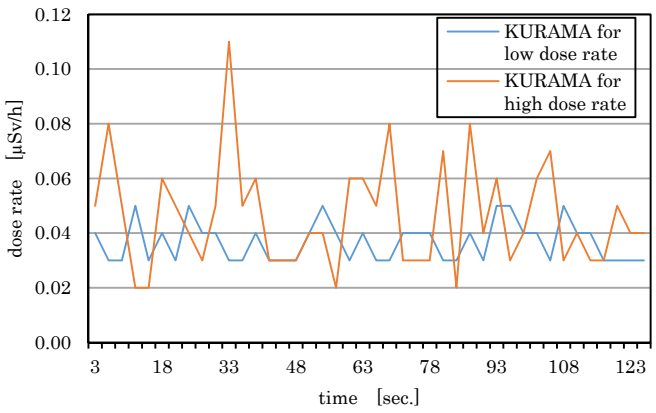

Figure 19: Measured value dispersion check.

variation at low dose rates, at geographic points with a dose rate less than 1 μSv/h, and to use the high-dose-rate CsI detector at geographic points with a dose rate greater than 1 μSv/h.

(2) Conducting walking surveys

With the purpose of studying the operation of walking surveys and acquiring basic data, we conducted walking surveys at places with differing conditions. Examples of such walking surveys are described below.

A. Walking survey in western Fukushima City

We conducted a walking survey on a trial basis in western Fukushima City. At the center of this geographic area is a surface paved with asphalt, with ditches along the edges. There were no obstructions on the outside of the asphalt surface, leaving the surface wide open and surrounded by grass.

Results of a walking survey conducted at this geographic point are shown in Figure 20. The paved surface at the center of the range of the walking survey had a low dose rate compared with that of the surroundings. It is considered that this low dose rate is due to the easy decontamination of the paved surface and the strong effect of weathering. In addition, the radiation dose in the vicinity of the ditch was higher than that of the surroundings. This is probably because there was an inflow of radioactive material from the surrounding area.

We conducted a high-density walking survey and tested interpolation with a GIS tool (Figure 21). Interpolation was conducted with IDW. The interpolated radiation dose rate in the paved area was low, and the dose rate in the vicinity of the ditch was high.

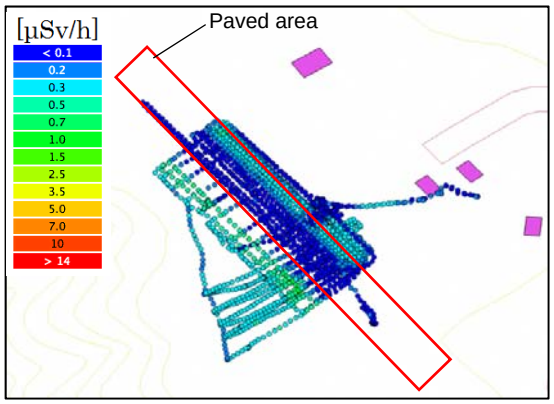

Figure 20: Results of a walking survey in western Fukushima City.

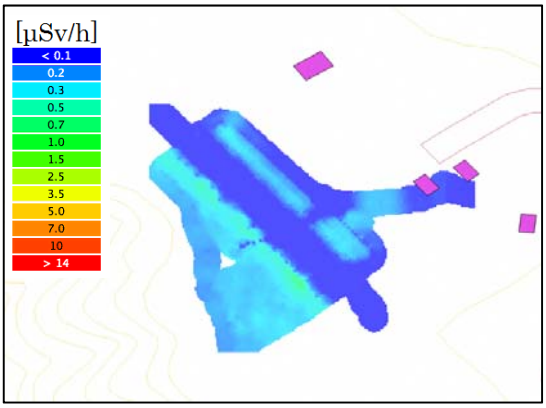

Figure 21: Results of interpolation with IDW.

B. Walking survey in the periphery of a temporary storage area

We conducted a walking survey in a temporary storage area and its periphery in the Nakadori region of Fukushima Prefecture (Figure 22). The area inside the red frame in the figure is the temporary storage area. The dose rate near the temporary storage area was equal to or less than the dose rate in the periphery, and no effect of external decontaminated waste on the outside area was seen in this temporary storage area.

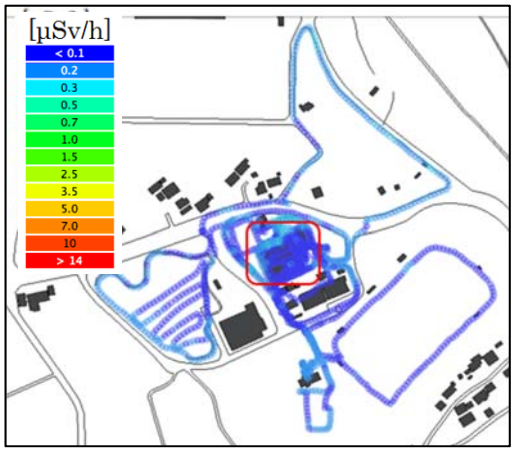

Figure 22: Dose map.
(with the temporary storage area indicated by the red frame.)

C. Walking survey in the Hamadori region (outside the evacuation zone)

We conducted a walking survey around rivers in the Hamadori region of Fukushima Prefecture (outside the evacuation zone) (Figures 23 and 24). There is a paved surface on the left side of the figure, with the rest of the study area being gravel or grassland. The dose rate was low on the paved surface and nearly uniform in other areas.

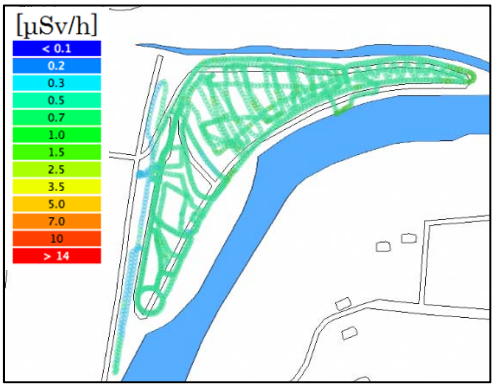

Figure 23: Dose map.

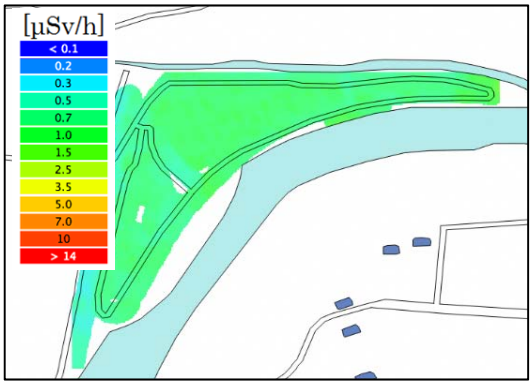

Figure 24: IDW interpolation result.

D. Walking survey in a difficult-to-return evacuation zone

We conducted a walking survey in a difficult-to-return evacuation zone in Fukushima Prefecture (Figures 25 and 26). The area where the walking survey was conducted was nearly uniform grassland. The dose rate was nearly uniform in the area, with no large deviation observed.

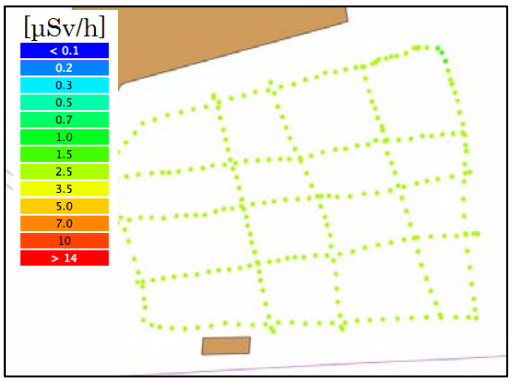

Figure 25: Dose map.

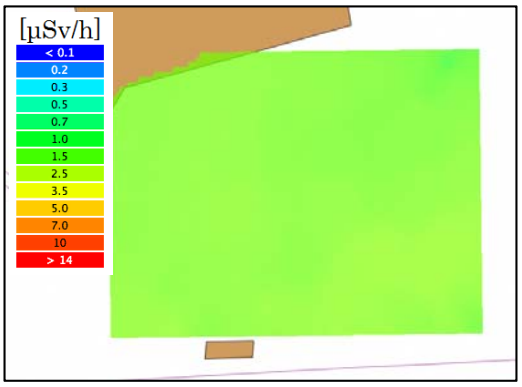

Figure 26: Results of interpolation by IDW.

4.4. Conclusions

Results were obtained in developing walking surveys by 2015.

In terms of developed equipment, the walking survey system adopted KURAMA, which was designed by Kyoto University and has a structure suitable for a walking survey. Additionally, to analyze the obtained data or to work with other monitoring methods, such as a UAV survey, we prepared a GIS data processing system. Furthermore, by collecting data for the determination of direction characteristics and calibration constants, it has become possible to measure the dose rate in a walking survey.

We conducted walking surveys at several points and confirmed that it is possible to measure the air dose rate and to create a contour map with a GIS processing system.

We published a manual for walking surveys and made the manual available to the general public.

In fiscal 2016, we are conducting walking surveys or lending necessary equipment at the request of municipalities.

5. FIP5: Study of proper treatment of waste containing radioactive materials at municipal solid waste incinerators

Abstract

At municipal solid-waste (MSW) incineration facilities in operation (stoker-type incinerators), we performed tests to characterise changes in the migration of radiocaesium to fly ash due to changes in the combustion temperature of the MSW incinerator, the addition of a radiocaesium evaporation accelerator or inhibitor, or the co-incineration of radiocaesium bearing used filter cloth from bag filters of MSW incineration facilities. We also performed radiocaesium leaching tests of incinerated ash (bottom ash and fly ash from stoker–type incinerators) and a laboratory test to examine a method to reduce radiocaesium solubility of ash from a MSW incineration facility (i.e., a stoker–type incinerator).

5.1. Purpose

Incinerating MSW that contains radiocaesium dispersed by the accident at the Fukushima Daiichi Nuclear Power Plant of Tokyo Electric Power Company causes radiocaesium to migrate to and become concentrated in bottom ash and fly ash. Bottom and fly ash generated in this way cannot be disposed of in a landfill, even if the radiocaesium concentration is below 8000 Bq/kg, a reference value set by law. Bottom ash and fly ash that must be stored in the incineration facilities has thus accumulated.

Although the level of radioactivity has decreased appreciably since the accident, ash containing radioactive substances is still being generated from the daily incineration of MSW. Proper treatment and disposal of the ash is an urgent issue (Figure 1)

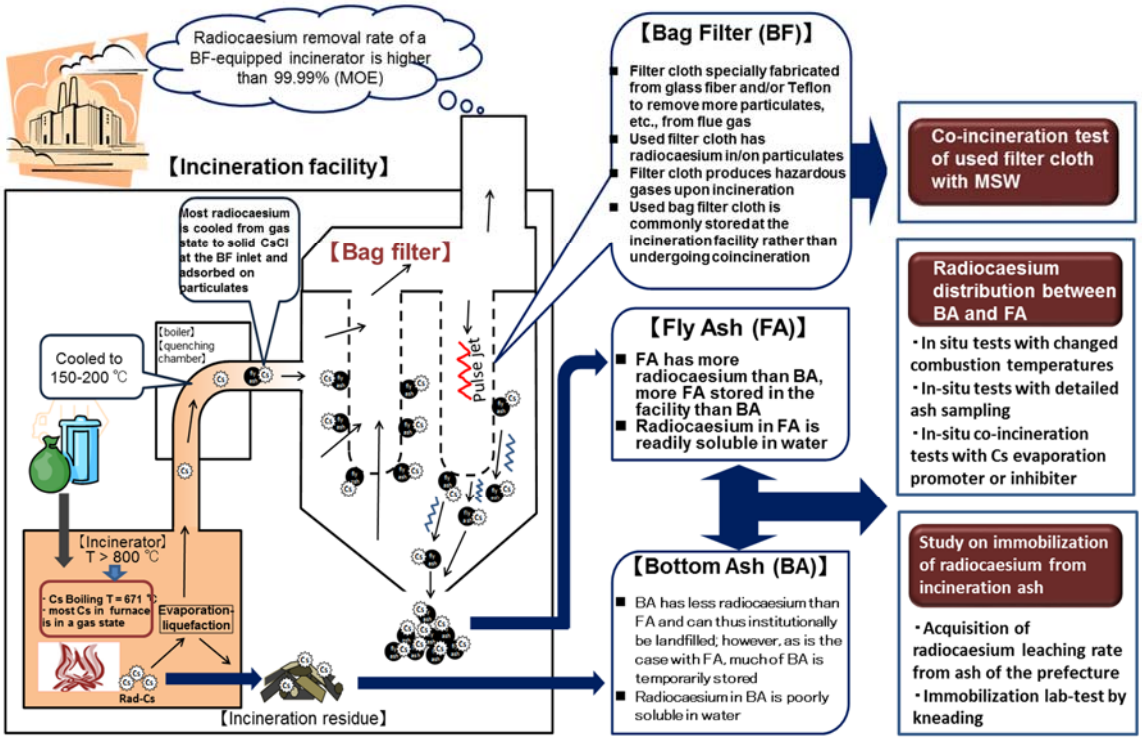

Figure 1: Waste incineration processes and research issues.

We thus conducted tests to confirm the effectiveness of methods to control the migration of radiocaesium to bottom ash and fly ash. After understanding general aspects of the radiocaesium leaching characteristics of incineration ash generated in Fukushima Prefecture, we examined technologies and methods to make radiocaesium in bottom ash and fly ash less soluble.

Used filter cloth from bag filters attached by fly ash containing radiocaesium is also generated by incineration facilities. The proper treatment of the cloth is another issue.

The co-incineration of the cloth with MSW is conceivable. To evaluate the feasibility of co-incineration, it is necessary to understand the co-incineration-induced changes in the radiocaesium distribution to bottom ash and fly ash and its effect on the incineration facility and the environment when co-incineration is conducted. We thus conducted co-incineration demonstration tests.

5.2. Content of implementation

(1) Radiocaesium distribution between bottom ash and fly ash

Radiocaesium generally tends to evaporate during incineration and to transfer to fly ash rather than remaining in bottom ash. The ratios of the distribution of radiocaesium to bottom ash and fly ash at incineration facilities in Fukushima Prefecture are given in Table 1. Approximately 60% of total radiocaesium is transferred to fly ash.

Table 1: Radiocaesium distribution between bottom ash and fly ash at MSW incineration facilities in Fukushima Prefecture.

Facilty	Capacity	Dust collection	Annual inicineration (2011fy)	Ash generation		Radiocaesium concentration		Radiocaesium distribution	
				BA	FA	BA	FA	BA	FA
	[t/d]		[t/y]	[t/y]		[Bq/kg]		[%]	
A	105	BF	16,035	2,053	632	12,220	49,400	45	55
B	120	BF	28,964	4,019	747	3,910	34,900	38	62
F	80	BF	20,230	2,190	1,076	16,640	33,900	50	50
G	100	EP	30,111	2,912	737	3,920	36,300	30	70
H	90	BF	16,948	1,392	681	1,494	6,640	31	69
J	60	BF	10,181	1,342	336	639	4,650	35	65
N	50	BF	837	93	41	3,140	13,110	35	65
P	50	BF	8,906	720	422	2,269	5,690	40	60
Q	150	EP	35,612	4,797	724	7,540	45,500	52	48
R	40	BF	12,401	2,190	262	2,200	17,360	51	49
S	30	BF	4,574	381	86	1,706	12,260	38	62

Note 1 Values in this table are not corrected for the amount of water and materials added.
Note 2 incinerators at all facilities are of the stoker furnace.
Note 3 Radiocaesium concentrations were measured in July 2011.
Note 4 Dust collection method, BF:bag filter; EP:electrostatic precipitator

We identified the following five main factors that have the potential to govern the transfer of radiocaesium: (a) combustion temperature, (b) air ratio, (c) waste composition, (d) addition of chemicals, and (e) particle size of ash.

Among these factors, (b) air ratio (air volume) affects various system parameters, including the flue

gas velocity, which potentially disturbs the combustion balance and affects proper incineration, (c) waste composition cannot be controlled, and (e) ash particle size is technically difficult to control. We thus focused on the relationships between the migration behaviour of radiocaesium and (a) combustion temperature and (d) addition of chemicals

A. Effect of combustion temperature

We performed tests in cooperation with Facilities A to D. All facilities were equipped with stoker furnaces.

We compared the distribution of radiocaesium to bottom ash and fly ash when the temperature at the incineration chamber outlet was increased (or decreased) 50°C from the normal operating temperature with the distribution during normal operation.

To obtain a combustion chamber outlet temperature of 50°C higher or lower than that in normal operation, we changed the temperature of combustion air supplied to the combustion chamber (i.e., primary air) by approximately 50°C from the temperature maintained during normal operation. The amount of combustion air (i.e., primary air) was not changed to prevent changes in the production of bottom ash and fly ash due to ash blow up. Other operating conditions, such as those related to the furnace water spray and the amount of secondary air, differ among facilities.

The true combustion temperature (combustion temperature range in the incinerator) could not be measured directly. Therefore, we used the combustion chamber outlet temperature measured by the facility as an index of the combustion temperature and evaluated the impact of the chamber outlet temperature changes on radiocaesium migration. At Facility C, however, we inserted a thermocouple into the incineration chamber to measure the internal temperature as an index of the combustion temperature because the automatic control of secondary air flow could not be disengaged, and changes in the combustion chamber outlet temperature might not correspond to actual changes in the incinerator internal temperature.

The test operation was continued for 1 day (i.e., 24 h) under the same conditions based on the time needed to stabilize the combustion state and the long retention time of the bottom ash in the system.

We sampled fly ash and flue gas at least 1 h after the establishment of the test conditions.

For bottom ash, owing to the facility-specific retention time inside the incinerator and ash discharger, we predetermined for each facility a sampling time based on the retention times estimated in a simple model and a tracer test (where metal cans were thrown into the waste hopper and their arrival was observed at a planned sampling point).

Figure 2 shows sampling points for bottom ash, fly ash, and exhaust gas, and estimated retention times of bottom ash inside the system for Facility A.

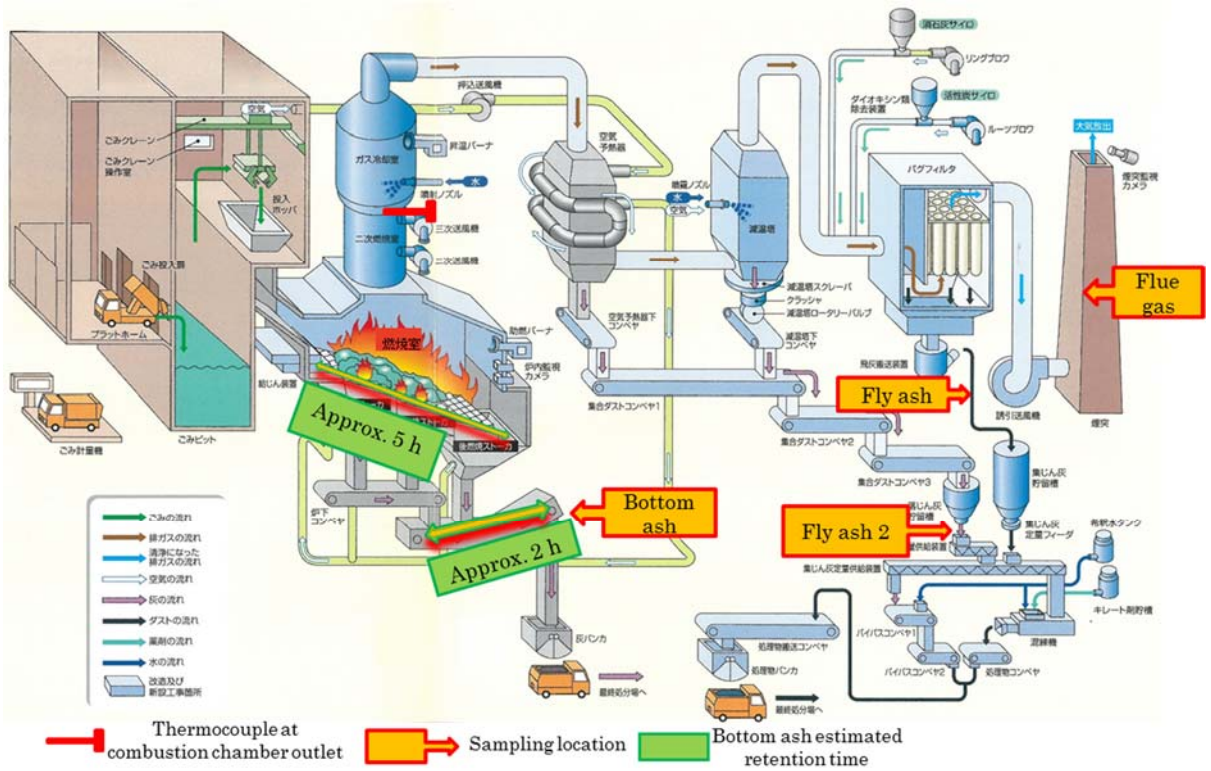

Figure 2: Sampling positions and estimated residence times of bottom ash, fly ash, and exhaust gas at incinerator Facility A.

The measurements and analysis procedures are shown in Table 2 for the bottom ash, fly ash, and flue gas sampled as described above.

Table 2: Samples and measurement items.

Waste Composition	Moisture content, ash content, combust content, material composition, lower calorific value、elemental analysis（C、H、N、O、S、Cl）
Bottom Ash	Radiocaesium concentration(Note 1), ignition loss(Note 2) elemental analysis（Cs、Na、K、Ca、Mg、Al、Si、P、Fe）
Fly Ash	Radiocaesium concentration(Note 1), elemental analysis（Cs、Na、K、Ca、Mg、Al、Si、P、Fe）
Flue Gas	Radiocaesium concentration(Note 3), Dioxins(Note 2)

Note 1 :Four samples of bottom ash and fly ash were collected every hour. Four were mixed and distributed for the analysis. Radiocaesium concentration of Four samples before mixing were also subject to NaI gamma ray spectrometer.
Note 2 :Conducted to check that there is no incomplete combustion under low temperature operation.
Note 3 :Conducted to check that there is not increased radiocaesium under high temperature operation and operation with radiocaesium evaporation promotoin agents added.

Analytical results for the waste composition are given in Table 3 and constitute the most basic information about waste. Compositional differences are thought to define the behaviour of radiocaesium in the combustion process.

Table 3: Waste composition analysis.

Facility			A			B		C		D	
Collection date(2014)			6/26	6/27	10/15	7/9	7/10	7/29	7/30	11/25	11/28
Apparent specific gravity		[kg/m^3]	220	217	131	139	223	97	126	184	176
Moisture content		[%]	45.65	47.12	39.18	43.16	45.13	36.38	45.78	49.38	45.15
Ash content		[%]	9.72	6.32	10.16	8	7.36	5.54	6.14	8.15	6.86
Lower callorific value		[kJ/kg]	8,460	9,380	9,920	8,330	9,420	12,100	10,130	7,700	8,620
Compsition of dried waste	Paper/cloth	[%]	53	38.4	39.4	59.2	45.4	56.3	37.5	39	49.7
	Plastic/synthetic resin/rubber/leather	[%]	22.6	27.1	18.6	15.5	21.2	22.7	32.9	21.4	24.1
	Wood/bamboo/straw	[%]	13.7	10	24.8	8.1	11.2	6.7	12	14.1	8.3
	Kitchen waste	[%]	3.7	14.3	9.5	13.9	10.4	9.2	8.4	14.9	10
	Non-burnable	[%]	2.3	2.4	5.1	0.4	4.6	0.6	2.5	4.3	0.7
	Other(under 5mm)	[%]	4.7	7.8	2.6	2.9	7.2	4.5	6.7	6.3	7.2
Ash content of dried waste	Paper/cloth	[%]	5.6	4.4	5	7.7	2.9	4.9	4.3	3.7	4.5
	Plastic/synthetic resin/rubber/leather	[%]	1.9	1.2	1	0.9	1.4	1.2	1.6	1.9	2.7
	Wood/bamboo/straw	[%]	4.7	1.1	3.1	1.6	0.4	0.4	0.7	0.8	0.9
	Kitchen waste	[%]	0.7	1	1.1	2.5	1.5	0.6	0.6	3.1	1.7
	Non-burnable	[%]	2.3	2.4	5.1	0.4	4.6	0.6	2.5	4.3	0.7
	Other(under 5mm)	[%]	2.7	1.9	1.3	1.1	2.6	1	1.6	2.3	2
	Total	[%]	17.9	12	16.6	14.2	13.4	8.7	11.3	16.1	12.5
Elemental composition	Carbon	[%]	40.36	49.98	47.11	44.15	48.27	50.91	54.47	44.37	46.9
	Hydrogen	[%]	6.36	8.1	7.19	6.49	7.19	8.23	9.3	7.07	7.1
	Nitrogen	[%]	0.71	0.81	1.16	1.18	1.48	0.56	0.66	0.97	0.61
	Sulphur	[%]	0.08	0.07	0	0.07	0.08	0.06	0.07	0.06	0.07
	Chlorine	[%]	0.31	0.16	0.81	0.15	0.57	0.42	0.42	0.21	0.21
	Oxygen	[%]	36.2	31.07	31.48	34.2	33.19	31.68	26	34.97	33.17

We did not observe a clear relation between the composition of waste and the area or season in which the waste was generated. The waste incinerated at Facilities A and B had calorific values of 8,330 to 9,920 kJ/kg, while all values exceeded 10,000 kJ/kg at Facility C, which had higher caloric value for waste in summer. Meanwhile, although Facility D received autumn waste at the end of November, it had the lowest calorific value.

B. Continuous sampling test

We conducted a tests in order to understand the relations between combustion temperature and radiocaesium distribution during normal furnace operation. Stoker furnace equipped two facilities (B and F) hosted continuous five days bottom and fly ash sampling of every two hours. Ash sampled were subject to radiocaesium concentration measurement by NaI spectroscopy.

The first four samples obtained each day were mixed together, divided and distributed for Ge measurements and an elemental (Cs, Na, K, Ca, Mg, Al, Si, P, and Fe) analysis. These data were used to examine the relationship between the combustion temperature during normal operation and migration behaviour (distribution to bottom ash/fly ash) of radiocaesium.

Sampling points and times were determined according to the methods employed in subsection (1) A.

C. Effects of a radiocaesium evaporation accelerator and inhibitor

We examined the effects of adding hydrated lime ($Ca(OH)_2$), which is expected to promote the

evaporation of radiocaesium, and bentonite (clay), which is expected to inhibit the evaporation of radiocaesium.

① Test of hydrated lime (2.4%) and bentonite (2.2%) addition at Facility A

② Test of hydrated lime (2.6%, 5.5%) addition at Facility A to determine the reproducibility of the effect observed in test ①.

③ Test of hydrated lime (2.2%) addition at Facility D to determine whether the results obtained in tests ① and ② are facility-specific.

④ The materials were sprayed on the surface of each crane of waste thrown into the hopper.

(2) Proper treatment of used filter cloths of bag filters

We conducted three test runs at both Facility B using glass-fibre made filter cloths and at Facility E using Tefaire® filter cloths. In one run, ordinary incineration was performed without used filter cloths co-incineration (Run-1). In the other two runs, co-incineration of used filter cloths with MSW was performed, but the used filter cloth throw-in ratio and interval differed betweenRun-2 and Run-3 (Table 4). At Facility B, two used filter cloth throw-in ratios were set according to a questionnaire survey of facilities having with actual experience with co-incineration treatment. These were the mean value of 0.20% and the maximum value of 0.40%. At Facility E, the throw-in ratio was set to 0.03% according to 'Cleaning Technical Report, No. 8' issued by the Clean Authority of Tokyo (2008) and other data[7)8)]. The incinerators at both facilities are stoker-type incinerators.

Table 4: Details of the used bag filter cloth co-incineration test.

Facility name			B (60 t/furnace·day)			E (75 t/furnace·day)		
Filter cloth material			Glass fibre			Tefaire®		
Run			RUN 1	RUN 2	RUN 3	RUN 1	RUN 2	RUN 3
Co-incineration ratio			Normal operation	0.2%	0.4%	Normal operation	0.03%	
Filter cloth input amount				6.4 kg/H	12.8 kg/H		0.90 kg/H	
Input amount and time interval, time continued				(1.5/0.5 H), 6 h	3/0.5 H, 6 H		0.5/1 H, 6 H	1.5/3H, 6 H
Measurement item	Used filter cloth	Radiocaesium	○			○		
	Flue gas	Radiocaesium	○	○	○	○	–	○
		Hydrogen chloride	–	○	○	–	○	○
		Sulphur oxide	–	○	○	–	○	○
		Nitrogen oxide	–	○	○	–	○	○
		Dioxins (*2)	–	–	○	–	–	○
		Fluorine compounds	–	–	–	○	○ (four times)	○ (four times)
	Bottom ash	Radiocaesium (*1)	○	○	○	○	○	○
		Ignition loss (*2)	–	–	○	–	–	○
	Fly ash	Radiocaesium (*1)	○	○	○	○	○	○
*1) Radiocaesium samples were collected once per hour for NaI measurements, for a total of five samples, four of which were mixed into one sample and then divided for Ge measurements. *2) Conducted in the RUN under the most severe conditions.			There were two cases of the co-incineration ratio (average 0.20% and maximum 0.40%) based on questionnaire survey results of facilities that previously conducted co-incineration before. Filter cloth dimensions: φ164 mm × 5250 mm (L). The manufacturer's standard value was used for weight: 2.38 kg each, calculated from a density of 880 g/m^2. Radiocaesium concentration of the filter cloth subject to co-incineration: 600 Bq/kg.			The co-incineration ratio was set at 0.03%, according to "Seiso Giho No. 8 2008 Tokyo 23 Special District Authority". Filter cloth dimensions: φ140 mm × 6000 mm (L). The manufacturer's standard value for weight was used: 1.71 kg each calculated from a density of 650 g/m^2, but the measured value at the facility was 2.0 kg each. Radiocaesium concentration of the filter cloth subject to co-incineration: 1260 Bq/kg.		

Regarding the effects of co-incineration on the migration behaviour of radiocaesium due to fly ash that contains radiocaesium adhering to the filter cloth, the effect of used cloths with glass fibre for which combustion is difficult in the established conditions, and the increase in the concentration of fluorine compounds due to the combustion of Tefaire®, we collected and analysed bottom ash, fly ash, and flue gas before and during the test or collected measurements obtained by the facility. For these items, we then compared the data obtained before inputting the filter cloth and during the test and surveyed the effects. Sampling points and times were set according to the methods described in subsection (1)A.

(3) Study on the reduction of radiocaesium leaching from fly ash

A. Data acquisition of radiocaesium leaching characteristics

We sampled bottom ash, fly ash and limited number of boiler ash from 15 incineration facilities in Fukushima Prefecture and performed radiocaesium leaching tests for a total of 64 samples to acquire radiocaesium leaching data. For some facilities, we sampled and tested summer and winter ash to evaluate seasonal changes in radiocaesium leaching properties. Leaching tests were performed in accordance with 'JIS K0058-1, As-is Agitation Test'; each sample was placed in a container as is, pure water was added at a volume that was 10 times greater than the amount of ash (L/kg), and the top liquid phase was agitated with a propeller.

B. Laboratory radiocaesium immobilisation test

As zeolite, bentonite, and sewage sludge are expected to reduce radiocaesium leaching from incineration ash, we used these three materials as additives to the sampled incineration ash. The test procedure simulates the actual fly ash kneading process. We added the materials to bottom ash, fly ash, and treated fly ash obtained from Facility K at various ratios (20% and 5% of dry ash weight) and added water (30%). The water-supplemented samples were thoroughly mixed and kept at various temperatures (25°C and 80°C) for different periods (one week and one month). Then, each sample was subjected to leaching tests.

5.3. Results

(1) Radiocaesium distribution between bottom ash and fly ash

A. Effect of combustion temperature

Data on the migration and distribution of radiocaesium are given in Table 5.

Ordinary untouched operation is regarded as a standard test.

The tests were conducted at four facilities, but we were unable to obtain a combustion chamber outlet temperature that was higher than that of standard operation during high-temperature operation at Facility C. Additionally, at Facility D, we were unable to obtain a combustion chamber outlet temperature that was lower than that of standard operation in low-temperature operation.

Table 5: Combustion temperature and migration of radiocaesium for each facility and each test.

Facility	Test date	Test	Primary air temp	Combustion chamber outlet temp	Radiocaesium concentration[Bq/kg] (measurement value)		Radiocaesium concentration[Bq/kg] (corrected value(※2))		Distribution ratio % of radiocaesium to fly ash	Fly ash/bottom ash radiocaesium concentration ratio(※3)
			[℃]	[℃]	Bottom ash	Fly ash	Bottom ash	Fly ash		
A	6/23	Standard1	125	904	1,580	8,300	1,900	13,000	60	6.8
	6/24	Standard2	121	912	1,750	10,300	2,100	16,000	63	7.6
	6/26	High temp1	183	964	2,020	10,800	2,500	17,000	61	6.8
	6/27	High temp2	189	950	1,460	13,500	1,900	21,000	72	11.1
	7/2	Hydrated lime2.4%	119	923	840	14,800	1,100	23,000	84	20.9
	7/3	Bentonite 2.2%	123	940	1,990	14,600	2,400	23,000	69	9.6
A Add	10/14	Standard	121	904	1,260	14,500	1,400	20,000	76	14.3
	10/16	Hydrated lime2.6%	116	891	920	15,700	1,200	22,000	83	18.3
	10/17	Hydrated lime5.5%	116	904	540	10,400	650	15,000	84	23.1
B	7/8	Low temp1	101	855	1,020	5,700	1,200	6,800	68	5.7
	7/9	Low temp2	103	842	900	4,600	980	5,500	67	5.6
	7/10	High temp1	200	946	940	5,100	1,000	6,100	68	6.1
	7/11	High temp2	194	956	590	4,700	630	5,600	76	8.9
C	7/28	Standard1	52	933 (1043)※1	930	7,800	1,100	12,000	71	10.9
	7/29	High temp1	100	931 (984)※1	1,110	6,400	1,300	9,900	64	7.6
	7/30	High temp2	100	924 (1040)※1	1,740	9,600	1,800	15,000	63	8.3
	7/31	Standard2	52	937 (1075)※1	1,490	9,500	1,700	15,000	64	8.8
D	11/25	Standard1	178	880	480	1,590	430	2,900	54	6.7
	11/26	Low temp1	129	867	480	1,450	430	2,600	52	6
	11/27	Low temp2	134	873	453	1,470	400	2,600	54	6.5
	11/28	Standard2	177	883	530	1,250	470	2,200	46	4.7
	11/29	Hydrated lime2.2%	178	893	410	1,280	360	2,300	53	6.4

(※1) In-core farnace tempreture measured with a provisionally installed thermocouple
(※2) Measured values were corrected for flue gas treatment agents and water added during the process.
(※3) Corrected values were used.

At Facilities A and B, where high-temperature runs produced high combustion chamber outlet temperatures, the ratio of distribution to fly ash increased on the second day of the high-temperature run. We obtained a rise of 2.6% in the distribution rates at Facility A and a rise of 0.8% at Facility B per 10°C combustion temperature by linear approximation, excluding data obtained on the first day (Figures 3 and 4).

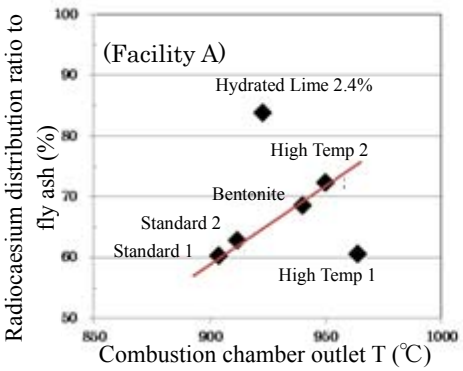

Figure 3: Rate of the distribution of radiocaesium to fly ash versus the combustion chamber outlet temperature (Facility A).

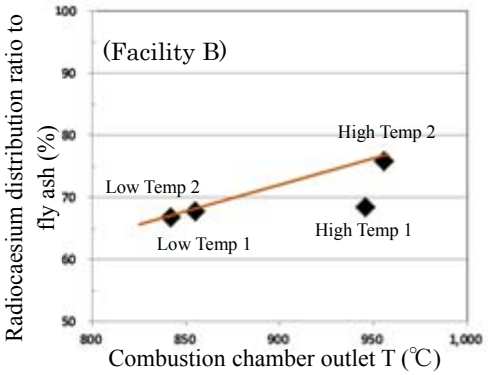

Figure 4: Rate of the distribution of radiocaesium to fly ash versus the combustion chamber outlet temperature (Facility B).

To examine variation in the temperature and migration status of radiocaesium before and after changing the combustion temperature conditions from standard to high-temperature operation, we sampled bottom ash and fly ash every 2 h for 2 days at Facility B, and measured by a NaI. In response to the change in operation mode from low-temperature operation to high-temperature operation, the combustion chamber outlet temperature increased approximately 100°C, from 850°C to 950°C, and the ratio of fly ash/bottom ash radiocaesium concentration increased along with the increasing temperature (Figure 5).

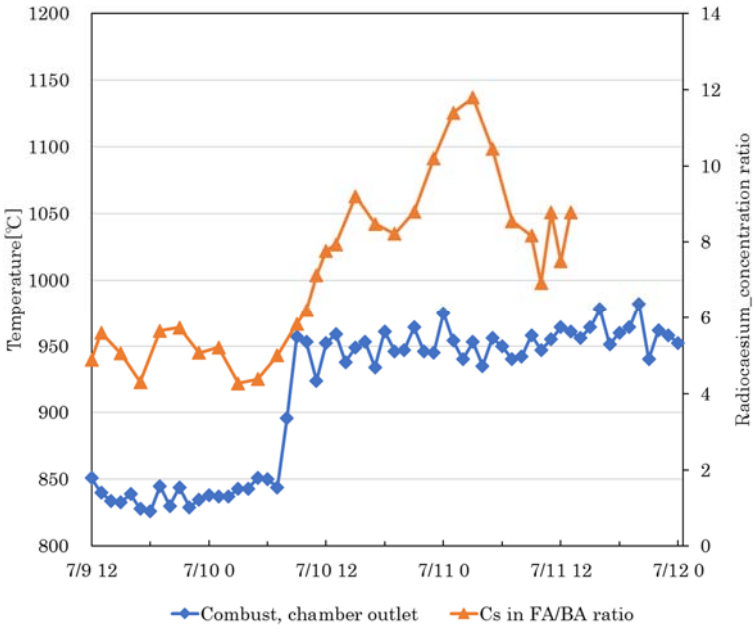

Figure 5: Combustion chamber outlet temperature and radiocaesium concentration ratio (Facility B).

B. Continuous sampling test

Figures 6 (Facility B) and 7 (Facility F) show the combustion chamber outlet temperature, NaI-detector-based radiocaesium concentration in bottom ash and fly ash, ratio of the radiocaesium distribution to fly ash based on NaI measurements, and ratio of the radiocaesium distribution ratio to fly ash based on Ge measurements.

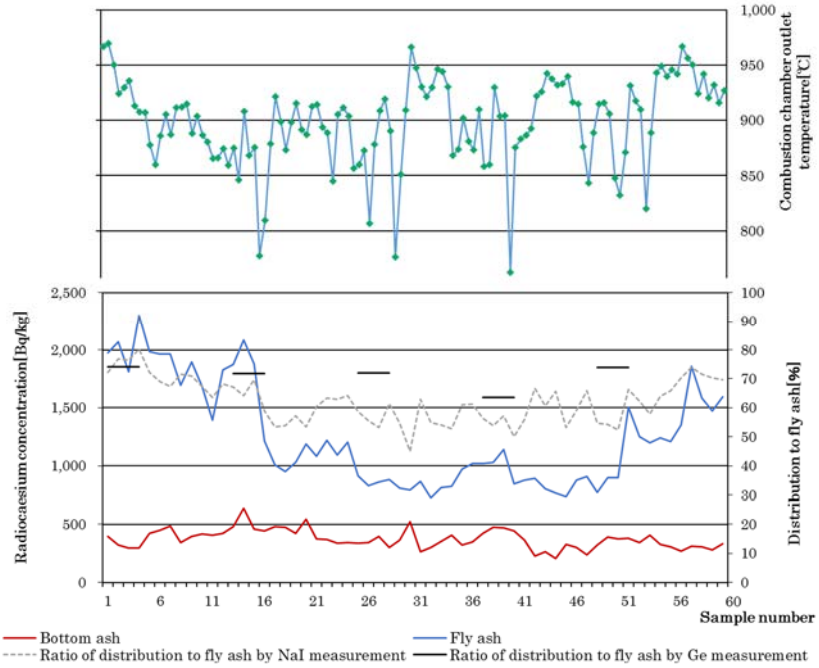

Figure 6: Radiocaesium concentrations in bottom ash and fly ash, radiocaesium distribution based on NaI and Ge measurements, and combustion chamber outlet temperature (dry ash at Facility B).

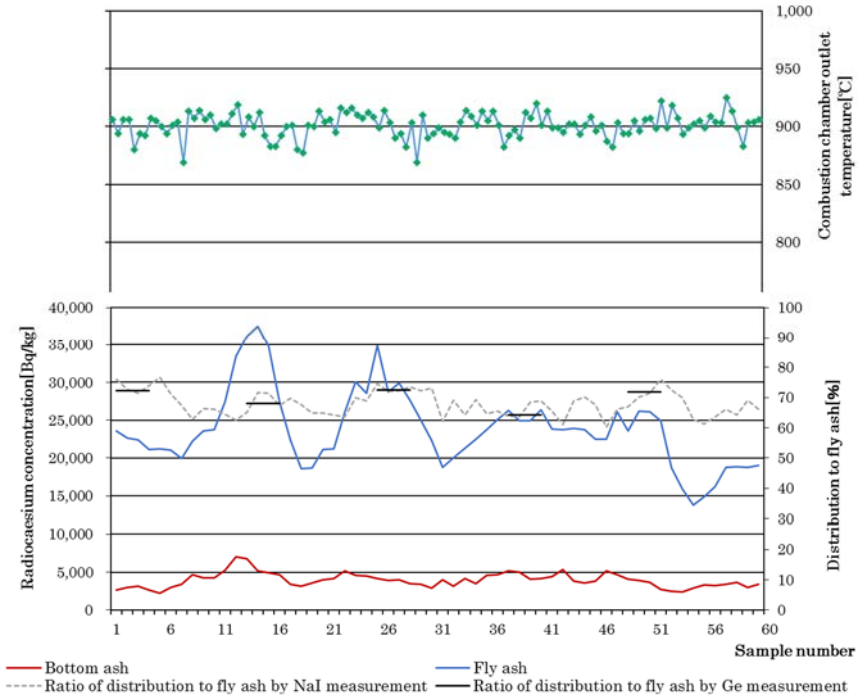

Figure 7: Radiocaesium concentrations in bottom ash and fly ash, radiocaesium distribution besed on NaI and Ge measurements, and combustion chamber outlet temperature (dry ash at Facility F).

It is difficult to detect a clear relationship between the combustion chamber outlet temperature and the distribution of radiocaesium to fly ash.

As shown in the plots of the temperature against the ratio of the radiocaesium distribution to fly ash based on NaI measurements (Figures 8 and 9), the increase in the combustion chamber outlet temperature at Facility B was accompanied by an increase in the ratio of the radiocaesium distribution to fly ash. Sudden drops in temperature may correspond to the inputs of sewage sludge, and it should be noted that the waste composition also changed substantially. The range of outlet temperatures for the combustion chamber of Facility F was small, and no clear relationship between the radiocaesium distribution ratio and combustion chamber outlet temperature was observed.

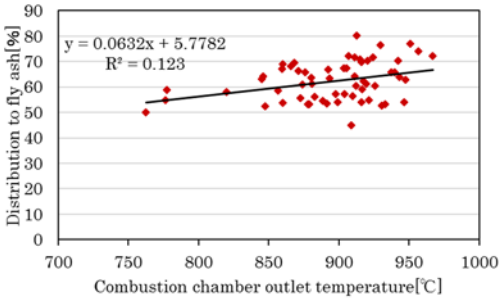

Figure 8: Combustion chamber outlet temperature and radiocaesium distribution to fly ash (Facility B); the radiocaesium concentration was measured by NaI.

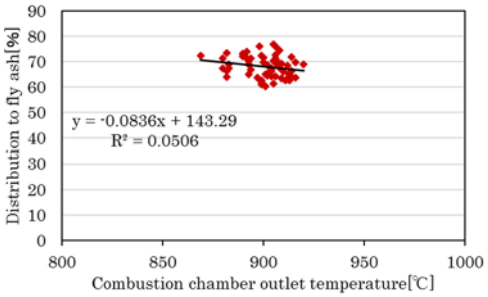

Figure 9: Combustion chamber outlet temperature and radiocaesium distribution to fly ash (Facility F); radiocaesium concentration was measured by NaI.

Regarding the relationship between basicity and radiocaesium distribution, at Facilities F, we detected positive correlations between the basicity of the waste calculated from the chemical composition of ash sampled during the 5-day continuous sampling test and the radiocaesium distribution ratio to fly ash (Figure 11). However, we found no positive correlations at the Facility B(Figure 10).

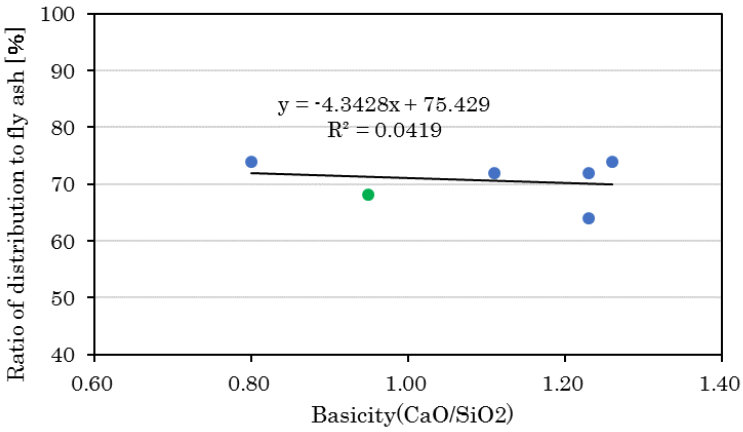

Figure 10: Basicity and radiocaesium distribution to fly ash calculated from the ash composition (Facility B).

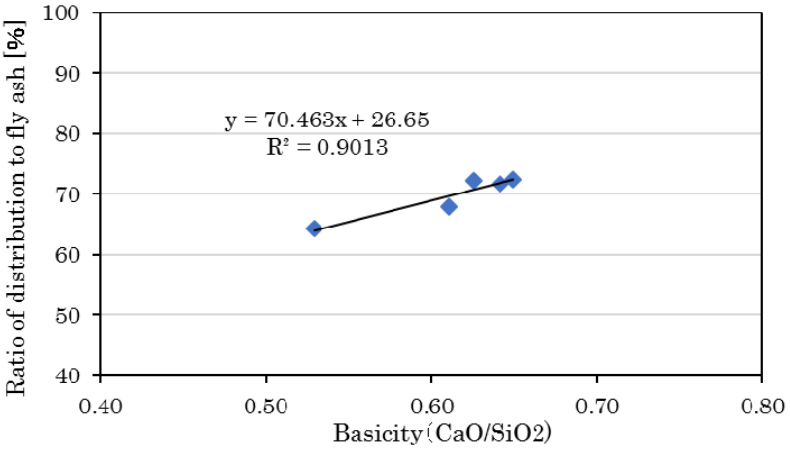

Figure 11: Basicity and radiocaesium distribution to fly ash calculated from the ash composition (Facility F).

C. Effects of a radiocaesium evaporation accelerator and inhibitor

The addition of hydrated lime $Ca(OH)_2$, (subsection 5.2.(1) C ①) at Facility A increased the ratio of radiocaesium distribution to fly ash remarkably (9.3% increase per 1% addition). However, the inhibitory effect of bentonite could not be confirmed (Figure 12).

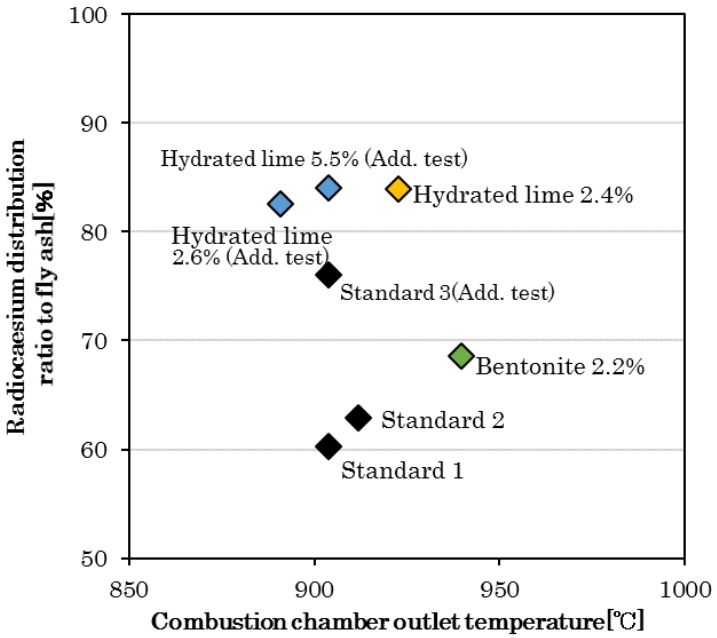

Figure 12: Effect of additives on the radiocaesium distribution to fly ash (Facility A).

We conducted additional tests to determine the general effects of hydrated lime; an effect was confirmed at Facility A, but it was weaker than that observed in the first test. Additionally, hydrated lime had no effect at Facility D (Figure 13).

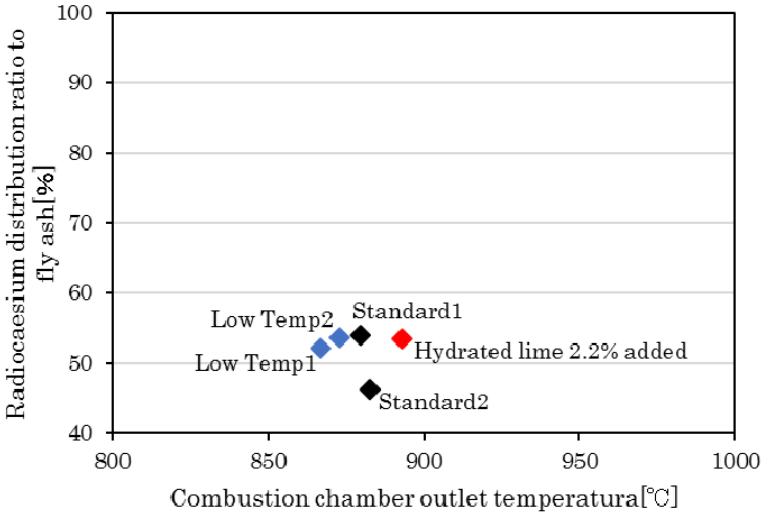

Figure 13: Effect of hydrated lime on the radiocaesium distribution to fly ash (Facility D).

A higher basicity of incinerated waste of Facility D should accelerate the evaporation of radiocaesium[1]. The basicity of the waste, based on the chemical analysis of bottom ash and fly ash conducted at Facilities A to D, is given in Table 6. The basicity of waste at Facility A was lower than that at other facilities. It is probable that the obvious effect observed at Facility A was due to the addition of the basicity-increasing material, hydrated lime, to low-basicity waste. In the case of Facility D, it is possible that the basicity-increasing material was added to waste whose basicity was somewhat high, and the hydrated lime thus did not promote the evaporation of radiocaesium.

Table 6: Basicity of waste calculated from the chemical compositions of BA and FA.

Facility	A						B		C		D		
Ash sampling date(2014)	6/23	6/26	7/2	10/14	10/16	10/17	7/8	7/10	7/28	7/29	11/25	11/26	11/29
Hydrated lime added[%]	-	-	2.4	-	2.6	5.5	-	-	-	-	-	-	2.2
CaO/SiO_2	0.44	0.55	1.03※1	0.65	1.02※2	1.42※2	0.82	1.11	0.96	0.62	0.67	0.75	1.42※3
	0.49						0.95		0.77		0.71		
$(CaO+MgO+Al_2O_3)/SiO_2$	0.81	0.97	1.43※1	1.07	1.46※2	1.89※2	1.38	1.79	1.58	1.13	1.11	1.22	1.89※3
	0.88						1.56		1.33		1.16		
Radiocaesium distribution to FA[%]	60	61	84	76	83	84	68	68	71	64	54	52	53

Calculation of basisity for days that hydrated lime was added: We used the average of analyzed chemical composition values and added hydrated lime quantity of 6/24 and 7/2(※1), the analyzed value of 10/14 for 10/16 and 10/17(※2), and the average of analyzed value and added hydrated lime quantity of 11/25 and 11/26 for 11/29(※3).

In this test, strict operating conditions were used that differ from typical operating conditions, and it was thought that these conditions increased the radiocaesium concentration in flue gas. We therefore conducted measurements of flue gas and dioxins. We did not detect radiocaesium in the flue

gas. Furthermore, the dioxin concentration in the flue gas and ignition loss values of bottom ash met relevant regulations (Table 7).

Table 7: DXNs concentration in flue gas and ignition loss of bottom ash.

Facility	Operating condition	Measurement date		DXNs in flue [ng-TEQ/m^{3}N]		IL of BA [%]	
				Measured	Criteria	Measured	Criteria
B	Low-T	2014	July 8	0.032	5	5.9	10
	Low-T		July 8	0.019		6.0	
C	Low-T	2014	Nov. 26	0.0004	0.1	<0.1	10
	Low-T		Nov. 27	0.00038		0.2	

(2) Proper treatment test of used filter cloths of bag filters

The co-incineration of used filter cloth with MSW was confirmed to be safe and feasible under the proper management of the co-incineration ratio.

Based on many measurements, used filter cloth co-incineration did not affect the measurements, but increased the concentration of radiocaesium in ash (Table 8).

Table 8: Radiocaesium concentration in bottom ash and fly ash.

Facility		**B**			**E**		
Test RUN No.		RUN 1	RUN 2	RUN 3	RUN 1	RUN 2	RUN 3
Used filter cloths input(pieces)		-	1.5/0.5H	3.0/0.5H	-	0.5/1.0H	1.5/3.0H
Radiocaesium concentration (Cs-134＋Cs-137) [Bq/kg]	Used filter cloths	600			1,260		
	Bottom ash	318	400	800	266	157	105
	Fly ash	2,400	3,260	3,640	1,400	1,210	1,220

An increase was observed at Facility B and no increase was observed at Facility E. The increase is thought to be caused by a change in the radiocaesium concentration in co-incinerated MSW, rather than the input of used filter cloth. This is supported by two pieces of evidence. First, the increase was higher than the value calculated from the radiocaesium concentration of the input filter cloth. Second, the increased values remained within the range of variation of the measurements obtained by the facility in 2015. No radiocaesium was detected in flue gas and no effects of co-incineration on flue gas were observed. Table 9 presents the results for Facility E.

Regarding concerned fluorine gas when Tefaire cloths were co-incinerated, measured values were less than approximately 1 mg/m^{3}N.

There were no changes in the ignition loss of bottom ash, harmful acidic substances, and dioxins in flue gas at either facility. These parameters are conceivably change when combustion conditions deteriorate (Table 10).

Table 9: Radiocaesium concentration in flue gas during bag filter cloth co-incineration tests.

Facility				B			E		
Sampling point				Bag filter outlet			Bag filter outlet		
Sampling date(2015)				7/28	7/29	7/30	10/26	10/27	10/28
RUN no. and used filter cloth input rate(pieces)				RUN1	RUN2	RUN3	RUN 1	RUN 2	RUN 3
				-	1.5/0.5H	3.0/0.5H	-	0.5/H	1.5/H
Radiocaesium concentration in flue gas [Bq/m^{3}N]	Filter		Cs-134	<0.3	<0.3	<0.3	<0.3	<0.3	<0.3
			Cs-137	<0.3	<0.3	<0.3	<0.3	<0.3	<0.3
	Drain		Cs-134	<0.3	<0.3	<0.3	<0.3	<0.3	<0.3
			Cs-137	<0.3	<0.3	<0.3	<0.3	<0.3	<0.3
Wet flue gas			[m^{3}N/h]	56,000	63,900	64,600	37,600	38,500	35,300
Dry flue gas			[m^{3}N/h]	44,400	54,700	52,200	26,100	27,100	25,600
Moisture content			[%]	20.8	14.5	19.1	30.2	29.6	27.1
Gas composition	CO_2		[%]	2.9	2.5	3.2	5.6	6.7	6.3
	O_2		[%]	17.6	17.9	17.1	14.7	13.5	13.8
	CO		[%]	<0.1	<0.1	<0.1	<0.01	<0.01	<0.01
	N_2		[%]	79.5	79.6	79.7	79.7	79.8	79.9

Table 10: Harmful acidic substances and dioxins in flue gas, and ignition loss of bottom ash.

Facility			B			E		
RUN No.			RUN2	RUN3	Past figure	RUN2	RUN3	Past figure
Flue gas	SOx	[m^{3}N/h]	<5	<5	<10 (2015)	<5	<5	<3.5～80 (2015)
	NOx	[ppm]	140	160	140～150 (2015)	150	170	99～180 (2015)
	HCl	[mg/m^{3}N]	<10	<10	27～32 (2015)	120	150	<5～310 (2015)
	HF	[mg/m^{3}N]	-	-	-	<1.1	<1	<1 (2015)
	Dioxins	[ng-TEQ /m^{3}N]	-	0.01	0.046～0.072 (2015)	-	0.0028	0.060～0.099 (2015)
Bottom ash	Ignition loss	[%]	-	5.1	5.0～8.1 (2015)	-	5.1	1.3～6.2 (2015)

(3) Study of the reduction of radiocaesium leaching from fly ash

A. Data acquisition of radiocaesium leaching characteristics

We sampled bottom ash and fly ash from 15 MSW incineration facilities in Fukushima Prefecture and performed radiocaesium leaching tests using these samples. The test results indicate that radiocaesium leaching from bottom ash was limited (below 1% to 16%), but leaching from fly ash was extreamly high (35% to 94%), as is generally known (Tables 11-1, 2, 3, and 4). Please note that 'BA' and 'FA' in the tables are the abbreviations of 'bottom ash' and 'fly ash' respectively.

Table 11-1: Radiocaesium leaching test results (1).

Facility		A				B										C		D		E	
Samplimg date		2014				2015										2014		2014		2015	
		6/23		7/2		9/7		9/8		9/9		9/10		9/11		7/28		11/25		10/26	
Sample type		BA	FA	BA	FA	BA	FA	BA	FA	BA	FA	BA	FA	BA	FA	BA	FA	BA	FA	BA	FA
Radiocaesium concentration in solid [Bq/kg]	Cs-134	400	2,100	300	3,900	45	380	43	320	25	280	65	250	24	190	300	1,700	92	390	56	300
	Cs-137	1,400	6,100	760	11,000	220	1,600	230	1,500	180	1,100	230	1,100	130	960	790	5,500	350	1,100	210	1,100
	Total	1,800	8,200	1,060	14,900	265	1,980	273	1,820	205	1,380	295	1,350	154	1,150	1,090	7,200	442	1,490	266	1,400
【Leaching test】 Radiocaesium concentration in liquid [Bq/L]	Cs-134	0.1	130	0.1	230	0.1	31	0.1	28	0.1	20	0.1	15	0.1	18	0.1	130	2	16	0.1	22
	Cs-137	1	360	3	670	1	130	0.1	110	0.1	94	0.1	70	0.1	77	2	380	5	54	0.1	92
	Total	1	490	3	900	1	161	0.2	138	0.2	114	0.2	85	0.2	95	2	510	7	70	0.2	114
Leaching rate	[%]	0.6	59	3.6	61	3.8	81	0	76	0.0	83	0	63	0	83	2.2	65	16	47	0	81

Table 11-2: Radiocaesium leaching test results (2).

Facility		F										G			H		I		
Samplimg date		2015										2016			2016		2016		
		10/13	10/12	10/14	10/13	10/15	10/14	10/16	10/15	10/17	10/16	3/11			3/1		3/17		
Sample type		BA	FA	BA	FA	BA	FA	BA	FA	BA	FA	BA	FA	FA-t	BA	FA-t	BA	FA	FA-t
Radiocaesium concentration in solid [Bq/kg]	Cs-134	550	4,100	1,000	6,300	700	5,500	930	4,700	580	4,300	42	310	300	9	50	200	2,300	840
	Cs-137	2,300	17,000	4,500	27,000	3,100	23,000	3,900	20,000	2,500	18,000	220	1,600	1,500	40	260	1,200	11,000	4,200
	Total	2,850	21,100	5,500	33,300	3,800	28,500	4,830	24,700	3,080	22,300	260	1,900	1,800	49	310	1,400	13,000	5,000
【Leaching test】 Radiocaesium concentration in liquid [Bq/L]	Cs-134	3	290	3	350	2	330	1	310	2	300	<0.1	21	24	<0.1	5	1	75	80
	Cs-137	12	1,200	11	1,500	8	1,400	6	1,300	10	1,300	0.2	100	120	0.1	24	6	270	390
	Total	15	1,490	14	1,850	10	1,730	7	1,610	12	1,600	<0.3	120	140	<0.2	29	7	450	470
Leaching rate	[%]	5	71	3	56	3	61	1	65	4	72	<1	63	78	<4	94	5	35	94

Table 11-3: Radiocaesium leaching test results (3).

Facility		J				K								L			
Sampiling date(2016 fy)		8/24	2/10	8/24	2/10	8/24	2/10	8/24	2/10	8/24	2/10	8/24	2/10	8/25	2/9	8/25	2/9
Sample type		BA		FA		BA		FA		Boiler ash		FA-t		BA		FA	
		S	W	S	W	S	W	S	W	S	W	S	W	S	W	S	W
Radiocaesium concentration in solid [Bq/kg]	Cs-134	<6	10	48.3	81	74	10	340	129	553	298	274	103	31	16	244	232
	Cs-137	44	67	315	560	404	67	2,010	841	3,110	1,960	1,640	718	174	105	1,480	1,570
	Total	<50	77	363	641	478	77	2,350	970	3,660	2,260	1,910	821	205	121	1,720	1,800
【Leaching test】 Radiocaesium concentration in liquid [Bq/L]	Cs-134	<0.6	<0.4	3.9	6	<0.8	<0.4	29	10.2	19.6	11.5	26	9.2	<0.9	<0.4	19	19.5
	Cs-137	<0.7	<0.4	24.6	42	0.8	<0.4	157	66.7	117	76.3	138	62.1	<0.7	0.5	113	134
	Total	<1.3	<0.8	28.5	48	<1.6	<0.8	186	76.9	137	87.8	164	71.3	<1.6	<0.9	132	154
Leaching rate[%]	Cs-134+ Cs-137	<26.0	<10.4	78.5	74.9	<3.3	<10.4	79.1	79.3	37.4	38.8	85.9	86.8	<7.8	<7.4	76.7	85.6
	CS-137	<15.9	<6.0	78.1	75	2	<6.0	78.1	79.3	37.6	38.9	84.1	86.5	<4.0	4.8	76.4	85.4

Table 11-4: Radiocaesium leaching test results (4).

Facility		M								N				O					
Sampiling date(2016 fy)		8/25	1/20	8/25	1/30	9/6	2/8	8/25	1/30	9/30	2/9	9/30	2/9	9/30	2/10	9/30	2/10	9/30	2/10
Sample type		BA		FA		Boiler ash		FA-t		BA		FA		BA		FA		FA-t	
		S	W	S	W	S	W	S	W	S	W	S	W	S	W	S	W	S	W
Radiocaesium concentration in solid [Bq/kg]	Cs-134	452	438	1,290	1,460	1,530	893	815	908	76	69	836	450	28	15	219	170	171	111
	Cs-137	2,460	2,780	6,960	9,150	8,570	5,720	4,710	5,860	409	464	4,750	3,040	187	103	1,190	1,120	995	754
	Total	2,910	3,220	8,250	10,600	10,100	6,610	5,530	6,770	485	533	5,590	3,490	215	118	1,410	1,290	1,170	865
【Leaching test】 Radiocaesium concentration in liquid [Bq/L]	Cs-134	<0.9	<0.5	51	82	46	17.7	48	56.9	<0.6	<0.6	59	35.8	<0.7	<0.4	11	7.5	7.8	5.3
	Cs-137	1	<0.7	284	521	270	117	271	365	0.9	2.2	344	235	<0.8	<0.4	64	51.5	44.5	35.3
	Total	<1.9	<1.2	335	603	316	135	319	422	<1.5	<2.8	403	271	<1.5	<0.8	75	59	52.3	40.6
Leaching rate[%]	Cs-134+ Cs-137	<0.7	<0.4	40.6	56.9	31.3	20.4	57.7	62.3	<3.1	<5.3	72.1	77.7	<7.0	<6.8	52.9	45.7	44.7	46.9
	CS-137	0.4	<0.3	40.8	56.9	31.5	20.4	57.5	62.3	2.2	4.7	72.4	77.2	<4.3	<3.9	53.4	46	44.7	46.8

For ash from Facilities D and M, we should note that the radiocaesium leaching rate was low for fly ash but high for bottom ash. In addition, the radiocaesium concentration in incinerated ash may differ greatly among facilities. We saw no clear seasonal trends in the radiocaesium leaching rates when comparing summer and winter (Figures 14 and 15).

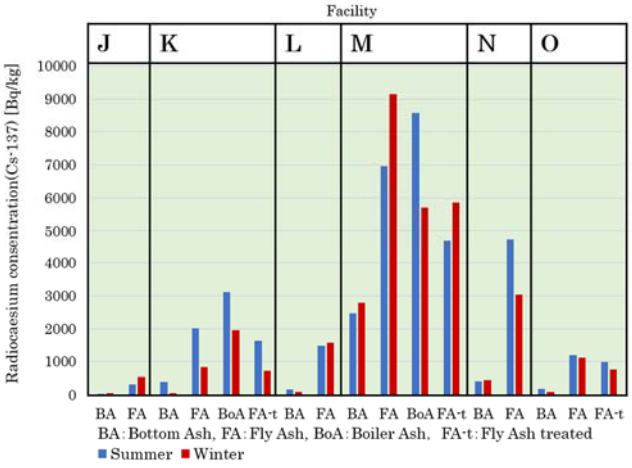

Figure 14: Facility-by-facility radiocaesium concentration in summer and winter samples.

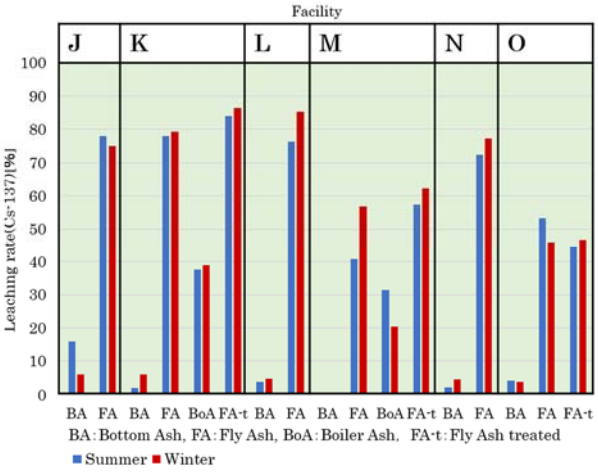

Figure 15: Facility-by-facility radiocaesium leaching rate from summer and winter incineration ash.

Here, fly ash refers to crude ash captured by a bag filter not yet treated by chelating agent addition or other methods. Treated fly ash is described as FA-t. If possible, we also sampled and measured boiler ash whose generation is small and indicated as “BoA”. Radiocaesium concentration of BoA is closer to FA and radiocaesium leaching rate shows intermediate value between BA and FA.

B. Laboratory radiocaesium immobilisation test

Table 12 and Figure 16 show relationships between test specimen conditions (ash type, additive material type, addition rate, curing temperature and curing time) and the radiocaesium leaching rate.

Table 12: Laboratory radiocaesium immobilisation test.

Ash type	Added chemicals	Addition ratio	Curing temperature[℃]	Curing period	Cs leaching rate [%]
Fly ash	Chemicals not added				79.1
	Zeolite	5%	25	1week	13
				1month	18.3
			80	1week	51.2
				1month	57.8
		20%	25	1week	4.3
				1month	4.8
			80	1week	17.3
				1month	24.2
	Bentonite	5%	25	1week	41.9
				1month	45.5
			80	1week	53.4
				1month	67.2
		20%	25	1week	14.1
				1month	14.8
			80	1week	17.2
				1month	28.7
	Sewage sludge	5%	25	1week	71.5
				1month	79.2
			80	1week	81.7
				1month	87.9
		20%	25	1week	66.2
				1month	61
			80	1week	66.5
				1month	67.9

Ash type	Added chemicals	Addition ratio	Curing temperature[℃]	Curing period	Cs leaching rate [%]
Treated fly ash	Chemicals not added				85.9
	Zeolite	20%	80	1month	24.8
	Bentonite				14.7
	Sewage sludge				59.4
Bottom ash	Chemicals not added				2
	Zeolite	5%	25	1week	<0.9
				1month	<1.1
			80	1week	<0.9
				1month	<1.1
		20%	25	1week	<1.0
				1month	<1.0
			80	1week	<1.1
				1month	<1.0
	Bentonite	5%	25	1week	<1.0
				1month	1
			80	1week	<1.0
				1month	<0.9
		20%	25	1week	<1.1
				1month	<1.1
			80	1week	<1.2
				1month	<1.0

Black numerals indicate elution rates calculated from caesium-134 and caesium-137, and red and blue numerals indicate elution rates calculated from caesium-137 (Red indicates the most immobilised case).

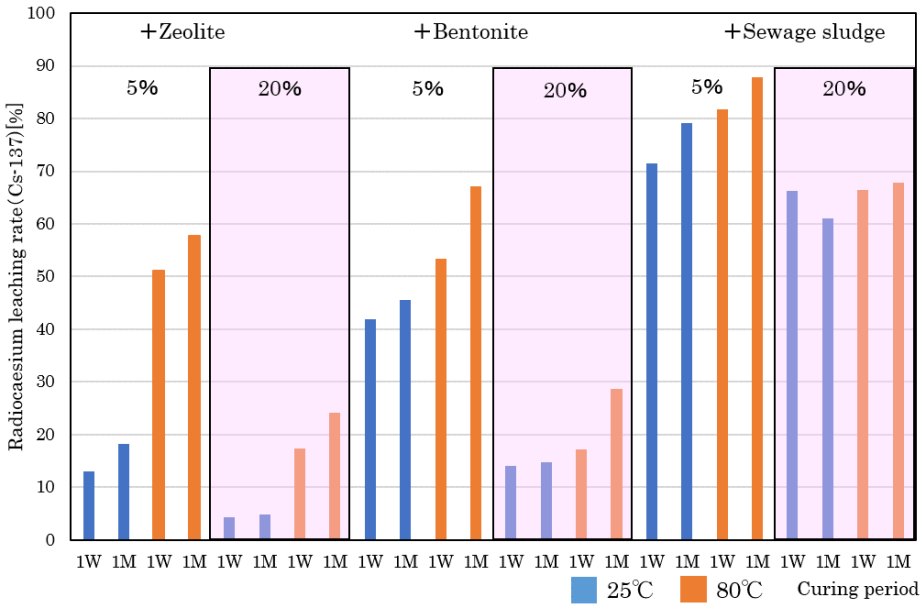

Figure 16: Relationship between leaching rate and additive, rate of addition, cure temperature and cure duration (Fly ash).

A very obvious reduction of radiocaesium leaching rate was observed for fly ash. The addition of 20% zeolite and 1 week of curing at 25°C resulted in the greatest reduction in the radiocaesium leaching rate, from 79.1% to less than 5%.

The materials added to fly ash showed leaching rate reduction in decreasing order as follows: zeolite, bentonite and sewage sludge. Both zeolite and bentonite showed1/3 lower leaching rates for the addition of 20% than for 5%. Zeolite was not effective at a higher cure temperature (80°C) compared with bentonite. For both zeolite and bentonite, longer (one month) curing duration had slightly adverse effects on the leaching rate reduction.

5.4. Conclusions

Table 13 summarizes the achievements. Various methods have been developed to control the radiocaesium distribution in bottom ash and fly ash during the MSW incineration process. These include changing the combustion temperature. However, we found that it was difficult to change the temperature within a range that is applicable to an incinerator in operation because the Waste Management and Public Cleaning Law prescribes maintenance and management standards. The addition of chemicals to the waste has promoted radiocaesium migration to fly ash to a great extent but the reproducibility of this effect was poor. Waste composition possibly affects the promotion or inhibition of migration in response to added chemicals. We will determine their impact by laboratory tests, where waste composition is easy to control.

With respect to the co-incineration of waste bag filter cloths with MSW at their original facility, we verified that co-incineration is a safe and appropriate treatment method when the ratio of the cloths in the mixture is managed appropriately.

We checked radiocaesium leaching characteristics from MSW incineration ash of facilities in the prefecture by radiocaesium leaching tests. According to the test result, the leaching rate differs remarkably between bottom ash (35% to 94%) and fly ash (less than 1% to 16%), differs depending on the facility, and does not show any significant seasonal changes. We will add and update data periodically.

In the laboratory radiocaesium immobilisation test, zeolite and bentonite, especially zeolite showed excellent ability to reduce the leaching rate of radiocaesium from fly ash from 79% to less than 5%. This result shows its possible practical application. We will further examine better methods for the addition and mixing of the material and ash, and identify materials capable of more effective radiocaesium leaching reduction. We plan to improve the understanding of the longevity of the leaching reduction effect and the effect of chelation.

Some of the achievements to date were presented at the Japan Waste Management Association Meeting[8),9)]. The information has also been provided to Fukushima Prefecture's general waste management division and municipalities as well as the special district authorities in the prefecture at the waste management meeting held by the general waste management division. We will continue to provide information to contribute to the proper treatment of waste contaminated with radioactive materials.

Table 13: Achievements to date.

Test		No. of facility cooperated	Results
(A) Radiocaesium distribution between bottom ash and fly ash	(A)-1 Effect of combustion temperature	4	Tests were conducted at four facilities but the expected combustion temperature was not obtained in some cases. In cases where high combustion temperature could be obtained, radiocaesium distribution to fly ash increased on the second day run (Distribution ratio up rise of 0.8% and 26% per 10℃ rise of combustion temperature).
	(A)-2 Continuous sampling test	2	Relationships between combustion temperature during usual operation and radiocaesium migration behaviours (distribution to bottom ash and fly ash) were investgated. No clear relationships were found.
	(A)-3 Effect of a radiocaesium evaporation accelerator and inhibitor	2	In the first test, when hydrated lime ($Ca(OH)_2$) was sprayed over the waste as a evaporation promoter, the radiocaesium distribution to fly ash increased remarkably (distribution rate up 9.3% per 1% addition). However bentonite addition did not show any evaporation prohibiting effect. We conducted additional tets to check the reproducibility and facility dependence of hydrated lime's radiocaesium evaporation effect. Hydrated lime showed the evaporation effect again to some extent but not as remarkable as in the first test.
(B) Proper treatment of used filter cloths of bag filters		2	As to the co-incineration of used filter cloths contaminated with fly ash containing radiocaesium with MSW, we confirmed that it is safe and proper treatment by managing the co-incineration ratio appropriately.
(C) Study of the reduction of radiocaesium leaching from fly ash	(C)-1 Date acquisition of radiocaesium leaching characteristics	15	We conducted testing on radiocaesium leaching from bottom ash and fly ash at 15 general waste incineration facilities in Fukushima Prefecture. Leaching of radiocaesium from bottom ash was limited (below 1% to 16%). However, fairly high leaching rate (35% to 94%) from fly ash was confirmed. In was confirmed that that the radiocaesium concentration in ash and the leaching rate differ depending on the facility and that the seasonal variation of radiocaesium leaching from incinerated ash is small.
	(C)-2 Laboratory radiocaesium immobilisation test	1	Zeolite and bentonite showed excellent ability to immobilize radiocaesium in fly ash. In particular, zeolite showed high performance. When zeolite was added 20% to fly ash, the leaching rate decreased from 79% to 4.3%. This result implicates possible practical use of the material.

References

1) Hidetoshi Kuramochi (2013) "Incineration of waste contaminated with radioactive materials: Issues and scientific findings so far (research review)", Safety Engineering, vol. 52, No. 5, pp282-290

2) Taku Iguchi and Takashi Kawano (2013) "Research on radiocaesium behavior during waste incineration", Proceedings of the Second Research Meeting of the Society for Remediation of Radioactive Contamination in Environment - p141, 2013

3) Kenichi Harada, Kouga Fukushima, Hidetoshi Kuramochi, Makoto Otake, Shinichi Sugita, and Toru Yamaki (2014), "Demonstrated Incineration of Grasses Contaminated by Radioactive Material", Proceedings of the 35th Japan Wastw Management Association Meeting, V-103

4) Mitsuhiro Tada, Yohei Tomita, Yasuhiro Miyakoshi, and Eiichi Shibuya (2013) "Cesium behavior in the incineration process and development of volatilization prevention technology" Proceedings for the Second Research Meeting of the Society for Remediation of Radioactive Contamination in Environment - p65

5) Masaki Takaoka (2013) "Measurement of radioactive materials in flue gas at waste incineration facilities", Journal of Japan Society of Material Cycles and Waste Management, Vol.24, No.4, pp258-266

6) Toru Kameo, Naoki Maruyama, and Nobukazau Sano (2003), and Clean Authority of Tokyo, "Regarding the disposal of waste filter cloths from bag filters", Cleaning Technology Report (Clean Authority of Tokyo), No. 3, pp57-63

7) Eiichi Wakaizumi (2008), "Regarding the incineration disposal of Tefaire® filter cloths at incineration facilities" Cleaning Technology Report (Clean Authority of Tokyo), No. 8, pp15-19

8) Shinichi Yamasaki, Hirofumi Yoshita, Hitoshi Suzuki, Minako Kamota, Hidetoshi Kuramochi, Kazuko

Yui, Minoru Okoshi, Nobuyuki Odawara, and Atsushi Fujimagari (2016), “Regarding the result of survey of radioactive material migration to bottom ash and fly ash under combustion temperature controlled incineration”, Proceedings of the 37th Japan Waste Management Association Meeting, V-3-123

9) Hirofumi Yoshita, Koki Kokubun, Naoharu Murasawa, and Shinichi Yamasaki (2017), “Regarding the result of demonstrative coincineration test of waste bag filter cloths with municipal solid waste”, Proceedings of the 37th Japan Waste Management Association Meeting, V-3-122

10) Waste Management and Public Cleansing Law (Law No. 137 of 1970)

Contents of major support received from the IAEA

1. FIP1 Survey of radionuclide movement in river systems

- Provision of the TODAM model, a numerical simulation of contaminant migration in a river network, for the quantitative estimation of radionuclides deposited in rivers.
- Technical guidance on the selection of monitoring points and monitoring items, with an emphasis on the importance of continuous monitoring at each monitoring point, based on previous studies of Chernobyl and Mayak.
- Advice about the operation of TODAM model using the monitoring data by the prefecture, that is, the importance of measuring the K_d value (solid-liquid distribution coefficient) and sediment particle size distribution at each observation point, as well as ion concentrations in rivers.
- Advice about the effectiveness of combining wide-area monitoring and simulation models, and the importance of including small lakes as research subjects for improving our understanding of the dynamics of radioactive materials in rivers.
- Advice about the need to assess the impact of decontamination and analyzing data excluding artificial effects.
- Support for on-site inspections concerning radionuclides monitoring in Ukraine, Germany, Slovakia, and so on.

2. FIP2: Survey of radionuclide movement with wild life

- Provision of foreign literature describing the relationship between wild animals and radionuclides, such as radionuclide migration to wild animals, including boars and deer, in various regions following the Chernobyl nuclear disaster and changes in radiocaesium levels in the bodies of birds, such as the American gallinule and American wood duck, at the Savannah River Ecology Laboratory.
- Provision of information about recent scientific results concerning the bioaccumulation of radiocaesium and in vivo radiocaesium concentration measurement technology.
- Discussions of study results and data analysis methods, such as the potential for mushrooms to explain a higher radiocaesium concentration in wild boars than those in other taxa in Fukushima Prefecture, based on observation that mushrooms (deer truffles) cause a high radiocaesium concentration in the muscle tissues of wild boars in Europe.
- Explanation of the impact of the Chernobyl disaster on wildlife animal groups in surrounding areas, the dynamics of wolves and other animals and survey methods to clarify these impacts.

3. FIP3: Countermeasures for radioactive materials in rivers and lakes

- Provision of information related to the environmental dynamics of radioactive materials in rivers and lakes.
- Provision of information related to global environmental remediation activities in rivers and lakes, including the removal of radioactive materials (countermeasures against the discharge of radioactive material from the heavily contaminated floodplain in the vicinity of the Chernobyl nuclear power

plant, and countermeasures against the inflow of radioactive materials into the Kiev Reservoir).

- Facilitation of a visit to the Chernobyl accident site.
- Recommendation regarding the evaluation of a radiocaesium decontamination test in a riverside (e.g., selection of the study site, simulation before decontamination, particle size of sediment, and density of the plant community).
- Advice on the study of countermeasures against radiocaesium in riverside parks (investigation of the history of floods, dikes and dredging to prevent recontamination).
- Recommendations about the study of Fukushima prefectural residents' anxiety and issues related to the water environment (including the age and sex of residents as factors).
- Support related to the preparation of published materials (papers).

4. FIP4: Developing of environmental mapping technology using GPS walking surveys

- Provision of information about efforts made by various institutions, such as the United States Environmental Protection Agency and Lawrence Berkeley National Laboratory, to perform local radiation dose mapping.
- Suggestion that inverse-distance weighting (IDW) is more appropriate than Kriging as a means of interpolation for walking surveys using GIS and that the shielding effect of buildings and the like must be considered.
- Advice to judge measurement conditions of walking surveys according to the conditions at each measurement point, as uniform measuring conditions are not always necessary.

5. FIP5: Study of proper treatment of waste containing radioactive materials at municipal solid waste incinerators

- Provision of information related to treatment methods employed in other countries for fly ash, treatment methods employed in other countries for low-level radioactive waste (i.e. incineration, melting treatment of metal, and plasma melting) and instruments for measuring the concentrations of radioactive substances in waste.
- Technical advice about the incineration of general waste, such as the need for studies conducted from the perspective of the radiocaesium balance of payments, the importance of comparative analyses of actual test data and model analysis results, and the need to optimize test conditions and assess waste quality.
- Advice about the importance of countermeasures against the generation of hydrogen fluoride in the mixed incineration of bag filters (made from Teflon).
- Advice regarding the safety (e.g. exposure protection and management) of facility workers.
- Suggestion that reducing radiocaesium elution from fly ash is important for the margin of safety when landfilling fly ash.